UNIVERSITÄT BONN

Characterization of Enzymes Involved in Lipid Biosynthesis from the Photosynthetic Bacteria *Synechocystis* PCC6803 and *Blastochloris viridis*

Dissertation

zur

Erlangung des Doktorgrades (Dr. rer. nat.)

der

Mathematisch-Naturwissenschaftlichen Fakultät

der

Rheinischen Friedrich-Wilhelms-Universität Bonn

vorgelegt von

Mohammed Aizouq

aus Salmieh, Syrien

Bonn, 2019

Angefertigt mit Genehmigung der Mathematisch-Naturwissenschaftlichen Fakultät der Rheinischen Friedrich-Wilhelms-Universität Bonn

1. Gutachter: Prof. Dr. Peter Dörmann
2. Gutachter: Priv. Doz. Dr. Christiane Dahl

Tag der Promotion: 02.03.2020

Erscheinungsjahr: 2020

Table of Contents

Table of Figures[1]

[1] Figure x. y: x is the section number in the thesis. Y is the figure number in the section.

Tables

Abbreviations

ACP	Acyl carrier protein
Amp	Ampicillin
BSA	Bovine serum albumin
cDNA	Complementary DNA
CHAPS	3-[(3-Cholamidopropyl) dimethylammonio]-1-propanesulfonate
CoA	Coenzyme A
Col-0 / 2	Columbia 0 / 2
CTAB	Cetyltrimethylammonium bromide
DAG	Diacylglycerol
ddH2O	Double deionized water
DGDG	Digalactosyldiacylglycerol
DMSO	Dimethyl sulfoxide
DNA	Deoxyribonucleic acid
DNA	Deoxyribonucleic acid
dNTP	Deoxyribonucleotide triphosphates
DW	Dry weight
EDTA	Ethylenediaminetetraacetic acid
ELT	Esterases/lipases/thioesterases
ER	Endoplasmic reticulum
EtBr	Ethidium bromide
FAMEs	Fatty acid methyl esters
FAPEs	Fatty acid phytyl esters
FATEs	Fatty acid tocopheryl esters
FFA	Free fatty acids
FID	Flame ionisation detector
FW	Fresh weight
g	Standard gravity (9.81 m s^{-2})
G3P	Glycerol-3-phosphate
Gal	Galactose
GC	Gas Chromatography
Glc	Glucose
GlcA	Glucuronic acid
GlcGalDG	Glucosylgalactosyldiacylglycerol
h	Hour
HEPES	4-(2-Hydroxyethyl)-1-piperazineethanesulfonic acid
His-tag	Histidine tag
HPLC	High-pressure liquid chromatography
I.S.	Internal standard
IPTG	Isopropyl β-D-1-thiogalactopyranoside
Kan^R	Kanamycin
kb	Kilo base pairs
kDa	Kilo Dalton
LB	Luria-Bertani medium
LC	Liquid chromatography
LPA	Lysophosphatidic acid

m/z	Mass-to-charge ratio
MGDG	Monogalactosyldiacylglycerol
MS	Mass spectrometry
MS medium	Murashige and Skoog medium
NASC	Nottingham Arabidopsis Seed Collection
NCBI	National Center for Biotechnology Information Search database
OD	Optical density
ORF	Open reading frame
PABA	*para*-aminobenzoic acid
PAGE	Polyacrylamide gel electrophoresis
PAM	Pulse-amplitude modulated
PC	Phosphatidylcholine
PCR	Polymerase chain reaction
PE	Phosphatidylethanolamine
PES	Phytyl ester synthase
PG	Phosphatidylgylcerol
PI	Phosphatidylinositol
PS	Phosphatidylserine
Q-TOF	Quadrupole time-of-flight
RNA	Ribonucleic acid
rpm	Rounds per minute
RT	Room temperature
SD	Standard deviation
SDS	Sodium dodecyl sulfate
sn	Stereospecific numbering
SPE	Solid phase extraction
SQDG	Sulfoquinovosyl diacylglycerol
TAE	Tris-acetate-EDTA
TAGs	Triacylglycerols
T-DNA	Transfer DNA
TES	2-[[1,3-dihydroxy-2-(hydroxymethyl)propan-2-yl]amino]ethanesulfonic acid
TLC	Thin layer chromatography
Tris	Tris(hydroxymethyl)aminomethane
UDP	Uridine diphosphate
UV	Ultra violet
v/v	Volume per volume (ml per 100 ml)
w/v	Weight per volume (g per 100 ml)
WT	Wild type

Fatty acids are abbreviated as X:Y, where X indicates the number of carbon atoms and Y refers to the number of double bonds. Carbon atoms and double bonds for the fatty acid moieties in glycerolipids, which contain more than one fatty acid are summarized, for example, 48:0-TAG represents tri-16:0 TAG.

1. Introduction

1.1. Photosynthesis in Bacteria

Photosynthesis is the fundamental process essential for all life on earth. Although the concept of photosynthesis is typically related to plants and eukaryotic algae, much of the understanding of the molecular details concerning light capturing and light reactions comes from studying photosynthetic bacteria (Deisenhofer and Michel 1989). Much like the name indicates, photosynthetic bacteria are prokaryotic organisms which contain photosynthetic reaction centres and pigments that are able to absorb light. Most of the photosynthetic bacteria contain bacteriochlorophyll (BChl) with the exception of the cyanobacteria which contain the same chlorophyll *a* as plants. Different substitutions around the tetrapyrrole ring and changes of the length of the side chain of the bacteriochlorophyll molecule result in structures found in several bacteriochlorophyll types like bacteriochlorophyll *a, b, c, cs, d, e*, and *g*. Based on the ability to produce oxygen, photoautotrophic bacteria can be classified into oxygenic autotrophs and anoxygenic autotrophs. To date, cyanobacteria represent the only group of the oxygenic autotrophic bacteria. The anoxygenic autotrophic bacteria are also able to assimilate CO_2. Unlike cyanobacteria, they cannot use water as electron donor. The anoxygenic autotrophic bacteria can be divided into the following main groups: purple bacteria, green bacteria (chloroflexi), heliobacteria and chlorobi. The anoxygenic autotrophs can also be divided according to their ability to cope with oxygen in the bacterial growth media, i.e. aerobic, anaerobic and semi-aerobic anoxygenic bacteria (Koblížek 2015; Shahak et al. 1999; Blankenship 1995).

1.2. Cyanobacteria

Cyanobacteria (also termed Cyanophytes, Cyanophyceae or blue-green bacteria) are gram-negative prokaryotes. They are the oldest and the only known prokaryotes capable of plant-like oxygen producing photosynthesis. Fossil records claim that cyanobacteria existed up to 3.5 billion years ago (Schopf 1993; Schopf 2006). This means they were the first organisms to start the accumulation of oxygen in our atmosphere (Line 2002; Catling et al. 2002). Cyanobacteria share several physiological and biochemical characteristics with the plant chloroplasts. According to the endosymbiotic theory, cyanobacteria are considered to be the ancestors of today's chloroplasts (Reyes-Prieto et al. 2007; Timmis et al. 2004). Presently, cyanobacteria in the biosphere are responsible for 20-30% of the earth's photosynthetic production. This makes them good candidates for many biotechnological applications. Moreover, they are attracting growing attention as host organisms for the production of biofuel.

1.2.1. The Model *Synechocystis* sp. PCC 6803

The glucose tolerant strain of *Synechocystis* sp. PCC 6803 (Williams 1988), hereafter is referred to as *Synechocystis*, is one of the most extensively studied cyanobacteria. It belongs to the family Oscillatoriophycideae of the Chroococcales. They are versatile unicellular organisms which modulate their metabolic characteristics in response to the availability of light and carbon. This means that they can live photoautotrophically and photoheterotrophically. *Synechocystis* also shows fermentative activity when darkness and anoxic environment are combined (Gutthann et al. 2007).

With a size of 3.6 mega base pairs (Mbp), the genome of *Synechocystis* consists of a single chromosome that harbours about 3000 protein coding genes (Kaneko and Tabata 1997). It is known that *Synechocystis* cells contain several genome copies. The number of copies changes based on the growth phase. The glucose tolerant strain of *Synechocystis* contains about 142, 47 and 43 genome copies in the exponential phase, linear phase and stationary phase, respectively (Griese et al. 2011). In addition, *Synechocystis* contains several plasmids of different sizes ranging between 2.3 and 120 kilo base pairs (Kbp) (Kaneko et al. 2003). The plasmid pSYSA is the most important plasmid as it is believed to be involved in the toxin-antitoxin systems which is responsible for the segregational killing of the cell (Kopfmann and Hess 2013).

Synechocystis cells have a spherical shape after cell division. The cell is surrounded by an outer membrane and a cytoplasmic membrane. The space between the two membranes is called the periplasmic space which contains a layer of peptidoglycan (Liberton et al. 2006). The periplasmic space also provides a good environment for protein folding and stabilization before protein secretion to the outer environment (Miller and Salama 2018). The motility of *Synechocystis* cells is a positive phototaxic twitching, which is supported by surface pili (Bhaya et al. 2001). Thylakoids are the dominant membrane structure in *Synechocystis*. They are the site where photosynthesis takes place. Thylakoids are arranged in the *Synechocystis* cell as ring-shaped structures parallel to the plasma membrane. They converge to the plasma membrane at several points. These points are called biogenesis centres (previously thylakoid centres). They are important during the restoration of the PSII complex (Nickelsen and Rengstl 2013; Heinz et al. 2016).

The cyanobacterial origin of the plant's chloroplast is manifested by the highly conserved lipid composition between *Synechocystis* thylakoid membranes and the inner envelope and thylakoid membranes of chloroplasts of plants. This lipid composition is different from most of the other bacterial membranes where phospholipids are dominant. *Synechocystis* contains mainly three glycolipids i.e. monogalactosyldiacylglycerol (MGDG), digalactosyldiacylglycerol (DGDG) and sulfoquinovosyldiacylglycerol (SQDG). Since cyanobacteria do not synthesize

phosphatidylcholine (PC), phosphatidylethanolamine (PE) or phosphatidylinositol (PI), phosphatidylglycerol (PG) and phosphatidic acid (PA) are the only phospholipids (Murata et al. 1992; Okazaki et al. 2006). They also contain low amounts of monoglucosyldiacylglycerol (MGlcDG) which is the precursor of MGDG biosynthesis by an epimerization step (MgdE) (Sato and Murata 1982).

The molecular species of the glycerolipids in cyanobacteria are determined by the carbon chain lengths of fatty acids in addition to the number of the double bonds in these chains. Based on this fact, cyanobacteria can be divided according to their fatty acid composition into four groups. *Synechocystis* belongs to the group 4, containing 16:0, $16:1^{\Delta 9}$, 18:0, $18:1^{\Delta 9}$, $18:2^{\Delta 9,12}$, $\alpha 18:3^{\Delta 9,12,15}$, $\gamma 18:3^{\Delta 6,9,12}$ and $18:4^{\Delta 6,9,12,15}$ (Merritt et al. 1991; Murata et al. 1992; Los and Mironov 2015).

1.2.2. Photosynthesis in *Synechocystis*

The phototrophic way of life implies the capability of harnessing the physical energy of the light and converting it into chemical energy to produce organic mass. For this purpose, photosynthetic organisms have developed an effective apparatus for sunlight harvesting. Cyanobacteria (*Synechocystis*) harbour pigment-protein complexes known as photosystem I and II (PSI and PSII). PSII releases oxygen from water oxidation and PSI depends on the reduction of $NADP^+$ (Nelson and Yocum 2006). The PSII subunit structure in cyanobacteria is identical to that of PSII of plants. Nevertheless, the PSII in cyanobacteria is associated to a chlorophyll-free light harvesting antenna called phycobilisomes (PBSs). Phycobilisomes contain water soluble pigments termed as phycobilins like phycoerythrin, phycoerythrocyanin or phycocyanin (Chang et al. 2015). Phycobilins like chlorophyll belong to the tetrapyrroles family formed by the condensation of eight molecules of aminolevulinic acid (Cornah et al. 2003). In contrast to light harvesting complex (LHC) in plants, which is embedded within the thylakoid membrane, the PBS locates on the plasma-oriented surface of the thylakoid membrane. Phycobilins are radiated out from the centre to increase the surface area to harvest more light in the shallow marine environment (Figure 1.1).

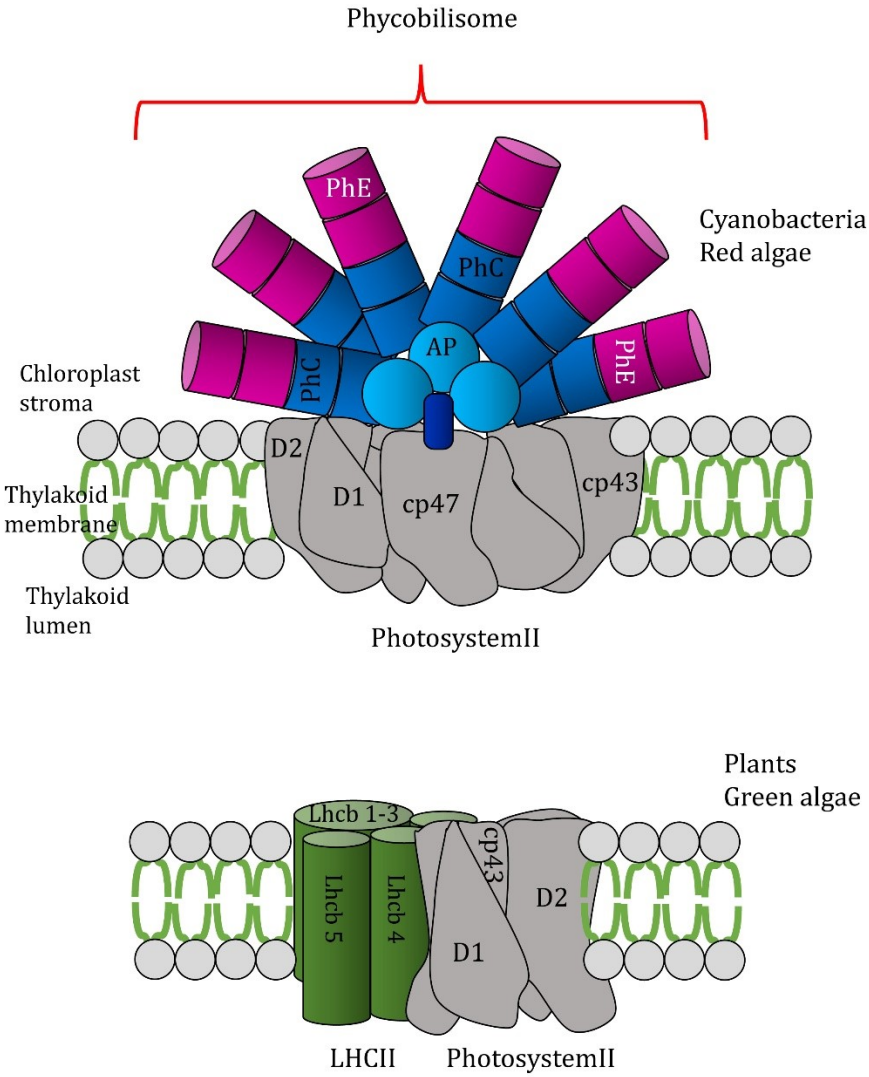

Figure 1. 1: Photosystem II complex in plants and cyanobacteria.
The figure shows the identical photosystem subunits in plants and cyanobacteria and the unique phycobilisome in cyanobacteria. PhE: phycoerythrin, PhC: phycocyanin, AP: Allophycocyanin. This figure is re-created from https://www.kegg.jp/entry/ter00196

1.2.3. Chlorophyll Synthesis and Degradation in *Synechocystis*

Synechocystis, like many other cyanobacteria, contains chlorophyll, phycocyanobilins and carotenoids as main photosynthetic pigments. Chlorophyll *a* (Chl *a*) is the only chlorophyll form in *Synechocystis*, and because of the similarity between the photosystems in cyanobacteria and plants, it is believed that the chlorophyll turnover and the regulation of the respective genes in *Synechocystis* might be related to the same processes in plants. The chlorophyll *a* molecule in plants, green algae and cyanobacteria consists of the porphyrin ring with a magnesium atom in the centre (chlorophyllide) and a branched phytol chain esterified to the chlorophyllide. The biosynthesis of the two chlorophyll moieties in plants has been described in detail in several studies before (Bouvier et al. 2005; Eckhardt et al. 2004). In cyanobacteria, chlorophyllide is

formed by the tetrapyrrole biosynthesis pathway starting from the amino acid glutamate as a result of several biochemical reactions (Masuda 2008). Phytol belongs to the terpenoids, or isoprenoids. In cyanobacteria, terpenoids are synthesized via the methylerythritol-phosphate (MEP) pathway using glyceraldehyde 3-phosphate (G3P) and pyruvate produced by photosynthesis as substrates. One final product of the MEP pathway is geranylgeranyl diphosphate (geranylgeranyl-PP), which can be reduced to phytyl diphosphate (phytyl-PP) by the geranylgeranyl-PP reductase sll1091 (Shpilyov et al. 2005; Pattanaik and Lindberg 2015) (Figure 1.2). Chlorophyll is synthesized by esterifying the chlorophyllide to phytyl-PP by the chlorophyll synthase slr0056 (Oster et al. 1997)(Figure 1.2).

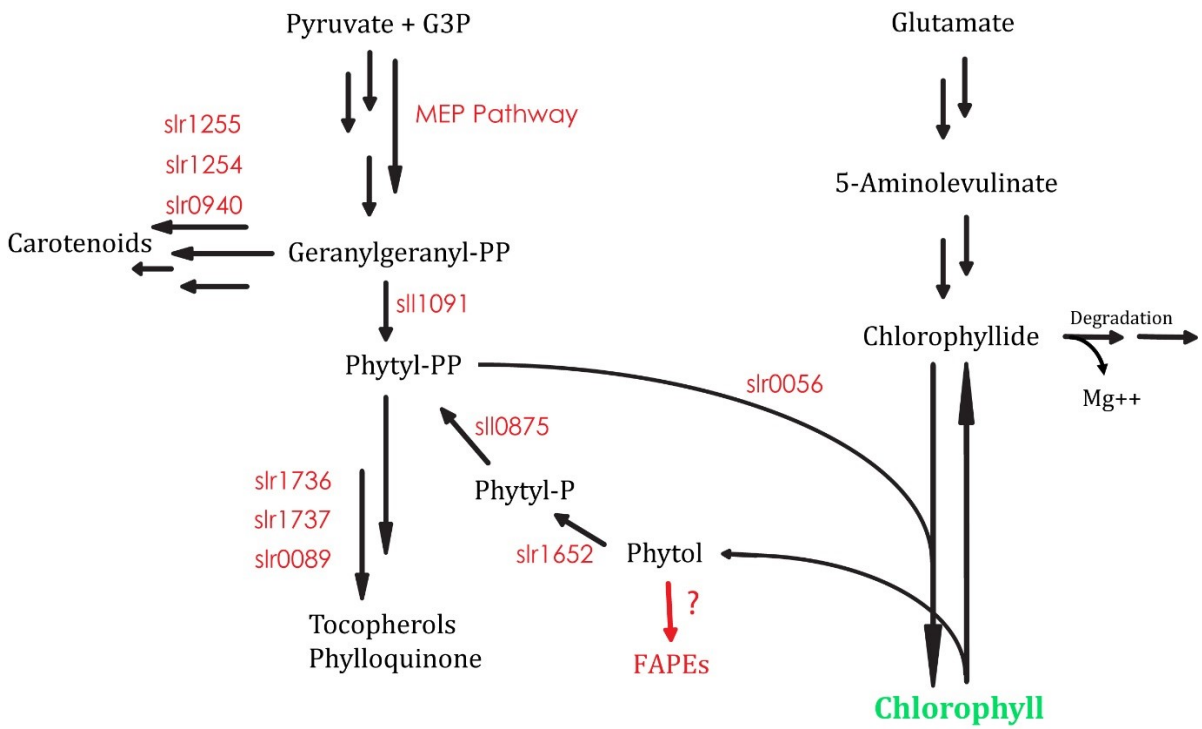

Figure 1. 2: Chlorophyll biosynthesis and degradation pathways in wild-type *Synechocystis*.
The scheme also shows the possible pathways to synthesise phytyl diphosphate (phytyl-PP) either by reduction of geranylgeranyl diphosphate (geranylgeranyl-PP) that is produced via the methylerythritol-phosphate (MEP) pathway or by phosphorylation of the chlorophyll-derived phytol to phytyl monophosphate (phytyl-P) and then to (phytyl-PP). (?) indicates enzymes that have not yet been identified in cyanobacteria. The red arrow indicates the potential fatty acid phytyl ester (FAPE) synthase which has not been described in *Synechocystis* before. The scheme is modified from (Backasch et al. 2005; Vavilin and Vermaas 2002; Pattanaik and Lindberg 2015).

The lifetime of chlorophyll in wild type *Synechocystis* growing under normal light conditions is about 300 h. This time is considered to be long compared to the cell doubling time which is about 14 h (Vavilin and Vermaas 2002). Thereafter, chlorophyll starts to be degraded naturally, catalysed by the chlorophyllase. The chlorophyll degradation rate might be increased by applying stress like highlight, or UV-B radiation (Gao et al. 2009; Kopečná et al. 2012). In darkness, chlorophyll starts to be degraded after 3 or 4 days which is the half lifetime of chlorophyll in darkness. The chlorophyll loss in darkness is not compensable because there is no *de novo*

synthesis as the chlorophyll biosynthesis is fully light-dependent (Wu and Vermaas 1995). During growth on nitrogen-free medium, considerable amounts of the chlorophyll-free phycobilisomes, which make up the light harvesting complexes in the photosystems of *Synechocystis*, start to be degraded. This explains why, in contrast to plants, chlorophyll in *Synechocystis* is less affected by nitrogen starvation (Li and Sherman 2002).

1.2.4. Phytol metabolism and phytyl ester biosynthesis in *Synechocystis*

Chlorophyll degradation is mediated by cleaving the ester bond of chlorophyll releasing chlorophyllide and free phytol. The degradation of chlorophyllide has been reviewed before (Eckhardt et al. 2004). Free phytol in *Synechocystis* might be phosphorylated to phytyl-P and then to phytyl-PP by the two kinase activities slr1652 and sll0875, respectively (Valentin et al. 2006; vom Dorp et al. 2015) (Figure 1.2). The resulting phytyl-PP can enter the chlorophyll synthesis/degradation cycle or can be incorporated into carotenoids, tocopherols (the four forms of tocopherols α, β, γ and δ are present in *Synechocystis*) or phylloquinone (vitamin K) (Maeda et al. 2005; Schledz et al. 2001).

In higher plants, phytyl esters accumulate in the plastoglobules of the chloroplast under chlorotic stress (Lippold et al. 2012). Two acyltransferases (PES1, PES2) of the esterase/lipase/thioesterase (ELT) family synthesise fatty acid phytyl esters (FAPEs) from phytol, which is derived from chlorophyll breakdown, and fatty acids (presumably acyl-CoA) from galactolipid turnover (vom Dorp et al. 2015) (Figure 1.3A). The first report of FAPEs in marine algae was the isolation from the dinoflagellate *Peridinium foliaceum*, which contains 5% of FAPEs of total lipids (Withers and Nevenzel 1977). Phytyl esters have been reported in the bryophytes *Megaceros flagellaris*, in mosses and also in zooplankton, especially in the famous arctic krill *Thysanoessa raschi* where phytol is almost the only fatty alcohol that is mainly esterified to 16:0 or 18:1 fatty acids (Sargent and Falk-Petersen 1981; Malcolm S.Buchanan 1996). The cyanobacterium *Synechococcus*, which is closely related to *Synechocystis*, was found to naturally accumulate small amounts of FAPEs (Lütke-Brinkhaus et al. 1985). Some studies suggested that phytol could be esterified by means of activities in non-photosynthetic bacteria. The authors demonstrated that some sediment marine bacteria like *Acinetobacter* sp., *Pseudomonas nautica*, *Marinobacter* sp., and *Marinobacter hydrocarbonoclasticus* are able to accumulate isoprenoid esters including phytol esters when growing on free isoprenoid alcohol in the presence of oxygen (Rontani et al. 1999).

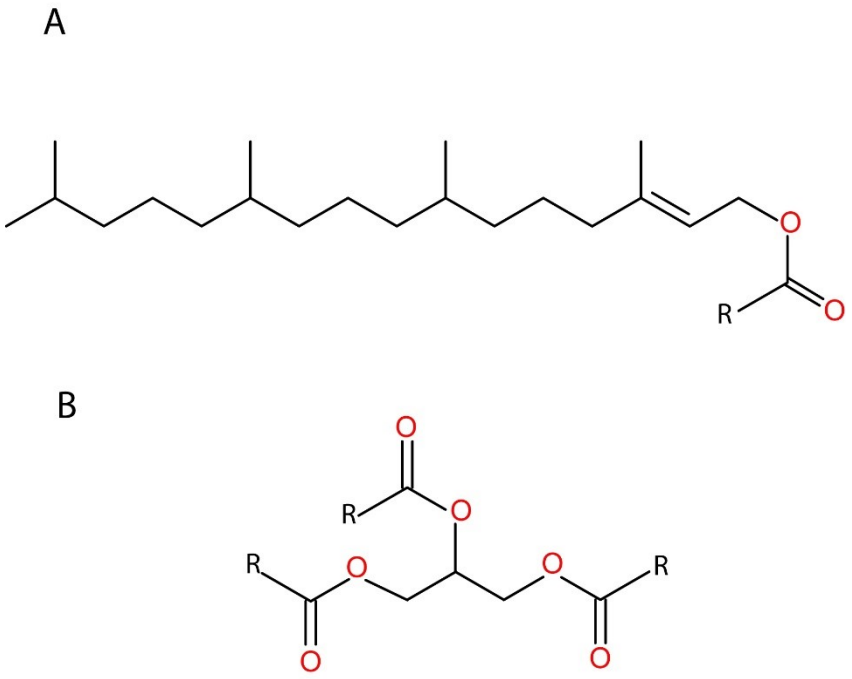

Figure 1. 3: **Chemical structure of the two storage lipids.**
(A) phytyl ester and **(B)** triacylglycerol (TAG). R: represent saturated or unsaturated alkyl chain residue (fatty acid).

1.3. Triacylglycerol (TAG) in Bacteria

Triacylglycerols (TAGs) are non-polar triesters of glycerol with three fatty acids (Figure 1.3B). TAGs are largely variable depending on the fatty acid composition. They are considered to be the most common storage lipid for carbon and energy in many organisms including plants, animals and fungi. The main storage lipids in bacteria, which are able to accumulate polyesters, belong to the poly hydroxyalkanoic acid group (PHA) (Anderson and Dawes 1990). However, it was reported that many members of the gram-positive Actinomycetes such as *Mycobacterium, Streptomyces, Rhodococcus, Nocardia* and others accumulate TAG (Röttig and Steinbüchel 2013; Alvarez et al. 2000; Barksdale and Kim 1977; Olukoshi and Packter 1994). Furthermore, the biosynthesis of TAG in the gram-negative bacterium *Acinetobacter* has already been described, however, TAG accumulation is very low (Makula et al. 1975). In addition to *Acinetobacter*, the marine bacterium *Alcanivorax borkumensis* seems to accumulate a minor amount of TAG (Kalscheuer et al. 2007). The main function of TAG in bacteria is to serve as reserve compound. According to Alvarez and Steinbüchel 2002, TAG in bacteria might have other functions like regulation of cellular membrane fluidity by keeping unusual fatty acids away from membrane phospholipids. In the cyanobacterial world, the biosynthesis of TAG is still a matter of debate. TAG has been potentially detected in several members of the Nostocales. The filamentous cyanobacterium *Nostoc commune* was found to accumulate a neutral lipid co-migrating with TAG after labelling the cells with radioactive glycerol (Tarante et al. 1993). Another lipid co-migrating with TAG was identified in the cyanobacterium *Nostoc punctiforme* (Peramuna and Summers

2014). TAG was also isolated from the thermophilic Nostocales *Mastigocladus* and *Tolypothrix* (Řezanka et al. 2012). To date, there is no report on TAG accumulation in non-filamentous or non-thermophilic cyanobacteria (Hu et al. 2008).

1.3.1. Acyltransferases Involved in Triacylglycerol Biosynthesis

The activity of an acyltransferase is essential for TAG biosynthesis. As the terminal step, the acyltransferase is necessary to produce a TAG molecule from a diacylglycerol (DAG) and an acyl donor, e.g. a fatty acyl-coenzyme A (CoA). This reaction is catalysed in plant seeds by the enzyme acyl-CoA:diacylglycerol acyltransferase1 (DGAT1). In another type of reaction catalysed by phospholipid:diacylglycerol acyltransferase1 (PDAT1), the acyl group donor is a phospholipid instead of a CoA. These two acyltransferases are the main TAG synthases in Arabidopsis seeds and they are considered to be unique for TAG synthesis (Zhang et al. 2009; Dahlqvist et al. 2000; Zou et al. 1999; Hobbs et al. 1999). DGAT2 is another acyltransferase in plants with a very low sequence homology to DGAT1 or PDAT1. DGAT2 is capable to produce TAG after heterologous expression (Lardizabal et al. 2001; Shockey et al. 2006; Cahoon et al. 2007). The two acyltransferase types DGAT1 and DGAT2 are present in plants, yeast and animals. Another acyltransferase is the bacterial acyltransferase Atfa (previously named WS/DGAT). It is the only reported acyltransferase involved in the biosynthesis of TAG in prokaryotes known to date. Atfa was characterized for the first time in *Acinetobacter calcoaceticus*. The Atfa-type acyltransferase has broad substrate specificity since it can synthesize wax esters (WE) and TAG by using acyl-CoAs as acyl donors and different-chain-length fatty alcohols or DAG as an acyl acceptor (Kalscheuer and Steinbüchel 2003). Homologs of Atfa are presented in bacteria that are reported to accumulate TAGs (see above) and also in plants, represented by the wax ester synthase/diacylglycerol acyltransferase (WSD) family of enzymes like WSD1 (Li et al. 2008).

1.3.2. Lipid Droplets in Cyanobacteria

Neutral lipids, mainly TAGs, are stored in so-called lipid droplets which are surrounded by a monolayer phospholipid membrane. They are found in the cytosol of plants, fungi and animal cells (Martin and Parton 2006). Many bacteria are capable of accumulating neutral lipids in lipid inclusion bodies (lipid droplets), which are located in the bacterial cytoplasm, like in *Rhodococcus* sp. and *Streptomyces* sp. (Alvarez and Steinbüchel 2002). The bacterium *Rhodococcus opacus* strain PD630 is able to produce three different types of intracellular inclusions during growth on different substrates. 98% of these intracellular inclusions are TAGs (Alvarez et al. 1996), as shown in Figure 1.4A. The chloroplasts of plants contain lipid droplets known as plastoglobules (Figure 1.4B). Plastoglubules are lipid droplets where the chloroplast stores TAGs, FAPEs, tocopherols and carotenoids. In addition, some enzymatic activities were detected in the plastoglobules like PES1, PES2 and VTE1 (tocopherol cyclase) (Kessler and Vidi 2007; Rottet et al. 2015). The fact that

chloroplasts of plants have evolved from cyanobacteria, suggests that most of the morphological and physiological characteristics of the chloroplast are derived from a cyanobacterial origin (Timmis et al. 2004; Reyes-Prieto et al. 2007). Cyanobacteria, particularly *Synechocystis* sp. PCC6803 and *Nostoc punctiforme,* were shown to contain lipid droplets similar to plastoglobules in plant chloroplasts. These lipid droplets start to accumulate in the cytoplasm in the stationary phase (Peramuna and Summers 2014; van de Meene et al. 2006) (Figure 1.4C).

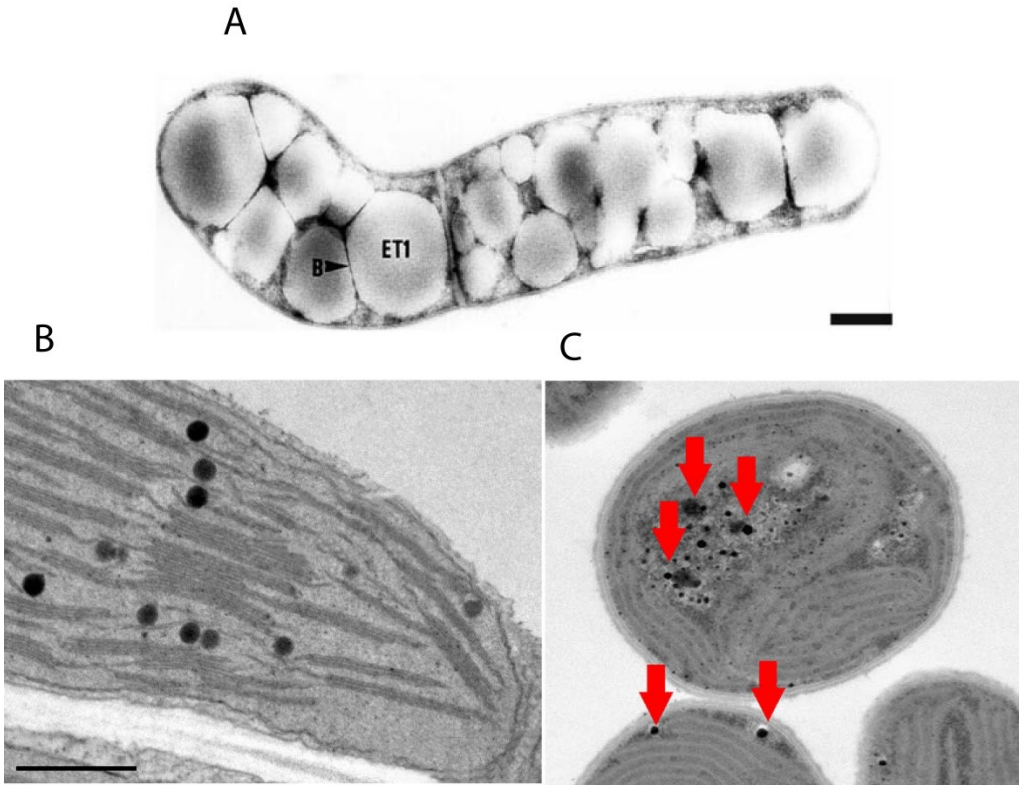

Figure 1. 4: **Lipid droplets in different organisms.**
(A) A cell of *Rhodococcus opacus* accumulating large amounts of TAG. ET1, electron-transparent inclusions body type 1. The arrowhead indicates the boundary B layer of the inclusion body. Bar: = 500 nm (Alvarez et al. 1996). **(B)** The spherical dark spots in *Arabidopsis* leaf chloroplasts are plastoglobules. Bar = 500 nm (Nacir and Bréhélin 2013). **(C)** Lipid droplets in *Synechocystis* WT are indicated with red arrows (Tahara et al. 2015)

1.4. The Galactolipid Biosynthesis Pathways in Plants and Bacteria

The galactolipids MGDG and DGDG are the most abundant membrane lipids in photosynthetic organisms including plants, green algae and cyanobacteria. MGDG and DGDG accumulate under normal growth conditions. However, DGDG, other glycolipids like sulfolipids as well as some non-phosphorous lipids accumulate in higher amounts during growth under phosphate deprivation to replace the phospholipids in plants, algae and bacteria (Güler et al. 1996; Härtel and Benning 2000; Minnikin and Abdolrahimzadeh 1974). Galactolipids play an essential role in the oxygenic photosynthesis of plants, green algae and cyanobacteria (Dörmann and Hölzl 2009). Chloroplasts

of plants contain about 45% and 15% MGDG and DGDG, respectively, of total glycerolipids (Siegenthaler and Murata 1998; Joyard and Douce 1987). X-ray crystallography and biochemical analyses of photosynthetic complexes from plants, algae and photosynthetic bacteria revealed that different glycerolipids including MGDG and DGDG are important components of photosynthetic reaction centres, of the photosystems PSI, PSII, the cytochrome b_6f complex and of the light harvesting complexes (Jones 2007; SS. Hasan et al. 2011).

The galactolipids MGDG and DGDG consist of one and two galactose moieties, respectively attached to DAG. The linkage between DAG and the galactose as well as between the two galactoses in the case of DGDG is a glycosidic bond. Based on the configuration of the glycosidic bond and the anomeric carbon, α and β anomeric configuration can be found (Figure 1.5).

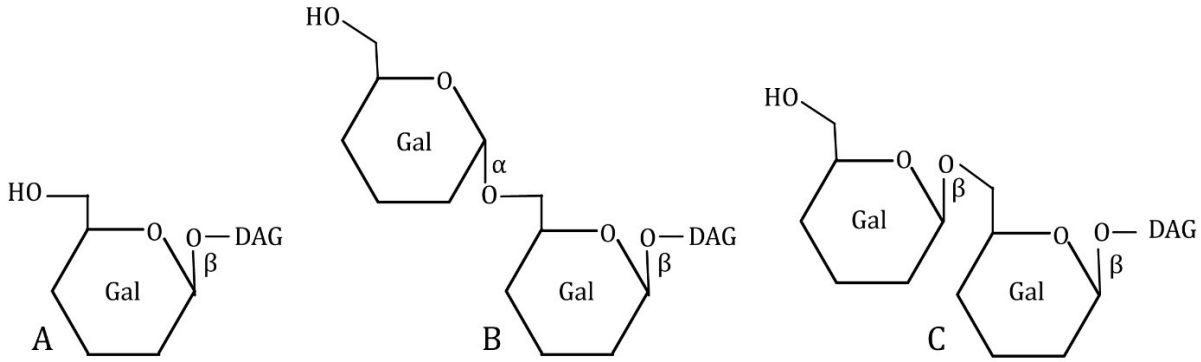

Figure 1. 5: Chemical structures of the sugar head group in the galactolipids MGDG and DGDG. **(A, B)** Natural isomers of βMGDG and αβDGDG, respectively, typically found in plants and algae. **(C)** The isomer of ββDGDG found in some bacteria. α, β: the anomeric configuration of the glycosidic linkages, DAG: diacylglycerol, Gal: galactose.

In plants, cyanobacteria and other bacteria, different pathways with different galactosyltransferases and glucosyltransferases exist which synthesize MGDG and DGDG (Figure 1.6). In *Arabidopsis thaliana*, MGDG is mainly produced my MGD1 which located in the inner envelope of the chloroplast. It transfers one galactose from uridine diphosphate-galactose (UDP-Gal) to DAG (Shimojima et al. 1997). The glycosidic linkage between the galactose and DAG is in β-anomeric configuration (βMGDG) (Hölzl and Dörmann 2007). DAG in plant chloroplasts can be derived from two pathways. DAG derived from the ER (eukaryotic lipids) contains mostly C18 fatty acid at the position *sn*2 and lacks C16. The second DAG form is derived from the chloroplast (prokaryotic lipids) and contains C16 fatty acid at the position *sn*2. Therefore, it is possible to distinguish the two DAG molecular species and the galactolipids derived from them. MGDG produced by MGD1 is composed of molecular species with prokaryotic and eukaryotic signature. After desaturation the main molecular species are 34:6 (*sn*1-18:3/*sn*2-16:3), and 36:6 (*sn*1-18:3/*sn*2-18:3) (Hölzl and Dörmann 2019). *Arabidopsis* contain further MGDG synthases, MGD2 and MGD3, which are localized in the outer envelope. They are only expressed under phosphate

deprivation (Kobayashi et al. 2009). MGDG produced by MGD2 and MGD3 is eukaryotic 34:3-MGDG (16:0/18:3). MGDG is the substrate for DGDG synthesis by the DGDG synthase DGD1. DGD1 from *Arabidopsis* is located in the outer envelope of the chloroplast. It transfers a second galactose to βMGDG by forming an α-anomeric linkage between the first and the second galactose (αβDGDG) (Hölzl and Dörmann 2007; Hölzl and Dörmann 2019) (Figure 1.6A). DGDG produced by DGD1 differs in its fatty acid composition compared to MGDG. The main species is 36:6 (18:3/18:3) and a minor species is 34:3 (18:3/16:0) (Klaus et al. 2002). Besides 34:6 (18:3/16:3) can be found only in very low amounts. Another DGDG synthase in *Arabidopsis* is DGD2. This enzyme is mainly active under phosphate deprivation when it produces eukaryotic 36:3 (16:0/18:3) with the respective MGDG substrate synthesized by MGD2 and MGD3.

Cyanobacteria have a different pathway to synthesise galactolipids (Figure 1.6B). Unlike plants, monoglucosyldiacylglycerol (MGlcDG), but not MGDG, is first synthesized from diacylglycerol and UDP-glucose by the MGlcDG synthase (MgdA) (Awai et al. 2006; Feige et al. 1980). The glucosyl moiety is linked in β- anomeric configuration to DAG (Coutinho et al. 2003). MGlcDG in *Synechocystis* is a substrate for the epimerase (MgdE), which converts MGlcDG into MGDG (Awai et al. 2014). DGDG in cyanobacteria is produced by the DGDG synthase DgdA utilising MGDG as a substrate. In contrast to plants, DGDG is not essential for growth in *Synechocystis*. Nonetheless, it is needed for an optimal autotrophic growth under phosphate limitation (Awai et al. 2007; Sakurai et al. 2007). The filamentous anoxygenic phototrophic *Chloroflexus* bacteria also accumulate MGDG and a diglycosyl lipid containing glucose and galactose. *Chloroflexus aurantiacus* contains two glycolipid glycosyltransferases, i.e. one galactosyltransferase, which is homologous to plant MGD1 and which synthesizes MGDG, and a second glucosyltransferase that transfers a glucose to MGDG resulting in βGlcβGalDG production (Hölzl et al. 2005b) (Figure 1.6C). Another member of *Chloroflexus* bacteria is *Chloroflexus aggregans* which also contains an MGDG synthase with sequence similarity to plant MGD1 (Yuzawa et al. 2012).

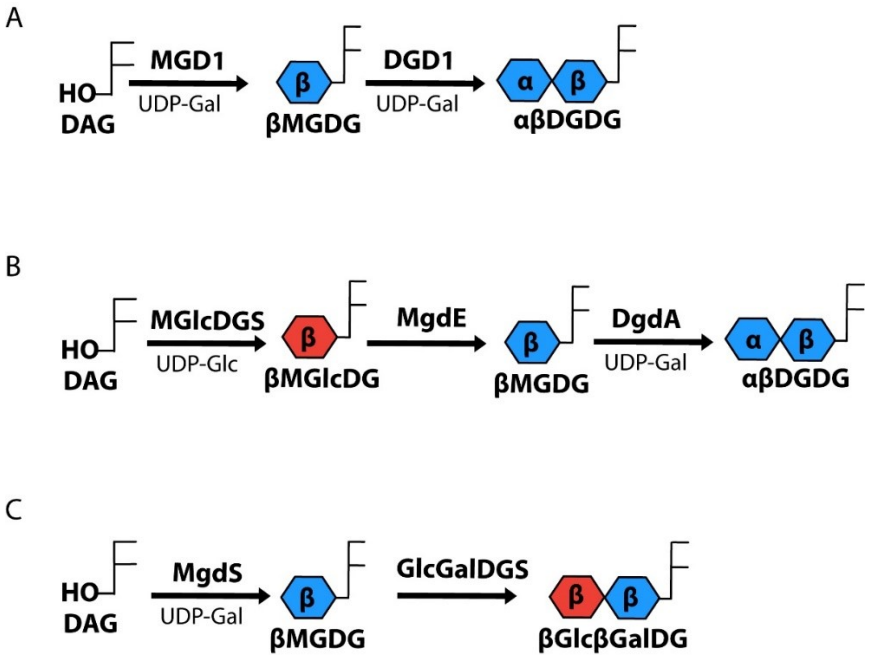

Figure 1. 6: **Pathways for the synthesis of MGDG, αβDGDG and ββGlcGalDG in different organisms.** **(A)** In plants and green algae, two enzymes, MGD1 and DGD1, transfer galactose residues onto diacylglycerol or MGDG to form βMGDG or αβDGDG, respectively. **(B)** Cyanobacterial βMGDG is formed by an epimerisation reaction of βMGlcDG by MgdE. **(C)** In *Chloroflexus aurantiacus* two glycosyltransferases are required to synthesize βMGDG and βGlcβGalDG

1.4.1. The Two *Arabidopsis* mutants *mgd1* and *dgd1*

βMGDG and αβDGDG are very important lipids for plants. The lack of one or both of these lipids has severe consequences for the chloroplast development, thylakoid membrane production, chlorophyll content and photosynthetic activity. A "leaky" mutation in the *MGD1* gene (*mgd1-1)* results in the reduction of 72% in the MGD1 mRNA and 42% of the MGDG content compared to the wild-type (Jarvis et al. 2000). Another mutant allele of *MGD1* in *mgd1-2* carries a null mutation. The *mgd1-2* mutant completely lacks MGDG and consequently DGDG. The homozygous plants of *mgd1-2* are dwarf and show an albino phenotype. Moreover, *mgd1-2* plants do not develop chloroplasts or thylakoid membranes. Therefore, they have lost the photosynthetic activity and the capacity for photoautotrophic growth (Kobayashi et al. 2007). Another null mutant allele of *MGD1* named *mgd1-3* (Hölzl unpublished) similar to *mgd1*-2 is used in this project.

The *dgd1* mutant of *Arabidopsis* is a null allele of the DGDG synthase gene DGD1. The *dgd1* mutant plants have a dwarfed growth and pale green leaves. In addition, they show a different ultrastructure of the thylakoid membrane accompanied with reduced photosynthetic capability (Dörmann et al. 1995). The plants have lost about 90% of αβDGDG, and the residual amount of αβDGDG in *dgd1* is derived from the activity of a second enzyme, DGD2 (Kelly et al. 2003).

1.4.2. The Processive Galactosyltransferase from *Blastochloris viridis* is involved in DGDG synthesis

Blastochloris viridis (*Rhodopseudomonas viridis*) is a member of the anoxygenic phototrophic bacteria in the phylum purple bacteria (Proteobacteria α-2 subclass) (Hiraishi 1997). In contrast to the other members of purple bacteria, *B. viridis* contains the bacteriochlorophyll (BChl) b instead of BChl *a*. This gives the culture a brownish green colour. The genome of *B. viridis* was completely sequenced in 2015 (Tsukatani et al. 2015). This bacterium is anaerobic with the capacity of microaerophilic growth (Lang and Oesterhelt 1989). Lipid analysis of *B. viridis* revealed that it contains βMGDG, ββDGDG, glucuronosyl diacylglycerol (GlcADG) and phospholipids (Figure 1.7 left) (Linscheid et al. 1997). ^{14}C labelling experiments emphasised that the MGDG in *B. viridis* is synthesised directly by glycosylation of diacylglycerol (DAG) like in plants and not by an epimerisation of a glucolipid as in cyanobacteria (Linscheid et al. 1997). The galactose residues in βMGDG and ββDGDG are all in β-anomeric configuration (Linscheid et al. 1997) . Protein BLAST searches for plant MGD1-related sequences revealed the presence of two galactosyltransferases in the genome of *B. viridis*, (Hölzl, unpublished). These two genes encode a nonprocessive enzyme producing βMGDG (BviMgdN), and a processive enzyme (BviMgdP) which converts diacylglycerol to ββDGDG, without accumulating βMGDG, when expressed in *E. coli* (Hölzl, unpublished) (Figure 1.7 right and 1.8).

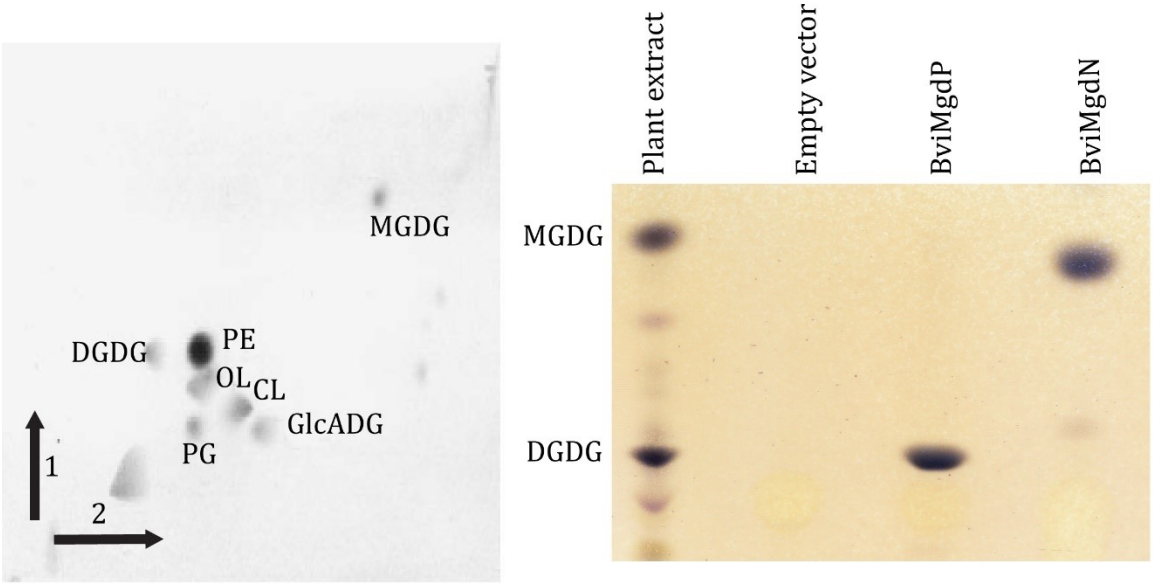

Figure 1. 7: **TLC plate shows bacterial lipid separation.**
Left: Separation of the polar lipids from *Blastochloris viridis* using a two-dimensional TLC plate (Linscheid et al. 1997). The plate shows the following lipids: MGDG: monogalactosyldiacylglycerol , DGDG digalactosyldiacylglycerol, GlcADG : glucuronosyldiacylglycerol, PC: phosphatidyl choline, PE: phosphatidyl ethanolamine, PG: phosphatidyl glycerol, CL: cardilipin, OL: ornithine lipid. The black arrows with 1 and 2 indicate the first and second dimension, respectively. **Right**: Separation of glycerolipids from *E. coli* cells expressing BviMgdP or BviMgdN from *B. viridis.* Lipids were extracted from *E. coli* and separated by thin layer chromatography. Glycolipids were stained with α-naphthol sulfuric acid. An *Arabidopsis* total leaf lipid extract was used as a standard. The DGDG in the plant standerd is αβDGDG. *E. coli* harbouring an empty vector was used as a negative control. BviMgdP is a processive enzyme that synthesizes ββDGDG directly from diacylglycerol. BviMgdN synthesises only βMGDG (Hölzl, unpublished).

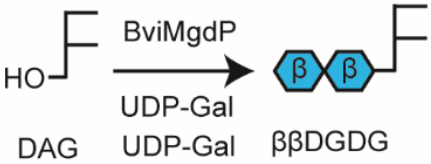

Figure 1. 8: **Potential pathways for the synthesis of the bacterial ββDGDG in the anoxygenic phototrophic bacterium *Blastochloris viridis*.**
The enzyme BviMgdP is able to transfer two galactose moieties to the diacylglycerol to form ββDGDG (Hölzl, unpublished)

1.5. Objectives

The evolution of eukaryotes including plants is based on selective pressure resulting in the accumulation of favourable sequences, as well as on gene transfer from other prokaryotes or eukaryotes. The incorporation of the prokaryotic progenitors for mitochondria and chloroplasts into the protoeukaryotic cell added another level of complexity to the genome organization of plant cells. Therefore, proteins accumulating in the chloroplasts of plants are derived from the cyanobacterial progenitor, from the host, or from the prokaryotic genes (in rare cases eukaryotic or viral genes) obtained by lateral gene transfer (Méheust et al. 2016). In this thesis, two bacterial genes which are homologous to plant genes encoding enzymes involved in chloroplast lipid synthesis were analysed.

Chloroplasts contain triacylglycerol (storage lipid) and phytyl esters (wax ester) derived from the chlorophyll phytol chain and fatty acids from membrane lipids. *A. thaliana* harbours two phytyl ester synthases, PES1 and PES2, which consists of a hydrolase domain and an acyltransferase domain. The presence of triacylglycerol and phytyl esters in cyanobacteria, however, remained unclear. In this study, the question whether *Synechocystis* contains triacylglycerols and phytyl esters was addressed. The *Synechocystis* enzymes with sequence similarity to PES1 or PES2 will be expressed in heterologous hosts and characterised for their capacity to synthesise triacylglycerol or phytyl esters. *Synechocystis* mutants will be generated and characterised.

The other part of the thesis refers to the analysis of the MGD1-type galactosyltransferase from *Blastochloris viridis*, presumably involved in the production of ββDGDG. The bacterial galactosyltransferase will be introduced into the galactolipid-deficient *Arabidopsis* mutants (*mgd1-3*, *dgd1*). Transformed plants will be analysed for lipid and chlorophyll content, and photosynthesis activity to determine the capability of the bacterial glycolipids to substitute for the plant glycolipids for complementation of growth and photosynthesis deficiency.

2. Materials and Methods

2.1. Equipment

6530 Accurate-mass quadrupole time-of-flight (Q-TOF) LC/MS	Agilent, Böblingen (DE)
7890 gas chromatography (GC) with flame ionisation detector (FID)	Agilent, Böblingen (DE)
7890 gas chromatography (GC) with mass spectrometry (MS)	Agilent, Böblingen (DE)
Autoclave	Systec, Linden (DE)
Balance 770	Kern, Balingen-Frommern (DE)
Balance PG503-S Delta Range	Mettler Toledo, Gießen (DE)
Binocular microscope SZX16	Olympus, Hamburg (D)
Block heater SBH130D/3	Stuart, Bibby Scientific, Staffordshire (USA)
Camera DP7Z for microscope	Olympus, Hamburg (D)
Centrifuge 5417R	Eppendorf, Hamburg (D)
Centrifuge 5810 R	Eppendorf, Hamburg (D)
Chemiluminescence documentation system	Bio-Rad, California (USA)
Freeze dryer Alpha 2-4	Christ, Osterode am Harz (DE)
Gel caster, Mighty small II	GE Healthcare Europe, Freiburg (DE)
Growing cabinet Rumed	Rubarth Apparate, Laatzen (DE)
High-performance liquid chromatography (HPLC) 1200 series	Agilent, Böblingen (DE)
Homogeniser Precellys 24	PeQlab, Erlangen (DE)
Horizontal electrophoresis chamber	Cti, Idstein (DE)
Incubator with light supply	Snijiders Scientific b.v., Tilburg (NL)
Incubator, Kelvitron	Thermo Scientific Heraeus, Waltham (US)
Inverted Microscope Eclipse TE300	Nikon, Düsseldorf (DE)
Junior Pulse-amplitude modulated (Junior PAM) chlorophyll fluorimeter	WALZ. Effeltrich (DE)
Light microscope B H-2	Olympus, Hamburg (D)
Magnetic stirrer MR30001	Heidolph Instruments, Schwabach (DE)
Micro pulser electroporator	BioRad Laboratories, München (DE)
pH meter inoLab pH Level 1	WTW, Weilheim (DE)
Photometer LI-185B	LI-COR, inc. (USA)
Photometer, Specord 205	Analytik Jena, Jena (DE)
Phytochamber SIMATiC OP17	York International, York (USA)
PowerPac Basic electrophoresis power supply	Bio-Rad Laboratories, München (DE)
Rotary evaporator LABOROTA 4001	Heidolph, Schwabach (DE)
Sample concentrator	Techne (Bibby Scientific), Stone (GB)
Semi-dry transfer cell Trans-BLOT SD	Bio-Rad Laboratories, München (DE)
Shaking Incubator with light supply	INFORS, Einsbach (DE)
Spectrophotometer Nanodrop 1000	PeQlab, Erlangen (DE)
Sterile bench model 1.8	Holten Lamin Air, Allerød (DK)
Synergy Water Purification System	Merck Millipore, Darmstadt (DE)

Thermocycler TPersonel 48	Biometra, Göttingen (DE)
Tube Rotator SB3	Stuart, Sta_ordshire (UK)
UV-transilluminator DP-001 T1A	Vilber Lourmat, Eberhardzell (DE)
Vortex Certomat MV	Braun Biotech, Melsungen (DE)
VortexGenie2	Scientific Industries, Bohemia (USA)
Water bath TW20	Julabo, Seelbach (DE)
Water bath TW20	Julabo, Seelbach (DE)
Water purification system ELIX 35	Merck Millipore, Darmstadt (DE)

2.2. Materials

2.2.1. Consumables

Auto sampler vials with inlets and screw caps with PTEF septa	VWR, Darmstadt (DE)
Centrifuge tubes (15 and 50 mL)	Greiner Bio-One, Frickenhausen (DE)
Ceramic beads different sizes	Mühlmeier Mahltechnik, Bärnau (DE)
Culture glass tubes (15.5 x 160 mm)	Schott, Mainz (DE)
Electroporation cuvettes	PeQlab, Erlangen (DE)
Glass Pasteur pipettes	Brand, Wertheim (DE)
Glass vials with and without thread 8 ml	VWR, Darmstadt (DE)
Glass vials with thread 40 ml	Schmidlin, Neuheim (CH)
Microcentrifuge tubes (1.5 and 2 mL)	Greiner Bio-One, Frickenhausen (DE)
PCR tubes	Brand, Wertheim (DE)
Petri dishes (94 x 16 and 145 x 20 mm)	Greiner Bio-One, Frickenhausen (DE)
Pipette tips	Axygen, Corning, Karlsruhe (DE) or Greiner Bio-One, Frickenhausen (DE)
Pots for plant cultivation	Pöppelmann, Lohne (DE)
PTFE screw caps for 8 mL glass vials	Schott, Mainz (DE)
PTFE septa for screw caps for 8 ml glass vials	Schmidlin, Neuheim (CH)
Soil (type Topf 1.5)	Gebrüder Patzer, Sinntal-Jossa (DE)
SPE silica column	Macherey-Nagel, Düren (DE)
Sterile filter for syringes 0.2 µm pore size	Schleicher and Schuell, Dassal (DE)
Syringes 30 and 5 ml	Labomedic, Bonn (DE)
Teflon septa for screw caps	Schmidlin, Neuheim (DE)
TLC plates Silica 60 Durasil with and without concentration zone	Macherey and Nagel, Düren (DE)
Trays for plants cultivation	Pöppelmann, Lohne (DE)
Square petri dishes 10 x 10 cm	Greiner Bio-One, Frickenhausen (DE)
Classic light bulb	Osram - 60 W – 230 V/E27
Vermiculite	Klemens Rolfs, Siegburg (DE)

2.2.2. Chemicals

3-[(3-Cholamidopropyl) dimethylammonio]-1-propanesulfonate CHAPS	AppliChem, Darmstadt (DE)
Acetic Acid	AppliChem, Darmstadt (DE)
Acetone	VWR, Darmstadt (DE)
Agarose	PeQLab, Erlangen (DE)
Ammonium acetate	Carl Roth, Karlsruhe (DE)
Ammonium ferric citrate	Sigma-Aldrich, Taufkirchen (DE)
Ammonium nitrate NH_4NO_3	AppliChem, Darmstadt (DE)
Arabinose	Carl Roth, Karlsruhe (DE)
Bacto Agar	Formedium, Norfolk (UK)
Boric Acid H_3BO_3	AppliChem, Darmstadt (DE)
Calcium chloride dihydrate $CaCl_2$. $2H_2O$	AppliChem, Darmstadt (DE)
Chloroform CH_3Cl	VWR, Darmstadt (DE)
Cobalt (II) nitrate hexahydrate $Co(NO_3)_2.6H_2O$	ICN Biomedicals, Inc. (USA)
Copper (II) sulfate pentahydrate $CuSO_4$. $5H_2O$	Merck Millipore, Darmstadt (DE)
Diethyl ether	Fisher Chemicals, Thermo Fisher Scientific, Braunschweig (DE)
Dimethyl sulfoxide DMSO	Sigma-Aldrich, Taufkirchen (DE)
Dipotassium phosphate K_2HPO_4	Carl Roth, Karlsruhe (DE)
Ethanol	Merck Millipore, Darmstadt (DE)
Ethidium bromide	Serva, Heidelberg (DE)
Ethylenediaminetetraacetic acid (EDTA)	AppliChem, Darmstadt (DE)
Glucose unhydrous	Formedium, Norfolk (UK)
Glycerol	AppliChem, Darmstadt (DE)
HEPES	AppliChem, Darmstadt (DE)
IPTG	Formedium, Norfolk (UK)
Isopropanol	VWR, Darmstadt (DE)
LB-Broth Lennox low salt	Formedium, Norfolk (UK)
Linoleic acid (18:2)	Honeywell Fluka, Schwerte (DE)
Magnesium sulfate heptahydrate $MgSO_4$. 7 H_2O	AppliChem, Darmstadt (DE)
Manganese chloride $MnCl_2$	AppliChem, Darmstadt (DE)
Methanol	Fisher Chemicals, Thermo Fisher Scientific, Braunschweig (DE)
Monopotassium phosphate KH_2PO_4	Carl Roth, Karlsruhe (DE)
MS salts including vitamins	Duchefa, Haarlem (NL)
n-Hexane	Carl Roth, Karlsruhe (DE)
n-Hexane	Merck Millipore, Darmstadt (DE)
Octadecanol (18:0ol)	Sigma-Aldrich, Taufkirchen (DE)
Peptone	Formedium, Norfolk (UK)
Phytoagar	Duchefa, Haarlem (NL)
Phytol (natural isomer)	Chem-Impex International, Illinois (USA)

Primuline	Sigma-Aldrich, Taufkirchen (DE)
Silwet Gold	Spiess Urania, Hamburg (DE)
Sodium carbonate $NaCO_3$	Merck Millipore, Darmstadt (DE)
Sodium chloride NaCl	Duchefa, Haarlem (NL)
Sodium molybdate Na_2MoO_4	Merck Millipore, Darmstadt (DE)
Sodium nitrate $NaNO_3$	Carl Roth, Karlsruhe (DE)
Sodium Thiosulfate Pentahydrate $Na_2S_2O_3$. 5 H_2O	Sigma-Aldrich, Taufkirchen (DE)
Sucrose	Duchefa, Haarlem (NL)
TES buffer	AppliChem, Darmstadt (DE)
Thionyl chloride $SOCl_2$	Fluka, Gillingham (UK)
Tocopherol (α, β, γ,δ)	Sigma-Aldrich, Taufkirchen (DE)
Toluene	VWR, Darmstadt (DE)
Trisodium citrate dihydrate $Na_3C_6H_5O_7$. 2 H_2O	AppliChem, Darmstadt (DE)
Zinc sulfate $ZnSO_4$	Merck Millipore, Darmstadt (DE)
Yeast extract	Formedium, Norfolk (UK)
Linoleic acid 18:2	Fluka, Gillingham (UK)
Acyl-CoAs	Sigma-Aldrich, Taufkirchen (DE)
Acyl-ACP	Sigma-Aldrich, Taufkirchen (DE)
Vitamin B12	
Procamocarb hydrochloride (Proplant)	Arysta- Düsseldorf (DE)
Para-aminobenzoic acid	Duchefa Biochemie (DE)

2.2.3. Antibiotics

All the following antibiotics were obtained from Duchefa, Haarlem (NL):

Ampicillin, carbenicillin, gentamicin, kanamycin, rifampicin, spectinomycin, streptomycin, tetracycline and chloramphenicol

When cultivating bacteria, media were supplied with appropriate antibiotics for selection of positive clones (Table. 1)

Table. 1: Antibiotic concentration used for bacterial selection.
X1000 stocks were prepared from each antibiotic and dissolved in water unless otherwise was mentioned.

Antibiotic	Concentration µg/ml		
	E. coli	*A. tumefaciens*	*Synechocystis*
Ampicillin (Amp)	100		
Carbenicillin (Carb)	50	250	
Gentamicin (Gm)	10	25	
Kanamycin (Kan)	30	50	30
Rifampicin (Rif, in DMSO)		60	
Spectinomycin (Spec)	25	100	
Streptomycin (Strep)	25	300	
Tetracycline (Tet, in ethanol)	10		
Chloramphenicol (Cam, in ethanol)	25		

2.2.4. Kits and Enzymes

CloneJET PCR Cloning Kit	Thermo Fisher Scientific, Karlsruhe (DE)
DCS DNA Polymerase	DNA Cloning Service (DCS), Hamburg (DE)
dNTPs	DNA Cloning Service (DCS), Hamburg (DE)
High speed plasmid mini kit	DNA Cloning Service (DCS), Hamburg (DE)
Lysozyme	Sigma-Aldrich, Taufkirchen (DE)
NucleoSpin Gel and PCR Clean-up Kit	Macherey-Nagel, Düren (DE)
NucleoSpin Plasmid Kit	Macherey-Nagel, Düren (DE)
Q5® High-Fidelity DNA Polymerase	New England Biolabs, Frankfurt, (DE)
Restriction endonucleases and Buffers	New England Biolabs, Frankfurt, (DE)
Restriction endonucleases and Buffers	Thermo Fisher Scientific, Karlsruhe (DE)
RNase A	Boehringer Mannheim, Roche, Grenzach-Wyhlen (DE)
T_4 DNA Ligase	New England Biolabs, Frankfurt, (DE)
Color Prestained Protein Standard, Broad Range (11–245 kDa)	New England Biolabs, Frankfurt a. M. (DE)
GeneRuler 1kb DNA ladder	Thermo Fisher Scientific, Braunschweig (DE)
ECL prime western blot detection kit	Thermo Fisher Scientific, Braunschweig (DE)

2.2.5. Lipid Internal Standards

Pentadecanoic acid (15:0)	Sigma-Aldrich, Taufkirchen (DE)
17:0-Phytol	Synthesised in the IMBIO
DGDG mix	Larodan, Malmö (S)
MGDG mix	Larodan, Malmö (S)
di14:0-PC	Avanti, Alabaster (USA)
di20:0-PC	Avanti, Alabaster (USA)
di14:0-PE	Avanti, Alabaster (USA)
di20:0-PE	Avanti, Alabaster (USA)
di14:0-PG	Avanti, Alabaster (USA)
di20:0-PG	Avanti, Alabaster (USA)
di14:0-PA	Avanti, Alabaster (USA)
di20:0-PA	Avanti, Alabaster (USA)
di14:0-PS	Avanti, Alabaster (USA)
PI from soybean	Larodan, Malmö (S)
34:0-MGDG from spinach	Larodan, Malmö (S)
36:0-MGDG from spinach	Larodan, Malmö (S)
34:0-DGDG from spinach	Larodan, Malmö (S)
36:0-DGDG from spinach	Larodan, Malmö (S)
34:0-SQDG from spinach	Larodan, Malmö (S)

rac Tocol	Sigma-Aldrich, Taufkirchen (DE)
TAG Tri-17:0	Larodan, Malmö (S)
TAG Tri-17:1	Larodan, Malmö (S)
N-acyl-sphingosine-galactoside (d18:1-c12:0)	Avanti, Alabaster (USA)

2.2.6. Cyanobacteria, Bacteria and Plants

Cyanobacteria

Synechocystis sp. PCC6803

WT	Pasteur Institute (FR)
Δ*slr1807*	Derived from the WT in this study
Δ*slr2103*	Derived from the WT in this study

Bacteria

Escherichia coli

Electroshox	Bioline, Luckenwalde (DE)
BL21 (AI)	Thermo Fisher Scientific
Blastochloris viridis DSM No. 133	DSMZ German collection of Microorganisms and cell cultures, Braunschweig (DE)
Caldilinea aerophila STL-*6-O1*^{T}	DSMZ German collection of Microorganisms and cell cultures, Braunschweig (DE)
Agrobacterium tumefaciens GV3101-pMP90	DNA Cloning Service, Hamburg (DE)

Plants

Arabidopsis thaliana

WT Columbia-0 and Columbia-2 — Nottingham Arabidopsis Seed Collection (NASC)

Mutant	**Mutant line**	**Ecotype**	**Origen**
mgd1	GABI 080C05	Columbia-0	NASC
dgd1	R376	Columbia-2	Dörmann et al., 1995, Plant Cell

2.2.7. Vectors and Recombinant Plasmids

Table. 2: Cloning vectors used in this study

Vector	Description	Reference
pJET1.2	Amp^R in *E. coli*	Thermo Fisher Scientific
pBin-35S-Lnt-DsRed	Kan^R in *A. tumefaciens*	Dr. Georg Hölzl, IMBIO, University of Bonn, unpublished
pQE-80L	Amp^R in *E. coli*	Qiagen
pTrcI_1-T5I_2-VKan	Kan^R in *E. coli*	Dr. Georg Hölzel, IMBIO, University of Bonn, unpublished
pTrc-T5I_2-VKan	Kan^R in *E. coli*	Dr. Georg Hölzl, IMBIO, University of Bonn, unpublished
pACYC-31	Cm^R and Tc^R in *E. coli*	(Kelly et al. 2016)

Table. 3: List of PCR products

The corresponding primers and the restriction sites are mentioned. All these PCR products were cloned first in the cloning vector pJET1.2 before transfer into the expression vector or deletion constructs

Insert *	Cloning restriction enzymes	Primers	source
slr1807	*Xba*I/*Xho*I	bn3230/bn3231	*Synechocystis*
slr2103	*Sac*I/*Pst*I	bn3268/bn3269	*Synechocystis*
BviMgdP (WP_055038454)	*Spe*I/*Sca*I	bn2874/bn2875	*B. viridis*
BviMGDN (WP_055036643)	*Xba*I/*Xho*I	bn2873/bn2696	*B. viridis*
CaeMgdS (CLDAP_04530)	*XbaI*/*Xho*I	bn3069/bn2993	*C. aerophila*
CaeDgdS (WP_014434037)	*Xba*I/*Sma*I-*Bam*HI	bn2994/bn2995	*C. aerophila*
BviGlcADS (BV133_371)	*XbaI/BamHI*	bn2577/bn2578	*B. viridis*
5'- slr2103	*-/NcoI*	bn2263/bn2264	*Synechocystis*
3'- slr2103	*MluI/-*	bn2265/bn2266	*Synechocystis*
nptII (Kan)	*MluI/NcoI*	bn1116/bn1117	pTrcHisC (Invitrogen)
5'- slr1807	*-/NcoI*	bn2259/bn2260	*Synechocystis*
3'- slr1807	*MluI/-*	bn2261/bn2262	*Synechocystis*

* The templates of these inserts are the genomic DNA of the corresponding organism with the exception of nptII which was amplified from an expression vector

Table. 4: List of recombinant Plasmids used in this study

Construct	Description	Stock
pQE80L-slr2103	Expression in *E. coli* BL21 (AI)	bn1361
pACYC-slr1807	Expression in *E. coli* BL21 (AI)	bn1362
pTrc-T5-BviMgdP-VKan*	Expression in *E. coli* BL21 (AI)	bn1363
pTrc-CaeDgdS-VKan	Expression in *E. coli* BL21 (AI)	bn1364
pTrc-T5-CaeMgdS-VKan	Expression in *E. coli* BL21 (AI)	bn1365
pTrc-CaeDgdS-T5-CaeMgdS-VKan	Expression in *E. coli* BL21 (AI)	bn1366
pTnV-Trc-BviGlcADS	Expression in *E. coli* BL21 (AI)	bn1367
pBin-35S-Lnt-BviMgdP-DsRed*	Expression in *A. thaliana*	bn1159
pJ-Δslr2103-kan	Deletion of slr2103 in *Synechocystis*	bn937
pJ-Δslr1807-kan	Deletion of slr1807 in *Synechocystis*	bn936

*These plasmids were cloned by Dr. Georg Hölzl (University of Bonn; unpublished). The other plasmids were cloned in this study.

The two plasmids pTrcI_1-T5I_2-VKan and pTrc-T5I_2-VKan are derived from the vector pTrcHisC (Invitrogen). They were modified by Dr. Georg Hölzl by deletion of the ampicillin resistance gene and addition of a sequence containing the leaky T5 promoter followed by a multiple cloning site to make the plasmids suitable for single expression (pTrc-T5I_2-VKan) or co-expression of two genes (pTrcI_1-T5I_2-VKan) (Hölzl et al. 2005a; Semeniuk et al. 2014). The BviMgdN gene was released from pJET1.2 with (*XbaI/Xho*I) and ligated into pTrc-T5I_2-VKan (*SpeI/SalI*). The BviMgdP gene was released from pJET1.2 with (*SpeI/ScaI*) and ligated into pTrc-T5I_2-VKan (*SpeI/ScaI*). For double expression, BviMgdN (*XbaI/Xho*I) and BviMgdP (*SpeI/ScaI*) were cloned in pTrcI_1-T5I_2-VKan in two steps. (Hölzl, unpublished).

The plasmid pBin-35S-Lnt-DsRed is derived from the vector pBinGlyRed1 (Edgar Cahoon, University of Nebraska). The glycinin promoter was deleted and replaced by the 35S promoter (*BamHI/MluI*). The N-terminal leader sequence of MGDS from *Nicotiana tabacum* (Lnt), which targets proteins to the inner envelope of the chloroplasts, was fused into the (*MluI*/*XbaI* sites, as an N-terminal signal sequence to BviMgdP (*XbaI*/*XhoI*). Thus, BviMgdP was targeted to the inner envelope of the chloroplast.

2.3. Methods

2.3.1. Methods in Molecular Biology

2.3.1.1. Isolation of the Genomic DNA

To isolate the genomic DNA from cyanobacteria or other bacteria, 1 ml of either cyanobacterial culture (OD_{750}: 1) or other bacterial culture (OD_{600}: 0.6) was harvested in a 1.5 ml micro-centrifuge tube by centrifuging with maximal speed for 1 min. The supernatant was discarded, and the pellet was frozen in liquid nitrogen. For *Arabidopsis* DNA isolation, one fresh leaf was placed in a 1.5 ml micro-centrifuge tube containing small ceramic beads. The leaf was frozen in liquid nitrogen and directly ground to powder using the Precellys homogenizer. 1 ml of CTAB buffer was added and the sample was incubated while shaking at a temperature of 65˚C for 20 min. Thereafter, 0.4 ml chloroform was added, and the sample was mixed thoroughly and centrifuged for phase separation at 3000 rpm for 5 min. The upper (aqueous) phase was subsequently transferred to fresh tubes and 0.7 ml isopropanol was added, the sample was mixed gently and put on ice for 10 min to precipitate the DNA. The DNA was harvested at 14000 rpm for 5 min and washed with ice cold 75% ethanol. At the end, 25 µl ddH_2O was added to dissolve the extracted DNA and the DNA was stored at -20˚C.

CTAB Buffer

CTAB	0.8% w/v
EDTA	22 mM
NaCl	800 mM
Sorbitol	140 mM
Tris –HCl pH 8	220mM

2.3.1.2. Mini Plasmid DNA Preparation from *E. coli*

Plasmids were isolated by centrifugation of 2 ml of an overnight *E. coli* liquid culture in a 2 ml micro-centrifuge tube. The supernatant was discarded, and the tube was dabbed on filter paper to remove as much as possible of the medium. The pellet was suspended later in 200 µl of BF buffer and 10 µl of lysozyme (20 mg/ml). The mixture was incubated at 95˚C for 1 min and placed on ice for another 1 min. The sample was centrifuged at 14000 rpm for 20 min and the supernatant was transferred to a fresh tube containing 480 µl of IS mixture for DNA precipitation. The mixture was inverted gently several times and then centrifuged for 12 min. The pellet was washed with 75% v/v ethanol. The ethanol was entirely removed, and the dried DNA was dissolved in 80 µl ddH_2O/RNase A (1 µl 10 mg/ml RNase A in 100 µl water). For sequencing, the plasmid DNA was isolated by using special kits (NucleoSpin Plasmid Kit) as required according to the manual.

BF Buffer		**IS Mixture**	
Sucrose	8% w/v	Isopropanol	400 µl
Triton X-100	0.5%	Ammonium acetate 5 M	80 µl
EDTA, pH 8	50 mM		
Tris–HCl pH 8	10 mM		

2.3.1.3. Polymerase Chain Reaction PCR

DNA fragments were amplified by polymerase chain reaction (PCR) including denaturation at 95˚C to separate the double DNA strain into two single strains, then the annealing step between 50 – 56˚C depending on the primers. Normally, the melting temperature (T_m) of the primers is calculated by adding 4˚C for each G or C and 2˚C for T and A. The annealing temperature is calculated as 4˚C less than the lowest melting temperature of the used primers. The final step is the extension at 72˚C by means of a heat stable DNA polymerase. PCR was followed by visualizing the DNA bands by agarose gel electrophoresis to confirm the size of the amplified DNA product (see below).

PCR was used in this study for the following purposes:

- **Amplification of bacterial ORFs or flanking regions** for cloning purposes. Q5 DNA polymerase was used here. Q5 polymerase was not added to the PCR master mix. Instead, it was added to the PCR later when the reaction had reached 95˚C to reduce the error rate. The reaction mixture and the PCR programme are shown in Table 5 and 6

Table. 5: Q5 polymerase reaction mixture

DNA	1.0 µl
Q5 DNA Polymerase	0.5 µl
X5 Q5 reaction buffer	10 µl
dNTPs (10mM)	1.0 µl
Forward primer (10 pmol/µl)	1.5 µl
Reverse primer (10 pmol/µl)	1.5 µl
Nuclease free dd-water	up to 50 µl

Table. 6: Q5 polymerase PCR programme

98˚C	30 sec	
98˚C	10 sec	X35
T_m - 4˚C	30 sec	
72˚C	30 sec/Kb	
72˚C	2 min	
5 -10˚C	5 min	

- **Genotyping of *Synechocystis* mutants** which were generated by disrupting the gene of interest by inserting an antibiotic resistance cassette in the wild type genome. A set of four primers was used to screen for mutants. Two of them bind in the resistance cassette at the 5' or 3' ends, and the other two bind in the flanking genomic sequences, one primer in each flanking region. PCR products were produced from one genomic primer and one cassette primer. Perceptibly, no PCR product will be produced with genomic DNA as a template. Oligonucleotide sequences are listed in 7.1.

Table. 7: DCS *Taq* polymerase reaction mixture

DNA	1.0 µl
DCS *Taq*-Polymerase	0.2 µl
Buffer B (X10)	1.5 µl
$MgCl_2$ (25mM)	1.5 µl
dNTPs (10mM)	0.3 µl
Forward primer (10 pmol/µl)	1.5 µl
Reverse primer (10 pmol/µl)	1.5 µl
Water	Up to 15 µl

Table. 8: DCS *Taq* polymerase PCR programme

95˚C	1 min	
95˚C	10 sec	X35
T_m - 4˚C	30 sec	
72˚C	1 min/kb	
72˚C	2 min	
15˚C	5 min	

- **Genotyping the *Arabidopsis mgd1* T-DNA insertion mutant**:

  The T-DNA insertions provide a way to screen for mutant alleles using PCR. PCR products were generated using a group of three primers. One primer binds up-stream of the insertion site in the genome. Other primer binds down-stream in the genome and the third primer binds in the insertion sequence. As a result, One PCR fragment was generated using the two genomic primers for the WT alleles. Other PCR fragment was generated using one genomic primer and the insertion primer for the homozygous mutant alleles. Accordingly, heterozygous mutant alleles gave two different PCR products one for the WT alleles and one for the mutant alleles. More details are shown in 3.14 PCR reaction mixture and programme are similar to ones indicated in Table 7 and 8.

- **Colony PCR:** A single colony of *E. coli* was grown overnight on an LB plate supplied with a specific antibiotic was used as template for this PCR. The colony was directly added to the PCR reaction mix. The presence of PCR product ensures that the cells contain the cloned insert in the vector. Primers were chosen so that one primer binds

to the insert sequence and the other primer binds to the vector. PCR reaction mixture and programme are also similar the ones indicated in Table 7 and 8 with 5 min instead of 1 min at 95˚C to allow the high temperature to break the cell wall.

2.3.1.4. Agarose gel-electrophoresis

The PCR products were separated on 1% (w/v) agarose gels by gel-electrophoresis. Conventional agarose gels were prepared by mixing agarose powder with 1 x Tris-acetate-EDTA (TAE) buffer and adding 2.5 µg/ml of ethidium bromide (EtBr). The gels were melted by heating and poured in a tray with a plastic comb. The PCR products or fragments derived from vector digestion were visualized on the gel under UV light. DNA samples were mixed with 6x DNA loading dye and were loaded on the gel. Electrophoresis was carried out at 120 V in 1 x (TAE) buffer for about 40 min. The DNA fragment sizes were determent by loading the GeneRuler 1kb DNA ladder.

50x TAE Buffer

Tris	2 M
Acetic acid	1 M
EDTA, pH 8	50 mM

Ethidium bromide stock solution 10 mg/ml in ddH_2O

6x Gel- loading buffer

Tris-HCl pH 7.6	10 mM
Glycerol	60% (v/v)
EDTA pH 8.0 NaOH	60 mM
Bromophenol blue	0.03% (w/v)
Xylene cyanol FF	0.03% (w/v)

2.3.1.5. Purification of PCR Products

The purification of PCR products from agarose gel was carried out by NucleoSpin Gel Kit or PCR Clean-up Kit according to the manual. The purified DNA was either directly used or was stored at – 20°C.

2.3.1.6. Sequencing

The inserts of some expression constructs were sequenced to make sure that no errors occurred during PCR or cloning. Highly purified vector DNA was isolated from the cells via kits (NucleoSpin Plasmid Kit) or purified from agarose gels as indicated above. Fragments were sequenced according to the manuals of the sequencing companies. The sequence files were analysed using FinchTV 1.4.0 (Geospiza, Inc.; Seattle, WA, USA; http://www.geospiza.com).

2.3.1.7. Control Digestion of DNA Plasmids

The strategy of control digestion is based on the ability of the restriction enzymes to cleave the DNA sequence at specific restriction sites. This strategy is used to quickly verify the success of the cloning strategy of plasmids. The goal of control digestion is to diagnose plasmids by cutting them into specific fragments. To this end, two or more restriction enzymes were selected to digest the plasmids according to the supplier's instructions in a total reaction volume of 10 µl. The resulting fragment patterns on the agarose gel indicate if the plasmid contains the expected fragment or not. The software Clone manager professional suit version 8 was used to determine the fragments sizes.

2.3.1.8. Ligation

The purpose of ligation is to ligate the inserted DNA to the digested vector backbone. The reaction is performed by the T4 DNA ligase. The concentrations of the insert and vector were estimated by the intensity of the bands on agarose gels (2.3.1.4). The ligation reaction took place in a reaction with a total volume of 10 µl mixture containing 0.5 µl T4 DNA ligase (4000 units/µl) and 1 µl of 10x T4 DNA ligase buffer containing ATP in addition to a vector and an insert in a molar ratio of 1:3. Thereafter, the reaction was incubated for 10 to 30 min at RT or overnight at 4°C. Then, the mixture was desalted for 2 h on micro dialysis membranes floating on ddH2O, and was either used directly or was stored at -20°C.

2.3.1.9. SDS Polyacrylamide Gel Electrophoresis (PAGE)

Sodium dodecyl sulphate-polyacrylamide gel electrophoresis (SDS PAGE) is a commonly used method for the separation of proteins according to electrophoresis mobility. To separate protein under electric field based on their molecular weight, proteins must be denaturized to their linear form. SDS as a detergent, β-mercaptoethanol as a reduction agent and high temperature were used to damage the tertiary structure of the protein. This damage brings the proteins from the folded to the linear form. Moreover, SDS will coat the protein with a homogenized negative charge, allowing to migrate through the polyacrylamide matrix and to separate according to the molecular weight. The protein samples were prepared by suspending 1 ml pelleted bacterial culture in 4x Laemmli buffer. This solution was heated at 95°C for 5 min to denature the protein (Laemmli 1970). The gel was prepared with 4% (w/v) acrylamide for stacking gel and 12% (w/v) for separating gel as shown below. Ammonium persulfate (APS) and tetramethylethylenediamine (TEMED) were added to the other ingredients directly before pouring the gel to start the polymerisation. Separation gel was sandwiched between a glass plate and an alumina plate. To flatten the upper rim of the stacking gel, isopropanol was added on top. After 30 min, the separation gel was polymerised. At this point, the isopropanol was completely removed and the

polymerisation of the stacking gel was initiated by adding APS and TEMED. Slots were structured by inserting plastic combs in the liquid stacking gel and another 30 min were required for polymerisation. The gel was placed in the gel chamber filled with running buffer (Tris 125 mM, glycine 960 mM, SDS 0.5% (w/v)). After loading the denatured samples, 25 mA per mini gel (8 x 8 cm) and 200 V was applied until the dye reached the separation gel. After that, the current was increased to 30 mA and let run for approximately an hour.

5x Laemmli buffer

Tris-HCl pH 6.9	500 mM
SDS	10% (w/v)
Glycerol	50% (v/v)
Bromophenol blue	0.03% (w/v)
EDTA	5 mM

4x Laemmli buffer was prepared by adding 50 µl β-mercaptoethanol and 50 µl ddH_2O to 400µl 5x Laemmli buffer.

Stock solution	4% Stacking gel	12% Separating gel
40% Acrylamide/bisacrylamide 29:1 (v/v)	1 ml	6.25 ml
0.5 M Tris-HCl pH 6.8	2.5 ml	6.25 ml
SDS 10% (w/v)	100 µl	250 µl
ddH_2O	6.3 ml	12.1 ml
TEMED	5 µl	10
APS 10% (w/v)	100 µl	150 µl

To visualize the protein bands, the polyacrylamide gel was stained with Coomassie Brilliant Blue R250 (Diezel et al. 1972). The separating gel was soaked in staining solution which was placed in a microwave oven until the solvent started to boil. Then, the gel in the staining solution was gently shaken for 5 min. Subsequently, the gel was washed several times with water to remove the alcohol and the acid. Finally, the gel was washed with destaining solution.

Staining solution		**Destaining solution**	
Ethanol	50% (v/v)	Glycerol	5%(v/v)
Acetic acid	7%(v/v)	Acetic acid	7.5%(v/v)
Coomassie Brilliant Blue R250	0.252(w/v)		

2.3.1.10. Western Blot and Immuno-detection

To detect specific proteins after gel electrophoreses, proteins were transferred from the gel onto a nitrocellulose membrane following the method described by Towbin et al. 1979. The

transfer was performed by semi-dry blotting using protein Towbin blot transfer buffer. To this end, blotting papers and nitrocellulose membrane were shaped in the size of the protein gel and they were soaked in Towbin transfer buffer. An assemblage was prepared as three sheets of the blotting paper, the nitrocellulose membrane, the polyacrylamide gel containing the protein and other three sheets of the blotting paper. The cathode was placed on top and the protein was transferred to the nitrocellulose membrane by blotting at a constant voltage of 15 V and 70 mA per mini gel for 60 min. After that, the nitrocellulose membrane was incubated with the blocking solution (2% bovine serum albumin (BSA) in TBSTXSB buffer) and was gently shaken for an hour in room temperature. Later on, the His-tagged proteins was bound by incubating the blocked membrane in the HisDetector Nickel-HRP conjugate (1:20 000 dilution in the blocking solution) for an hour in room temperature with gentle shaking. The membranes were washed 3x times with TBSTXSB buffer by incubating for 10 min. In between the membrane was rinsed with distilled water. The blots were developed with the ECL prime western blot detection kit (Thermo Fisher Scientific). The substrate for the horseradish peroxidase (HRP) was added to the membrane and the activity of protein binding was detected as dark bands by the chemiluminescence documentation system (Bio-Rad).

Towbin Transfer Buffer

Tris base	25 mM
Glycine	192 mM
Methanol	20% (v/v)
SDS	0.1% (w/v)

TBSTXSB buffer

Tris-HCl pH 8	10 mM
NaCl	155 mM
Triton X-100	0.01% (v/v)
SDS	0.75 mM
BSA	15.5 mM
Thimerosal	250 mM

2.3.1.11. Protein Quantification

Based on the method described by Smith et al. 1985, the total protein concentration was measured with the bicinchoninic acid (BCA) assay. To this end, 200 µl of 1:100 diluted protein extract was mixed with 200 µl freshly prepared BCA reagent. The mixture was heated to 60˚C for 15 min until the pink colour appeared. Then, the optical density at 550 nm was recorded with the Nano drop photometer and the protein concentration calculated automatically by the NanoDrop 1000 version 3.8.1 software, based on defined standard curves with bovine serum albumin (BSA).

BCA reagent

BCA solution: $CuSO_4$ (4% w/v) 50: 1

2.3.2. Cultivation and Transformation of Organisms

2.3.2.1. Cultivation and Transformation of *Escherichia coli*

Escherichia coli (E. coli) was cultivated in liquid or on solid Luria-Bertani (LB) medium (concentration of medium: 20 g/l). The cultures were incubated at 37°C with shaking 180 rpm. 1.5% (w/v) of bacto agar was added to LB medium for cultivation on plates. Both liquid and solid media were supplied with the appropriate antibiotic (Table 1). To transform *E. coli* cells via electroporation, 50 µl of competent cells were placed on ice for ca. 10 min and were then mixed with 2 to 5 µl purified plasmid DNA. The mixture was placed on ice for 5 min, then it was transferred to a precooled electroporation cuvette. After that, the cells were shocked with a pulse of 1800 V, and were suspended with 600 µl LB medium. Thereafter, the cells were incubated for 1 hour at 37°C for regeneration. Finally, the cells were spread on an LB plate and were incubated overnight at 37°C. A single colony was picked for protein expression.

2.3.2.1.1 Recombinant Protein Expression in *Escherichia coli*

4 ml of liquid LB medium, supplemented with appropriate antibiotic, was inoculated with a single colony containing the expression plasmid(s) and incubated at 37°C with a shaking rate of 180 rpm overnight. After that, the 2 ml of the pre-culture was used to inoculate the main culture (100 ml fresh LB medium) and it was grown under the same conditions. When the culture reached an OD_{600} of 0.6, it was cooled down and the expression of the protein was induced with 0.5 mM IPTG. In addition to IPTG, 0.1% (w/v) arabinose was used for induction of the T7 RNA polymerase under control of the araBAD promoter, when the BL21-AI strain was used for expression (Narayanan et al. 2011). The culture was incubated at 37°C for 4h or at 16°C overnight. Finally, the cells were used for feeding assays, protein or lipid extraction, or they were pelleted by centrifugation and stored at -20°C.

2.3.2.1.2 Feeding of *Escherichia coli* with Lipids

Protein expression in different cultures of *E. coli* BL21 (AI) containing different expression constructs (single and co-expression of slr1807 and slr2103 or empty vector) was induced as indicated above. The next morning, the incubation temperature was raised from 16 to 30°C and 0.1% (v/v) phytol with or without detergent (0.1% w/v CHAPS) was added to the cultures. For the TAG feeding assay a mixture of 30 µM of each of the two diacylglycerols, dioctanoin (di-8:0 DAG) and dipalmitin (di-16:0 DAG) dissolved in a small volume of toluene, and then 0.1% (w/v)

CHAPS were added to the *E. coli* cultures expressing the acyltransferase slr2103. Thereafter, the cultures were incubated at 30°C for 3h at 180 rpm shaking. The OD_{600} was determined for calculating cell density, and cells were harvested by centrifugation. The pellets were washed with water two times before the lipid extraction (2.3.3.1).

2.3.2.1.3 Enzyme Assay with Recombinant BviMgdP Proteins

E. coli BL21 (AI) expressing BviMgdP were grown and the expression of the protein was induced as described (2.3.2.1.1). The cells in 50 ml of the culture were collected by centrifugation at 1000 g for 12 min and the pellet was re-suspended in ice cold assay buffer 1 (4% of original volume of the culture). All steps after suspension were performed on ice. The suspension was distributed in 2 ml Precellys tubes with screw caps containing glass beads and the cells were disrupted with the Precellys homogenizer ten times at 6500 rpm for 10 sec. Thereafter, the suspension was combined and centrifuged at 4000 g for 5 min to remove cell debris. The supernatant was transferred to a fresh 2 ml tube and the protein concentration was determined by the BCA assay (2.3.1.11).

Enzyme assays for BviMgdP activity were performed in a final volume of 100 µL containing 200 µg of the crude protein extract, 1 mM UDP-galactose, 50 nmol of di18:2 DAG in ethanol in buffer 1. The reaction was incubated at 30°C for 1 h. The reaction was stopped by adding 1 ml of chloroform/methanol (2:1) and lipids were extracted and purified. Finally, lipids were analysed with Q-TOF MS/MS as described.

Assay buffer 1:

Tris-HCl, pH 8	50 mM
Glycerol	7% (v/v)

2.3.2.1.4 Assay with Recombinant slr2103 and/or slr1807 Proteins

The enzyme assay was performed after modification according to (Ischebeck et al. 2006) and (Patwari, 2019). To this end, *E. coli* cells expressing either slr2103 or slr1807 were grown and the protein expression was induced as indicated in (2.3.2.1.1). An aliquot of 1 ml of the culture was removed to analyse the protein expression by SDS-PAGE and western blot. The rest of the culture was spun down by centrifugation at 1000 g for 12 min and the pellet was washed with the homogenization buffer. All steps after the washing step were performed on ice. The pellet was suspended in 4 ml of the homogenization buffer and distributed into four fresh Precellys tubes with screw caps containing glass beads. The cells were homogenized in a Precellys homogenizer (6500 rpm x 1sec x 10 times) and combined afterwards. The suspension was centrifuged at 4000 g for 2 min to remove cell fragments. After that, the supernatant was centrifuged at 35,000 g for 45 min to obtain the microsomal membrane fraction. The protein concentration was measured as

described in (2.3.1.11). The microsomal membrane fraction was supplied with substrates including acyl-CoA, DAG or phytol to measure the acyltransferase activity. To this end, a final reaction of 200 µl total volume including the assay buffer, 50 µM acyl-CoA , 200 µM fatty alcohol (phytol) or DAG, dissolved in ethanol and 400 µg protein extract (microsomal fraction) were mixed and incubated for 20 min at 35˚C. The reaction was terminated by adding 1 ml of chloroform/methanol (2:1) and lipids were extracted and purified. Finally, lipids were analysed with Q-TOF MS/MS as described.

Homogenization buffer:

EDTA	1 mM
Sucrose	200 mM
Tris-HCl, pH 7.4	100 mM

Assay buffer:

$MgCl_2$	20 mM
CHAPS	0,1%
Tris-HCl, pH 7.4	100 mM
Bovine serum albumin (BSA)	1,25 $mg.ml^{-1}$
Sodium orthovanadate	10 mM

2.3.2.2. Cultivation and Transformation of *A. tumefaciens*

A. tumefaciens cells were grown in liquid or on solid YEP medium supplied with antibiotics (Table 1). The cells were incubated at 28°C for two days. The liquid culture was shaken at 180 rpm during the incubation. The transformation of *A. tumefaciens* cells was carried out as described above for *E. coli*, but using YEP medium instead of LB. The agrobacterial cells were harvested by centrifugation for 20 min at 4000g.

YEP medium

Peptone	10 g/l
Yeast extract	10 g/l
NaCl	5 g/l
Agar	15 g/l
pH 6.8	

2.3.2.3. Generation of Electro-Competent Bacterial Cells

E. coli or *A. tumefaciens* cells were grown from frozen glycerol stocks as a pre-culture in 20 ml SOB medium containing the suitable antibiotics (Table 1). 400 ml of SOB medium was inoculated with the pre-culture, and was incubated on 37 or 28°C for *E. coli* or *A. tumefaciens,* respectively until OD_{600} 0.5. The culture was cooled on ice for 30 min before it was centrifuged 4000 g at 4°C for 10 min. The pellet was suspended with 50 ml of pre-chilled 1mM HEPEs buffer. Then the cells

were harvested by centrifugation and washed three times with 250, 100 and 50 ml of pre-chilled sterile water. After that, the supernatant was decanted and the pellet was suspended one time in 20 ml pre-cooled sterile 20% glycerol and after a second round of decanting, another time with 2 ml 10% ice-cold glycerol. Then, 50 µl of the cells were aliquoted in 1.5 ml tubes. Finally, the tubes were frozen in liquid nitrogen and then either used directly or stored at -20°C.

SOB medium

Peptone	20 g/l
Yeast extract	5 g/l
NaCl	0.6 g/l
KCl	0.18 g/l
$MgSO_4$ 1 M	2 ml*
$MgCl_2$ 1 M	2 ml*

* Add after autoclaving

2.3.2.4. Cultivation of *Synechocystis* sp. PCC 6803

Synechocystis was cultivated photomixotrophically in liquid and on solidified BG-11 medium (Stanier et al. 1979). Mutated strain cultures were supplied with 30 µg/ml kanamycin. A pre-culture of 50 ml was inoculated from a plate with inoculation loop and was incubated at 28°C in incessant light with an intensity of 30 $\mu mol.m^{-2}.s^{-1}$ until the cells reached the exponential phase (~3 to 4 days) at an approximate optical density (OD_{750}) of 0.6. For experiments (growth curves and measuring lipids), cells were grown in batch cultures using Erlenmeyer flasks. To this end, 100 mL BG-11 medium in a 250 ml glass Erlenmeyer flask was inoculated with 1 ml from the pre-culture and was the cells grown at the same conditions for 7 to 11 days depending on the desired final growth phase (Singh and Sherman 2006). Finally, the OD_{750} was determined. Cultures were subjected to the stress by either incubating in dark combined with 0.5 M NaCl in BG-11 for three days, or they were harvested by centrifugation and were transferred to BG-11 lacked nitrogen (BG-11-N) and the cells grown for 5 days.

BG-11 Medium	Volume ml/l	Stock solution g/l
$MgSO_4$ x $7H_2O$	10	7.5
$CaCl_2$ x $2H_2O$	10	3.6
Na_3-citrate x $2H_2O$	10	0.6
Na_2-EDTA x $2H_2O$ pH 8	10	0.1
Trace metal mix	1	-
$NaNO_3$*/**	5	300
BG-11 mix*	1	-
Vitamin B12*	1	0.02
TES buffer pH 8.2 (NaOH)*	10	229.25
Glucose *	5	180.6

BG-11 mix		
K_2HPO_4 x $3H_2O$	2 0 g/l	
Na_2CO_3	10 g/l	
Fe-NH_4-citrate	3 g/l	
Trace Metal Mix		
H_3BO_3	2,86 g/l	
$MnCl_2$ x 4 H_2O	1,81 g/l	
$ZnSO_4$ x $7H_2O$	0,22 g/l	
Na_2MoO_4 x $2H_2O$	0,39 g/l	
$CuSO_4$ x $5H_2O$	0,0079 g/l	10 ml from 0.8 g/100ml Stock Sol.
$Co(NO_3)_2$ x $6H_2O$	0,0494 g/l	10 ml from 0.5 g/100ml Stock Sol.
Phytoagar	8 g/l	(autoclaved separately)

* Add after autoclaving

** It was omitted in the case of BG-11-N medium

Synechocystis cells were maintained on BG-11 agar plates under the same conditions mentioned before and they were re-streaked every 15 to 20 days on fresh plates. For long term preservation, 10 ml of the *Synechocystis* culture were concentrated in one ml fresh medium and 1 ml of 90% (v/v) sterile glycerol was added. The cells and glycerol were mixed gently and frozen in liquid nitrogen, then stored at -80°C. *Synechocystis* stocks have to be renewed every 6 months.

2.3.2.4.1 Generation of *Synechocystis* Δ*slr2103* and Δ*slr1807* Deletion Mutants

Synechocystis is spontaneously transformable. Foreign DNA can naturally be integrated into its genome by double-homologous recombination. This specific characteristic was used to generate deletion mutants of slr1807 and slr2103, to understand the functional *in vivo* role of the two genes (Figure 2.1). To this end, the upstream sequences (5') of the slr1807 and slr2103 genes were amplified from the genomic DNA of *Synechocystis* using the primer pairs bn2259/bn2260 and bn2263/bn2264, respectively (bn2260 and bn2264 contain an *NcoI* site). Both sequences were cloned into pJET1.2 (pJ-5'-slr1807 and pJ-5'-slr2103). In a similar way, the downstream sequences (3') of the two genes were amplified using the primer pairs bn2261/bn2262 for 3'-slr1807 and bn2265/bn2266 for 3'-slr2103 (bn2261 and bn2265 harbour an *MluI* site) and cloned in pJET1.2. (pJ-3'-slr1807 and pJ-3'-slr2103) (Figure appendix 7.1). The nptII gene which is the kanamycin resistance cassette (Kan^R) was amplified using the oligos bn1116 and bn1117 containing *MluI* and *NcoI* sites. The Kan^R cassette was also cloned in the pJET1.2 (pJ-nptII). The 5' flanking sequences from the two genes and the nptII gene were released using *NcoI*/*HindIII* and *NcoI* (partial digestion)/*MluI*, respectively. The two fragments were ligated in one step into the vector pJ-3'-slr1807 or pJ-3'-slr2103 (opened with *MluI*, *HindIII*). The resulted knock-out constructs pJ-Δslr1807-kan and pJ-Δslr2103-kan (Figure appendix 7.3) were transferred to the

glucose tolerant *Synechocystis* (2.3.2.4.2). Complete segregation for both mutant lines was accomplished by re-streaking the cells on antibiotic containing medium several times to eliminate the WT copies. The purity of homozygous lines was confirmed by genotyping via PCR (Figure 3.6).

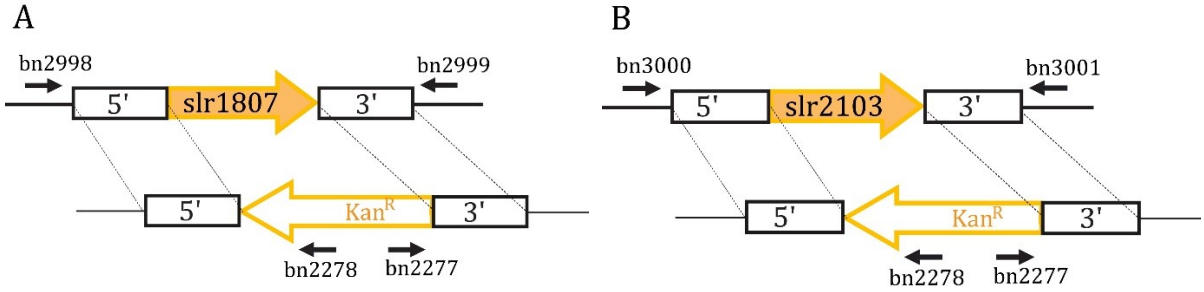

Figure 2. 1: Insertional deletion of the genes slr1807 and slr2103.
(A) Hydrolase-like sequence slr1807. **(B)** Acyltransferase- like sequence slr2103. The mutants were generated by double homologous cross over recombination. Boxes with 5' and 3' indicate the up and downstream flanking sequences, which were used for homologous recombination. A kanamycin cassette (arrow with Kan^R) was inserted into slr1807 and slr2103. Primers which were used to identify the two mutants are indicated by small black arrows.

2.3.2.4.2 Stable Transformation of *Synechocystis*

Synechocystis cells were transformed to generate deletion mutants by homologous recombination where the target genes were replaced with an antibiotic resistant cassette. The transformation protocol was a modified version based on the protocol described by Proels, 2014. Under sterile working conditions, 15 ml of a fresh *Synechocystis* culture was concentrated into 5 ml of fresh BG-11 medium. The concentrated culture was directly used for transformation; thus 1 ml of the culture was transferred to 2 ml micro-centrifuge tubes. Thereafter, 10 µg of circular plasmid DNA containing the desired construct was added to four micro-centrifuge tubes and the remaining one was used as a negative control. The tubes were mixed gently, and they were incubated still in the dark at 28°C for 24h. After dark incubation, 50, 100, 200 µl of each tube were platted on antibiotic-free BG-11 medium and were incubated under culturing conditions (2.3.2.4) for two or three days when the small colonies start to appear. Afterwards, an increasing concentration of kanamycin (Kan) was delivered to the cells until a maximum concentration of 15 µg/ml. To this end, the agar was lifted with a sterilized spatula and 1 ml of 15 µg/ml Kan was injected under the lifted agar onto the bottom of the petri dish. Then, the plates were sealed with gas permeable tape to avoid evaporation and were incubated. The antibiotic was gradually absorbed into the agar. The colonies started to appear in two to three weeks. By then, single colonies were picked and transferred to fresh BG-11 plates contains 15 µg/ml Kan. The plates were incubated and resulting colonies were frequently re-streaked on BG-11 plates containing increasing concentrations (20, 25 and 30 µg/ml) of kanamycin.

To ensure a complete segregation, the mutated cells were streaked on 30 µg/ml Kan BG-11 plates once every two weeks for five rounds. The success of the genomic integration in the cells

was confirmed by PCR as will be shown later (Chapter 3). Positive clones were maintained as mentioned in (2.3.2.4).

2.3.2.4.3 Feeding of *Synechocystis* with Phytol

WT and mutated strains were fed with natural phytol to detect an increase in the phytyl ester content in *Synechocystis*. The feeding process was simply accomplished by adding 0.1% (v/v) phytol (3.37 mM) to 100 ml *Synechocystis* culture. The culture was incubated under normal growth conditions for 12h. Then the cells were harvested and the pellet was washed 2 times with BG-11 medium, frozen in liquid nitrogen and either stored at -80°C or prepared for lipid extraction (2.3.3.1).

2.3.2.4.4 Spotting Assay

The sensitivity of *Synechocystis* WT and the mutated lines towards stress such as nitrogen starvation was tested. Pre-cultures were grown under the above-mentioned growth conditions until OD_{750} of 0.6. Then the culture was diluted with antibiotic free BG-11 to OD_{750} of 0.2 in a final volume of 25 ml. The culture was grown and freshly diluted to an OD_{750} of 0.2 one more time. Further, a series of 10fold dilutions of up to $1:10^6$ were prepared using a multichannel micropipette. Afterwards, 5 µl of each dilution was spotted on BG-11 plates with or without nitrogen source. The cell drops were let to dry, and the plates were incubated under a light source until no more colonies appeared (almost 2 weeks).

2.3.2.4.5 Growth Curves

Synechocystis growth curves in this study were recorded based on cultures which were grown at the same time and under the same conditions in triplicates. The first OD_{750} measurement of each culture was taken directly after adding phytol to the samples. Then the OD_{750} was measured every 12h. The experiment was repeated twice.

2.3.2.5. Techniques for Working with *Arabidopsis thaliana*

2.3.2.5.1 *Arabidopsis thaliana* Seed Surface Sterilization

The germination of the seeds was carried out under strictly sterile conditions to avoid contamination on the growth medium. Therefore, the surface of the seeds was sterilized before they were plated out. Selected seeds from all lines were collected in 1.5 ml centrifugation tubes and 1 ml of sterilisation solution was added. Next, the tubes were shaken vigorously for 12 min. Then the tubes were briefly centrifuged and the solution was poured away. Thereafter, the seeds were washed twice first with of 75% and then 96% ethanol. Then the ethanol was completely removed. Finally, the seeds were air dried on the sterile bench and were stored at 4°C.

Sterilization Solution

Sodium hypochlorite 12%	4 ml
Ethanol 96% (v/v)	25 ml
ddH_2O	24 ml

2.3.2.5.2 Cultivation of *Arabidopsis thaliana*

Surface sterilized seeds of *A. thaliana* WT (Col-0 or Col-2) and mutants (2.2.6) were sown on MS media plates containing 2% sucrose. The plates were sealed with gas-permeable tape and incubated overnight in the dark at 4°C for stratification. After that, the plates were incubated for approximately 10 days at 22°C under long day conditions (16 h light and 8 h dark) with 60% relative humidity and a light intensity of 120 µmol.m^{-2}.s^{-1}. The plants were either grown on the plates for further experiments or were transferred after the four leaves stage to 10 cm pots containing a ratio of soil/vermiculite (2:1). The plants on soil were grown in phyto-chambers at 150 µmol.m^{-2}.s^{-1} light for 16 h per day, 20°C and 55% relative humidity. The pots were watered with tap water, except the for the first time after transferring when the water was supplied with boric acid 0.15% (w/v) and fungicide (Proplant). For the phosphate starvation experiments, the plants were germinated on plates as describes before. Then they were placed under sterile conditions on synthetic *A. thaliana* nutrient medium (+P) or on phosphate deplete medium (-P), and were grown for another2 weeks.

Synthetic Medium for *A. thaliana*

		Micronutrients:	
KNO_3	2.5 mM	H_3BO_3	35 µM
$MgSO_4$	1 mM	$MnCl_2$	7 µM
$Ca(NO_3)_2$	1 mM	$CuSO_4$	0.25 µM
KH_2PO_4*	1 mM	$ZnSO_4$	0.5 µM
NH_4NO_3	1 mM	Na_2MoO_4	0.1 µM
Fe-EDTA	25 µM	NaCl	5 µM
		$CoCl_2$	5 µM

* KH_2PO_4 was omitted in the case of phosphate depleted medium

2.3.2.5.3 *Arabidopsis* Transformation Using *Agrobacterium tumefaciens*

Transformation of *A. thaliana* by the floral dipping method was performed according to Clough and Bent (1998). Transgenic agrobacterial cultures containing the desired binary plasmid were grown in 200 ml YEP medium containing appropriate antibiotics (2.3.2.2). On the day of transformation, the agrobacterial cells were harvested and the pellet was re-suspended in dipping solution. The whole shoots of 5 to 6 weeks old *Arabidopsis* plants were dipped in the dipping solutions for 15 sec, and were directly covered with plastic covers for a high humidity environment. After a long night (16h) incubation at RT, the transformed plants were placed in the

phyto-chamber. The shoots were covered with paper bags when the siliques had turned to be yellow. A few weeks later, the seeds were harvested when they had reached complete dryness.

Dipping Solution	
Tap water	100 ml
Sucrose	5% (w/v)
Silwet	0.05% (v/v)

2.3.2.6. Cultivation of *Blastochloris viridis*

B. viridis cells were cultivated in a medium that was developed and optimized by Darcy, 2006. 50 ml glass flasks with screw cap were filled to the top with the medium and inoculated from a plate with one full inoculation loop. The flasks were tightly closed, and the cells were grown autotrophically under semi-anaerobic conditions at 28°C under continuous light from a 60 watt classic light bulb source. The cells were maintained on agar plates with the same medium and stored in glycerol stocks at -80°C.

***B. viridis* Medium**	Amount l^{-1}
$(NH_4)_2SO_4$ 10% (w/v)	7 ml
Malate Solution	28 ml
Potassium Phosphate Solution	10.5 ml
Supersalts Solution	35 ml
Peptone	0.9 g
Yeast Extract	0.9 g
$MgCl_2$ 1% (w/v)	9.7 ml
$CaCl_2$ 1M	0.3 ml
PABA 50 µg/ml	0.5 ml
Vitamin B12	0.7 ml
ddH_2O	~800 ml
Tap Water	120 ml
Trace Element Solution	
$Cu(NO_3)_2 \times H_2O$	0.04 g
$MnSO_4 \times H_2O$	1.59 g
$ZnSO_4 \times 7H_2O$	0.24 g
H_3BO_3	2.8 g
$NaMoO_4 \times 2H_2O$	0.75 g

	Amount l^{-1}
Malate solution	
DL-malic acid	100 g
NaOH	60 g
Potassium phosphate solution	
KH_2PO_4	40 g
K_2HPO_4	60 g
Supersalts solution	
Na_2EDTA	0.4 g
$MgSO_4 \times 7H_2O$	4 g
$CaCL_2 \times H_2O$	1.5 g
$FeSO_4 \times 7H_2O$	0.2 g
Thiamine	20 mg
Trace Element Solution	20 ml
pH 7.5	

2.3.2.7. Cultivation of *Caldilinea aerophila*

PE medium was used to cultivate *C. aerophila* cells (Hanada et al. 1995). The cultivation was carried out in liquid medium under aerobic conditions. 20 ml of PE medium was inoculated with 0.5 ml pre-culture and the cells were incubated in a water bath at 55°C.

PE Medium	Amount l^{-1}		Amount l^{-1}
Sodium glutamate	0.5 g	**Vitamin mixture**	
Sodium succinate	0.5 g	Nicotinic acid	100 mg
Sodium acetate	0.5 g	Thiamine hydrochloride	100 mg
Yeast extract	0.5 g	Biotin	5 mg
Casamino acids	0.5 g	p-aminobenzoic acid	50 mg
Sodium thiosulfate	0.5 g	Vitamin B12	1 mg
KH_2PO_4	0.38 g	Calcium pantothenate	50 mg
K_2HPO_4	0.39 g	Pyridoxine hydrochloride	50 mg
$(NH_4)2SO_4$	0.5 g	Folic acid	50 mg
Vitamin mixture	10 ml		
Basal salt solution.	5 ml	pH 7.5	

Basal salt solution L^{-1}
1.11 g of $FeSO_4$ x $7H_2O$, 24.65 g of $MgSO_4$ x $7H_2O$, 2.94 g of $CaCl_2$ x $2H_2O$, 23.4 g of NaCI, 111 mg of $MnSO_4$ x $4H_2O$, 28.8 mg of $ZnSO_4$ x $7H_2O$, 29.2 mg of $Co(NO_3)_2$ x $6H_2O$, 25.2 mg of $CuSO_4$ x $5H_2O$, 24.2.mg of Na_2MoO_4 x $2H_2O$, 31.0 mg of H_3BO_3, 4.53 g of trisodium EDTA.

2.3.3. Methods in Biochemistry

2.3.3.1. Lipid Extraction

Total lipids of cells and leaf material were extracted using the biphasic separation method modified from (Bligh and Dyer, 1959). Briefly, 100 ml of cyanobacterial cells were harvested and washed with fresh BG-11. The pellet was transferred to micro-centrifugation tubes and extracted for 20 min with 1 ml of chloroform/methanol (1:2). The last step was repeated 3 times, the three extracts were combined and the internal standards were added. 1 ml 300 mM of ammonium acetate and 1 ml chloroform were added to the extraction to obtain phase separation. The organic phase was dried under a nitrogen stream and the lipids were either dissolved in hexane for further purification or stored at -20°C. For extracting lipids from the other bacterial strains and plants, a pellet obtained after centrifugation of 100ml bacterial culture, or a plant leaf (100 mg fresh weight), were boiled in water for 20 min. Lipids were extracted twice, first with chloroform/methanol (1:2) and second with chloroform/methanol (2:1). The first extract was dried using a stream of nitrogen and the second extract was combined with the dried lipid. The

combined extract was washed with 300 mM ammonium acetate and the organic phase was collected as mentioned before. For the measurement of galactolipids and phospholipids, the dried lipids were dissolved in 1 ml chloroform. Then, 10 µl lipids were mixed with 10 µl internal standard and 80 µl of the Q-TOF running solvent chloroform/methanol/300 mM ammonium acetate (300/665/35). Solvent and media control samples were extracted and analysed to exclude contaminations.

2.3.3.2. Solid Phase Extraction (SPE)

SPE was done in plastic columns containing silica material to separate lipids in fractions based on their polarity. According to vom Dorp et al. 2013, the dried lipids were dissolved in hexane and the columns were rinsed 3 times with hexane (15 or 3 ml for 500 or 100 mg silica column, respectively) for equilibration before the lipids were loaded. Afterwards, fatty acids phytyl esters FAPEs were eluted from the column using hexane and diethyl ether 99:1 (v/v). Tocopherols and TAGs were eluted using the same solvents in a ratio of 92:8 (v/v).

Columns were equilibrated with chloroform for the purification of galactolipids and phospholipids. While galactolipids were eluted with three times column volume of acetone/isopropanol 1:1 (v/v), phospholipids were eluted by applying three column volumes of 100% methanol.

2.3.3.3. Thin Layer Chromatography (TLC)

The first step of the lipid characterization was achieved with thin layer chromatography (TLC). About one tenth of the total lipid extract was separated on TLC plates using different solvent combinations as mobile phase. Galactolipids were separated in total lipids extracts by developing a TLC plate for 40 min using acetone/toluene/water 91:30:08 (v/v/v) as mobile phase. The plate was dried and stained with α-naphthol sulfuric acid staining to visualise the glycolipids (Hölzl et al. 2005a). Non-polar lipids were separated in total lipids extracts from *Synechocystis* using hexane/diethyl ether/acetic acid (70:30:1) or (90:10:1) as a mobile phase. The total lipids extract from an *A. thaliana* leaf and Birkenöl oil mixture (10 µl of 1:100 dilution) were used as standards for galactolipids and non-polar lipids, respectively. For further lipid analysis, the TLC plates were stained with Primuline (White et al. 1998) and observed under UV light. Then, the spots from the TLC plates were scrapped off and lipids were extracted from the silica material using chloroform/methanol 2:1(v/v) for further analyses.

2.3.3.4. Synthesis of Fatty Acid Methyl Esters (FAMEs)

The compositions of free fatty acids (FFAs) and fatty acid-derived compounds were quantified after they were converted into their corresponding methyl esters (Browse et al. 1986). To transfer

the esterified fatty acid from the lipid to a methyl group, 10 µl of the lipid extract was incubated with 1 ml of 1 N of methanolic hydrochloric acid and 100 µl of pentadecanoic acid 15:0 (5 µg/ml) as an internal standard. The reaction was incubated at 80°C for 15 min and was let to cool to room temperature. Thereafter, 1 ml of 0.5 M NaCl and 1 ml of n-hexane were added and the mixture was shaken and centrifuged to achieve a phase separation. The hexane phase was collected, 10 µl was dried and dissolved with 100 µl hexane and directly measured by GC-FID (2.3.3.8).

2.3.3.5. Quantification of Chlorophyll Content

Quantification of Chlorophyll a and Carotenoid Content in Synechocystis

The chlorophyll *a* and carotenoids contents in *Synechocystis* were measured as described by (Zavrel et al. 2015). To this end, 1 ml of culture was pelleted and the cells were resuspended in 1 ml of cold methanol. The sample was homogenised by vortexing and it was incubated in dark at 4°C for 20 min. The extract was centrifuged at 11000 rpm for 7 min and the supernatant was collected. The methanol extraction was repeated until the pellet turned blue. The absorbance of the methanol blank and the extracts were measured at 470, 665 and 720* nm by a spectrophotometer. The concentrations were determined according to the equations:

*Chl a (µg/ml) = 12.9447 * (A665 – A720)*
*Chl a (µM) = 14.4892 * (A665 – A720)*
*Carotenoids (µg/ml) = [1.0 * (A470 – A720) – 2.86 (Chl a µg/ml)]/221*

In case of using volumes of the cultures and/or the added methanol other than 1 ml, the concentrations were calculated according to:

$$\text{Pigment in the sample (µg/ml)} = \text{measured pigment concentration} * \frac{\text{volume of methanol (ml)}}{\text{volume of sample (ml)}}$$

Quantification of Chlorophyll Content in A. thaliana

The chlorophyll concentration in plant leaves was determined according to (Porra et al. 1989). Defined leaf samples frozen in liquid nitrogen were ground into powder after they. Chlorophyll was extracted with 1 ml 80% (v/v) acetone and absorbance OD of the extract was measured at 663.3, 646.6 and 750* nm by a spectrophotometer. From these readings, concentrations of chlorophyll a and chlorophyll b were calculated by using the following formulas:

$$Chl\ a\ (\mu g/ml) = 12.25 * (A663.6 - A750) - 2.55(A646.6 - A750)$$

$$Chl\ b\ (\mu g/ml) = 20.31 * (A646.6 - A750) - 4.91(A663.6 - A750)$$

* * The absorption at 750 and 720 nm was used as correction for the other absorptions

2.3.3.6. Chlorophyll Fluorescence

Pulse amplified modulation (PAM) fluorometry was used to measure the chlorophyll fluorescence in the plants and cyanobacteria. Following the manufacturer's instructions, photochemical quantum yield of photosystem II (YII) was calculated by the WinControl-3 software that operates the Junior-PAM. YII is calculated according to the equation $(F_m\text{-}F)/F_m$ where F_m and F are the fluorescence emission of a light-adapted plant under measuring light and after applying a saturating light pulse, respectively (Schreiber et al. 1986). The parameter YII reflects the efficiency of the photosystem performance. To record PAM chlorophyll fluorescence, dark-adapted (60 min) *Arabidopsis* plants from all lines were exposed for 5 min to different photosynthetically active irradiation levels, i.e. 150, 500, 1000 and 1500 $\mu mol.m^{-2}.s^{-1}$ to determine the impact of high light on photosynthesis activity (Hölzl et al. 2009; Hölzl et al. 2006). Thereafter, three groups of ten measurements were performed for each line at each irradiation level. To measure chlorophyll fluorescence in *Synechocystis*, a 15 ml culture was concentrated into 1 ml BG-11 medium and the light guide was dipped in the concentrated culture until a certain depth which was specified by a magnetic clip.

2.3.3.7. High-Performance Liquid Chromatography (HPLC)

HPLC was used for tocopherol measurement. Lipids were extracted and purified as mentioned in 2.3.3.1 and 2.3.3.2. Tocol (50 µl containing 500 ng) was used as an internal standard and a set of plant tocopherol mixture (α, β, γ and δ) was run before and after measuring the samples as positive control to determine the retention time. Tocopherols were separated on a LiChrospher diol column (Knauer, 250 x 4 mm, 2.1 µm particle size) with fluorescence detection (Agilent 1100 HPLC System). The Fluorescence was documented with an excitation at 290 nm and an emission at 330 nm (Kanwischer et al. 2005) modified. Hexane/tertiary butylmethylether 96:4 (v/v) was used as isocratic running solvent. The flow rate was 0.75 ml/min and the pressure was approximately 60 bar. The injection volume was 50 µl and the running time was 20 min. The data was analysed using the Agilent 1100 series HPLC system with a fluorescent light detector (FLD).

2.3.3.8. Gas Chromatography-Flame Ionization Detection (GC-FID)

The quantification of fatty acid methyl esters was important to quantify acyl lipids like galactolipids and phytyl esters, and was also required to quantify internal standards like 17:0-phytol (2.3.3.4). Methyl esters were quantified via GC-FID using the following parameters:

		temperature programme	
Column	Supelco SP-2380	Initial	100°C
length	25 m	25°C /min	to 160°C
Inner diameter	0.32 mm	10°C/min	to 220°C
film thickness	0.1 µm	25°C/min	to 100°C
Carrier gas	Helium		

Flow rate	7 ml/min	Injection/sample	2 µl

2.3.3.9. Measuring and Analysing Lipids by Q-TOF MS/MS

2.3.3.9.1 Internal Standards for Lipid Analysis by Q-TOF

Different lipids were quantified in relation to previously quantified internal standards (IS). For phospholipids, galactolipids and sulfolipids an internal standard mixture was prepared by Helga Peisker (IMBIO, University of Bonn) (Wewer et al. 2014). 10 µl of the IS mixture in chloroform/methanol (2:1) contains 10.35 nmol di14:0-PC, 13.25 nmol di20:0-PC, 9.33 nmol di14:0-PE, 12.1 nmol di20:0-PE, 9.92 nmol di14:0-PG, 11.25 nmol di20:0-PG, 6.96 nmol di14:0-PA, 7.145 nmol di20:0-PA, 1.41 nmol di14:0-PS, 15.9 nmol 34:0-PI, 7.278 nmol 34:0-MGDG, 6.75 nmol 36:0-MGDG, 10.134 nmol 34:0-DGDG, 22.2 nmol 36:0-DGDG and 21.2 nmol 34:0-SQDG. The dried lipid extract was dissolved with 1 ml chloroform, then 10 µl lipids was mixed with 10 µl IS and 80 µl Q-TOF running buffer.

The internal standards for TAGs and phytyl esters were prepared by Dr. Katharina Gutbrod (IMBIO, University of Bonn) (vom Dorp et al. 2013). 50 µl of the TAG IS mixture contains 1 nmol of each tri17:0-TAG and tri17:1-TAG. For FAPEs quantification, 50µl of the IS, containing 1 nmol of 17:0-phytol, was added to each sample. For the quantification of di18:2 DGDG which is the product of the enzyme assay with BviMgdP, a final concentration of 3 nmol of *N*-acyl-sphingosine-galactoside (d18:1-c12:0) was used as an internal standard (prepared by Dr. Katharina Gutbrod).

2.3.3.9.2 Measurement of Lipids with Direct Infusion Q-TOF Mass Spectrometry

FAPEs, glycerolipids and TAGs were measured by direct infusion Q-TOF MS/MS in the positive ionization mode. The methods were developed in the IMBIO by Helga Peisker, Dr. Vera Wewer and Dr. Katharina Gutbrod. Dried extracted lipids were dissolved in chloroform/methanol/300 mM ammonium acetate 300:665:35 (v/v/v) (Welti et al. 2002). Q-TOF MS/MS measurements were performed using an Agilent 1100/1200 series nanopump and HPLC-Chip Cube MS interface. The LC-pump was operated at a flow rate of 1 µl/min. Lipids were analysed in the positive ion mode on an Agilent 6530 Series Accurate-Mass Q-TOF LC/MS. Lipids were quantified by neutral loss or precursor ion scanning, and the relative calculations based on the internal standers I.S. Target lists and the parameters of lipid quantification are shown in the appendix (7.2). Data were visualized by the Agilent Mass Hunter Qualitative Analysis Software (Version B.06.00). Lipids were quantified using Microsoft Excel 2013. The Excel sheets are modified from the original copies provided by Helga Peisker and Dr. Katharina Gutbrod.

The instrumental parameters used for Q-TOF measurements are:

Infusion chip	FIA Chip II flow injection and infusion
Solvent:	chloroform/methanol/300 mM ammonium acetate 300:665:35 (v/v/v)
Flow rate:	1 µl/min
Injection:	5 or 3 µl
Drying gas:	nitrogen 8 ml/min
Fragmentor voltage:	200 V
gas temperature:	300°C
HPLC-Chip V_{cap}	1700 V
Scan rate:	1 spectrum/sec

2.3.3.9.3 **Untargeted Lipidomic Analyses via Q-TOF LC MS/MS**

Liquid chromatography (LC) coupled with mass spectrometry (MS) was performed using the untargeted approach. As shown in Figure 2.2, cultures of 100 ml of five biological replicas from each line of *Synechocystis* were separately grown under the same conditions (2.3.2.4). The OD_{750} was determined for normalization. The total lipid was extracted (2.3.3.1), dried under nitrogen, and dissolved in 100% methanol. The amount of the added methanol was adjusted to the OD_{750} measurements of the cultures for normalization to obtain comparable lipid concentrations. Thereafter, the lipids were diluted 100fold with 100% methanol and 200 µl were transferred to glass vials for measurements with Q-TOF LC/MS. Samples were run in the positive ionization mode for 60 min per sample. To obtain high quality data, the injection order of the samples was randomized, and a solvent blank was run after every two samples. In addition, several controls for the extraction steps and the growth medium were measured. Internal standards (IS) were not used for the untargeted LC approach. Lipids were separated on the Knauer Eurospher II C8, 150 x 3 mm, 3 µm particle size column. Two solvent systems were used as mobile phase i.e. 100% water, 0.1% (v/v) formic acid (A) and 100% methanol, 0.1% (v/v) formic acid (B). A gradient of solvents A and B was used to elute lipids from the column is shown in Table 9. The injection volume was 10 µl and the flow rate was 0.4 ml/min. The separation was accomplished using an Agilent 1100 Series binary pump connected to an Agilent 6530 Series Accurate-Mass Q-TOF LC/MS.

Parameters for LC-Q-TOF MS/MS Analysis:

Parameter	**Setting**
Drying gas	8 l/min N_2
Fragmentor voltage	200 V
Gas temperature	300°C
V_{cap}	3500 V
Scan rate	1 spectrum/s

Table. 9: Liquid chromatography gradient for non-targeted approach

Time	Eluents%	
	A	B
0	25	75
5	0	100
50	0	100
50.1	25	75
60	25	75

Data obtained from Q-TOF LC/MS was analysed by the Agilent MassHunter Qualitative Analysis software (Version B.06.00). After that, the raw data from MassHunter was analysed using the interactive metabolomic and lipidomic XCMS online database (https://xcmsonline.scripps.edu). The website allows users to upload groups of data sets. Prior to the upload, the MassHunter files were converted to. mzML form using ProteoWizard. After uploading the files, parameters were selected based on the instrumental platform in which the data were obtained from (HPLC/Q-TOF for this study). Finally, the files were submitted online. By using R-package, the raw data were processed for peaks detection and filtration, retention time correction, peak grouping and matching (Figure 2.2). Thereafter, the software statistically compared the relative ion intensities to identify changes in specific endogenous metabolites (Smith et al. 2006; Gowda et al. 2014; Margaria et al. 2008). Finally, the results output was exported from XCMS as tables and extracted ions chromatograms (EICs).

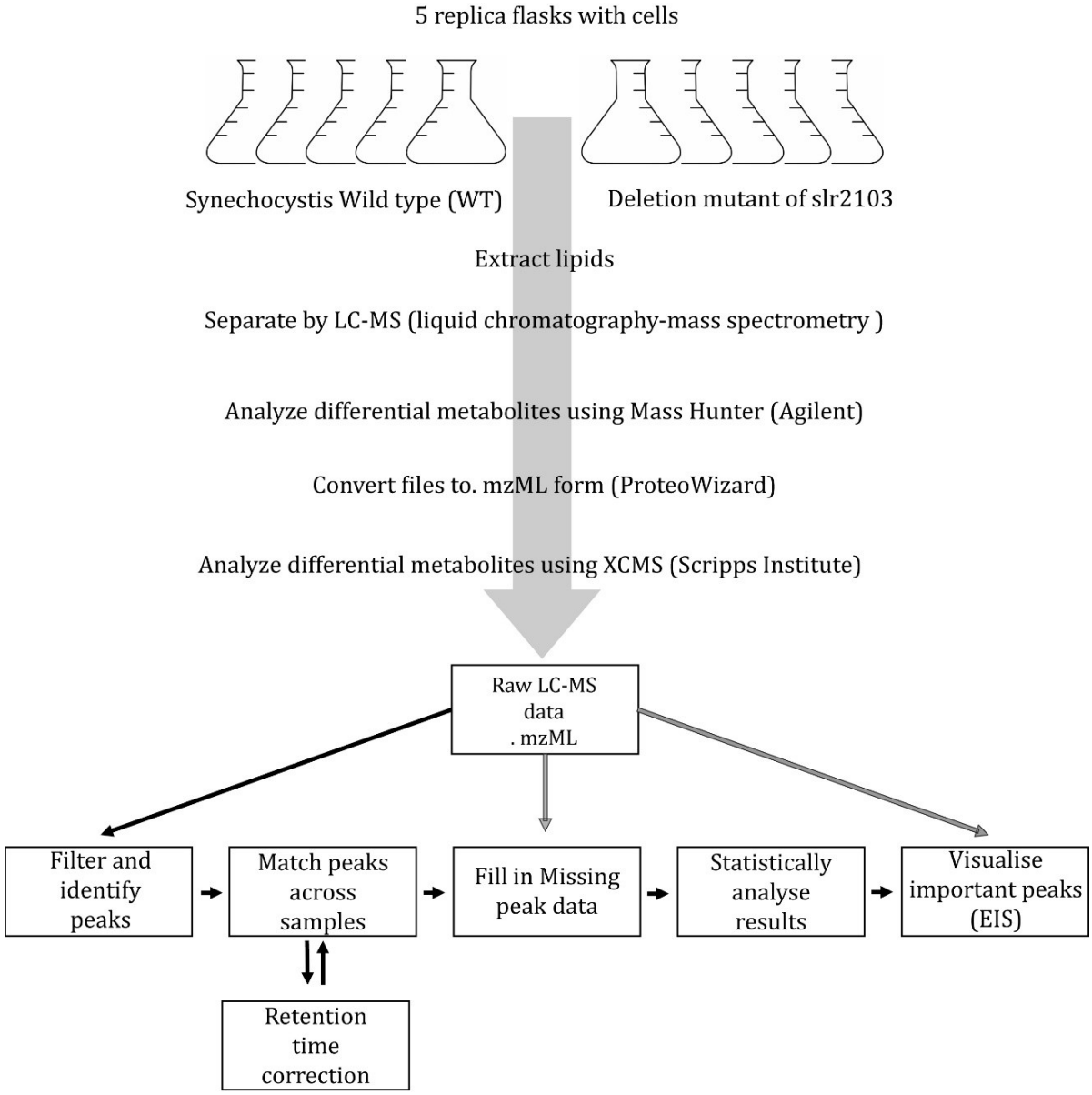

Figure 2. 2: Scheme of the untargeted approach workflow that used in this study.
Boxes indicate the workflow after uploading to XCMS. Black arrows indicate the normal process flow and the grey arrows show when XCMS re-reads the raw data files (Margaria et al. 2008)

2.3.4. Transmission Electron Microscopy (TEM)

For comparative ultrastructural analysis, cells of *Synechocystis* WT and Δ*slr2103* mutant were collected by centrifugation and resuspended in 8% agarose. After solidification, the agarose was cut into blocks of ~1 mm^3 and used for combined conventional and microwave assisted fixation, dehydration and resin embedding. Sectioning, and ultrastructural analysis were performed as described (Daghma et al. 2011). TEM was done in a cooperation with Dr. Michael Melzer from IPK Gatersleben.

2.3.5. Statistical Methods

All experiments were conducted with at least three replicas unless indicated otherwise. Means and standard deviation (SD) were calculated by Microsoft Office Excel or by the online version of XCMS (The Scripps Research Institute) as mentioned. Statistical significance for all experiments was calculated using Student's t-test. P values < 0.05 were labelled for each Figure. Errors of combination of sums were calculated from the square root of the sum of squares.

3. Results

3.1. Identification of the ELT-like Acyltransferase and Hydrolase in *Synechocystis*

In plant chloroplasts, fatty acid phytyl esters are synthesized by two enzymes, PES1 and PES2. They both belong to the Esterase/Lipase/Thioesterase (ELT) family. PES1 and PES2 are composed of an N-terminal hydrolase and a C-terminal acyltransferase domain (Lippold et al. 2012; vom Dorp et al. 2015). The similarity between chloroplast and *Synechocystis* suggested that *Synechocystis* might contain similar enzymes.

Protein BLAST searches with the C-terminal part of the *Arabidopsis* PES2 protein against the protein database of NCBI restricted to the subset organism *Synechocystis* PCC6803. The BLAST search showed that *Synechocystis* harbours four protein sequences with similarity to acyltransferases including slr2103, with highest sequence similarity to PES2, and sll1752, slr2060, and sll1848 with lower sequence similarity. Both slr2060 and sll1848 encode lysophosphatidic acid (LPA) acyltransferases as reported earlier (Weier et al. 2005; Okazaki et al. 2006). Furthermore, another BLAST search was conducted with the slr2103 protein sequence against the protein database of NCBI. The search revealed slr2103-like sequences in other cyanobacteria like *Cyanothece*, *Anabaena*, *Nostocales* and *Calothrix*. On the other hand, BLAST searches with PES2 sequence against the protein database in NCBI, revealed the presence of three PES2-like sequences with two domains (hydrolase and acyltransferase) in green algae (*Chlamydomonas reinhardtii*) and red algae (*Galdieria* and *Chondrus*). A phylogenetic tree was constructed with the amino acid sequences of the C-terminal acyltransferase portions of the plant, green and red algae, the cyanobacterial acyltransferases and with *Arabidopsis* DGAT1, which is involved in TAG synthesis (Figure 3.1). Furthermore, the *Acinetobacter* wax synthase/DGAT sequences (bacterial AtfA-type) and the related WSD1 sequence from *Arabidopsis* involved in wax ester synthesis were included. The sequences clustered into five groups: a plant-type ELT group containing the C-terminal sequences of *Arabidopsis* PES1, PES2 and the related proteins from green and red algae, a group of ELT-like cyanobacterial acyltransferases including slr2103, a group of the three distantly related LPA acyltransferase-like sequences from *Synechocystis*, as well as *Arabidopsis* DGAT1 and the two AtfA-type sequences. The slr2103 sequences are much closer related to the acyltransferase domain of *Arabidopsis* ELT sequences than to the *Arabidopsis* DGAT1 or the AtfA-type sequences. That indicates that slr2103 establishes a new group of bacterial acyltransferases.

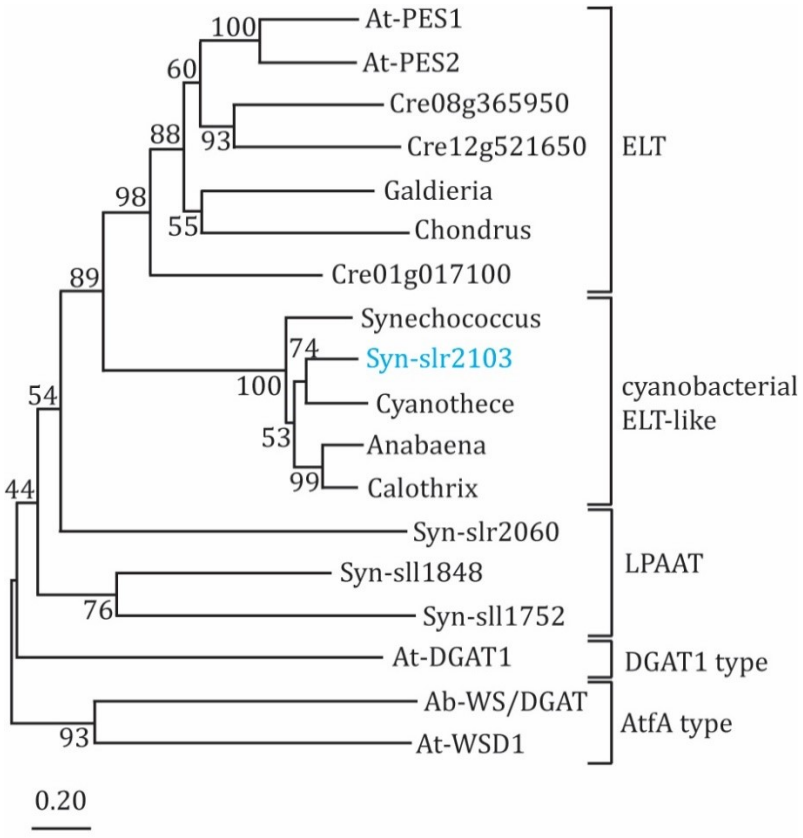

Figure 3. 1: Phylogenetic relationship of lipid acyltransferases from cyanobacteria, plants, green and red algae.
Protein sequences were aligned with ClustalW, and a phylogenetic tree constructed using the Neighbour Joining method with 1000 bootstrap repetitions (Mega 10.0.5). For the plant-type ELT (esterase/lipase/thioesterase) sequences, only the C-terminal acyltransferase-like parts were considered. *Acinetobacter* sp. ADP1 WS/DGAT, AF529086.1; *Anabaena* sp. (CA=ATCC 33047) WP_066380359; *Arabidopsis thaliana* PES1 (amino acids 401-704); PES2 (401-701); DGAT1; WSD1; *Calothrix brevissima* WP_096644248; *Chlamydomonas reinhardtii* Cre01g017100 (591-911), *Cre08g365950* (411-692), Cre12g521650 (631-873); *Chondrus crispus* XP_005713590 (601-965); *Cyanothece* sp. (PCC 7425) WP_012629067; *Galdieria sulphuraria* XP_005702844 (561-921); *Synechococcus* sp. (NKBG042902) WP_030007836; *Synechocystis* sp. (strain PCC 6803) slr2103; sll1848; slr2060; sll1752; Nostocales WP_045867658.

In the same manner, a protein BLAST search with the N-terminal hydrolase domain of PES2 from *Arabidopsis* against the protein sequence database in NCBI, showed that *Synechocystis* contains a hydrolase-like sequence slr1807 with low similarity. Another BLAST search with slr1807 showed that several members of cyanobacteria (*Cyanothece*, *Anabaena*, *Nostocales* and *Calothrix*) contain slr1807-like sequences. All of these hydrolase-like sequences belong to the α/β group of hydrolases. Similar sequences to slr1807 were also found in plants, green and red algae represented by the N-terminal domains in the PES2-like sequences. A phylogenetic tree was constructed with the amino acid sequences of the N-terminal hydrolase portions of the plant (N-terminal sequences from PES1 and PES2), green and red algae, and bacterial hydrolases (cyanobacteria and *Acinetobacter*). The sequences clustered mainly into three groups:

cyanobacterial hydrolases including slr1807, hydrolases from plants/green algae and hydrolases from red algae (Figure 3.2).

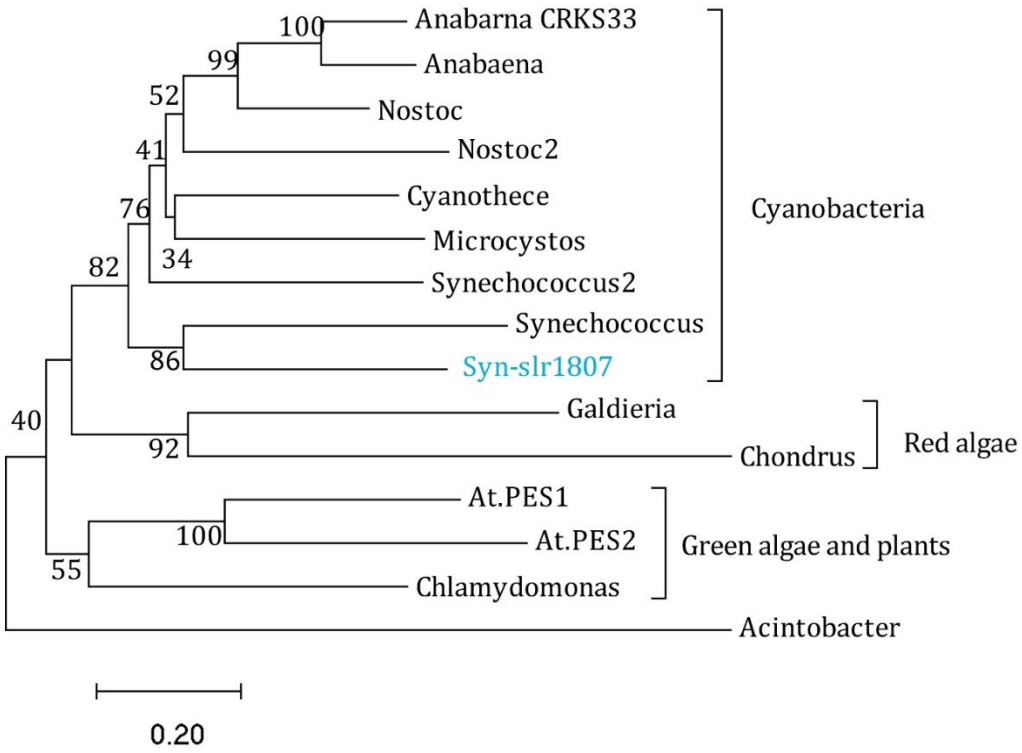

Figure 3. 2: Phylogenetic relationship of hydrolase-like sequences from cyanobacteria, plants, green and red algae.
Protein sequences were aligned with ClustalW, and a phylogenetic tree constructed using the Neighbour Joining method with 1000 bootstrap repetitions (Mega 10.0.5). For the plant-type ELT (esterase/lipase/thioesterase) sequences, only the N-terminal hydrolase-like parts were considered. *Anabaena* sp. (CRKS33) OBQ36611; *Anabaena* sp. (UBA12330) HCQ23126.1; *Nostoc flagelliforme* WP_100900107; *Nostoc* sp. (PA-18-2419) WP_138502455.1; *Microcystis aeruginosa* WP_002755084; *Cyanothece* sp. (PCC 7425) WP_012595380; *Synechococcus* sp. (PCC 7336) WP_017328020; *Synechococcus* sp. (1G10) WP_094553836; *Synechocystis* sp. (PCC 6803) slr1807; *Arabidopsis thaliana* PES1 (amino acids 91-400); PES2 (91-400); *Chlamydomonas reinhardtii* Cre12.g521650 (321-630); *Galdieria sulphuraria* XP_005702844 (281-560); *Chondrus crispus* XP_005713590 (311-600); *Acinetobacter baumannii* SCY24562.

As indicated above, an orthologue of PES2 with two-domain sequence does not exist in the genome of *Synechocystis.* Instead, *Synechocystis* harbours two shorter ORFs i.e. slr1807 and slr2103, each encoding a separate protein, with sequences similarities to the hydrolase and acyltransferase domains, respectively (Figure 3.3 and 3.4). The ORF slr1807 consists of 786 bp (1283741-1284526) encoding a 261 amino acid polypeptide with a calculated molecular mass of 29 kDa, whilst the ORF slr2103 contains 885 bp (1571731-1572615) encoding a 294 amino acids polypeptide with a calculated molecular mass of 32 kDa.

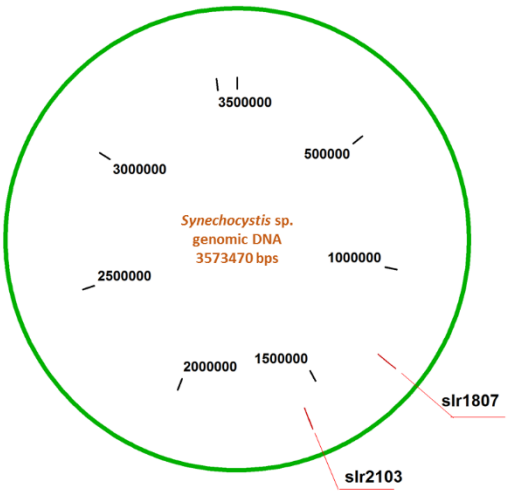

Figure 3. 3: Location of slr1807 and slr2103 in the genomic DNA of *Synechocystis*.
The sequence was obtained from NCBI, GenBank: BA000022.2 and the map with the location of slr1807 and slr2103 is produced by Clone manager professional suit version 8.

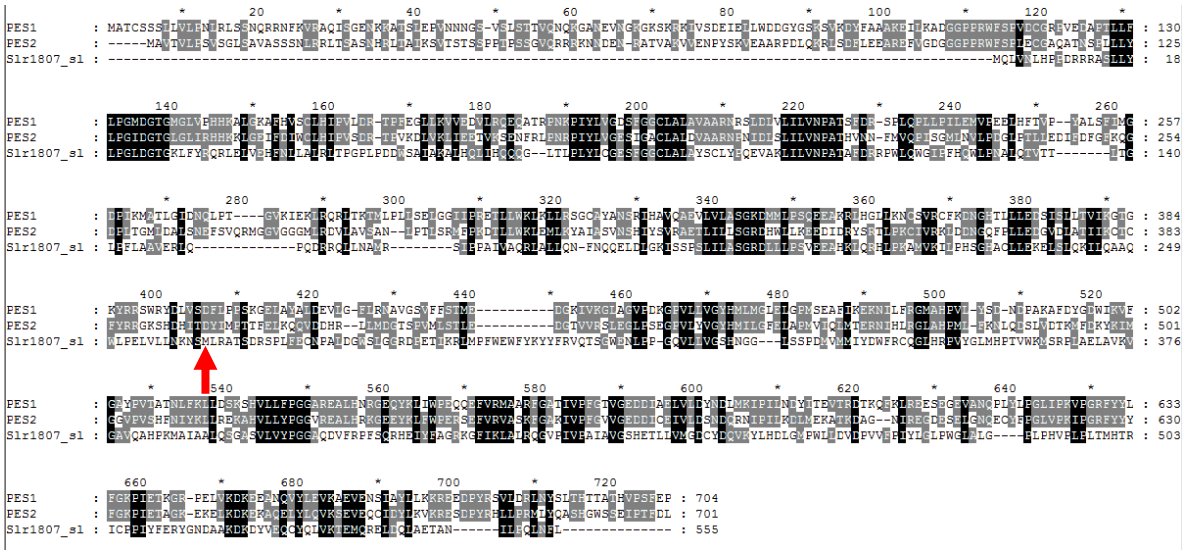

Figure 3. 4: Alignment of *Arabidopsis* PES1, PES2 and *Synechocystis* slr1807 and slr2103 amino acid Sequences.
The cyanobacterial proteins were artificially fused to show the similarity to the two different domains in the plant proteins. The red arrow indicates where the sequence of slr1807 ends and slr2103 begins. The letters with black background show similarity within the three sequences and the grey backgrounds show similarity with at least two sequences.

3.2. Generation of *Synechocystis Δslr2103* and *Δslr1807* Deletion Mutants

Synechocystis deletion mutants *Δslr2103* and *Δslr1807* was generated by inserting a kanamycin resistance cassette into the ORFs slr2103 and slr1807, respectively. An isogenic mutant line was isolated after re-streaking the cells on kanamycin containing medium. The purity of homozygous lines was confirmed by genotyping via PCR (Figure 3.5). Details are described in (2.3.2.4.1).

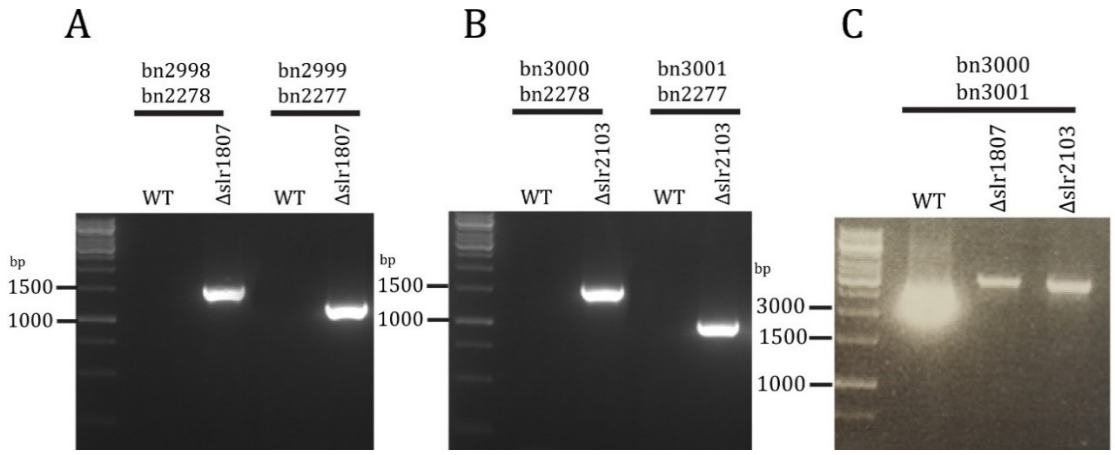

Figure 3. 5: **Genotyping of Δ*slr1807* and Δ*slr2103* mutants.**
Genomic DNA of the WT, slr1807 and slr2103 cells was used for PCR with primers as shown above. **(A)** Agarose gel with the separated PCR products obtained from genotyping of the 5' and 3' mutation sequences of *Δslr1807.* **(B)** Agarose gel with the separated PCR products obtained from genotyping of the 5' and 3' mutation sequences of *Δslr2103.* WT was used as negative control in A and B. **(C)** Identification of the knock out region. Primer list and the expected fragment sizes are listed in the appendix 7.1.

3.3. The Open Reading Frames slr1807 and slr2103 are Not Essential for *Synechocystis*

Synechocystis mutant strains lacking either slr1807 or slr2103 grow normally indicating that the two proteins are not essential. A cell spotting assay was performed as described in (2.3.2.4.4) under control conditions and nitrogen starvation (Figure 3.6). The assay showed similar viability of the two mutant cells compared to the WT growing under normal conditions or nitrogen deprivation.

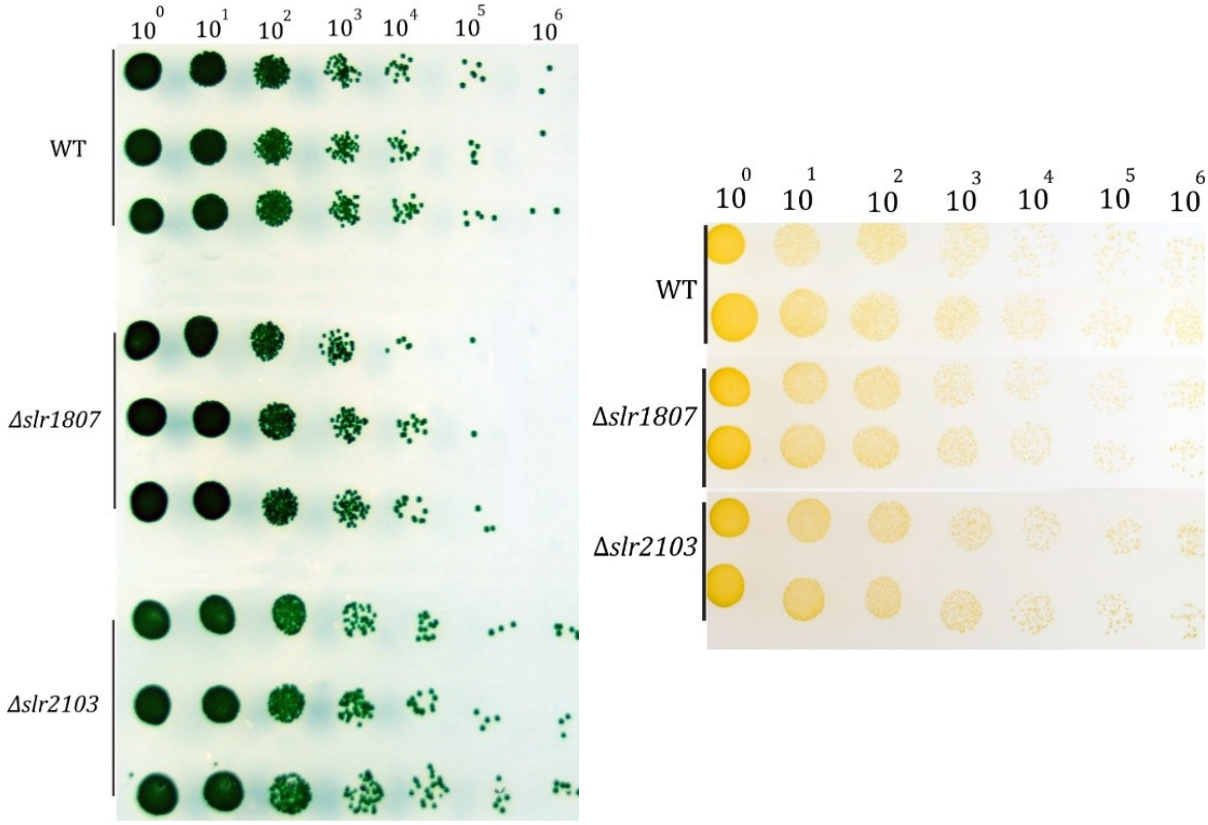

Figure 3. 6: The vitality of *Synechocystis* shown by a spotting assay.
The growth of the two mutants is not affected. *Synechocystis* WT, Δ*slr1807* and *Δslr2103* cells were grown in liquid medium (BG-11) to OD_{750} of 1.0. 10 µl aliquots of the cells were plated in a serial dilution on solid medium and grown under light until no new colonies appear. **(left)** Growth on BG-11 medium (control). **(right)** Growth on nitrogen deficient medium.

3.4. The Deletion of slr1807 or slr2103 has Minor Effects on Photosynthesis

To study the physiological changes in photosynthesis, the photosynthetic pigment content and quantum yields were determined in the mutants and compared to the WT. The chlorophyll and carotenoid contents were measured in the WT, Δ*slr1807*, Δ*slr2103* under control and stress conditions (combined dark/NaCl treatment). The chlorophyll *a* contents in the WT and the two mutants are similar under control conditions with a non-significant increase and decrease in the hydrolase and the acyltransferase mutants, respectively. The chlorophyll contents in the three lines were lower under stress conditions compared to the WT (Figure 3.7A). The carotenoid contents did not show significant changes between the WT and the two mutants growing under control or stress conditions (Figure 3.7B). The quantum yield of photosystem II (YII) was determined by chlorophyll fluorescence measurements of dark adapted *Synechocystis* cultures. YII was decreased from 0.34 in the WT to 0.32 and 0.31 in the hydrolase and the acyltransferase mutants, respectively (Figure 3.7C). These results show that loss of slr1807 or slr2103 exerts minor effects on photosynthesis.

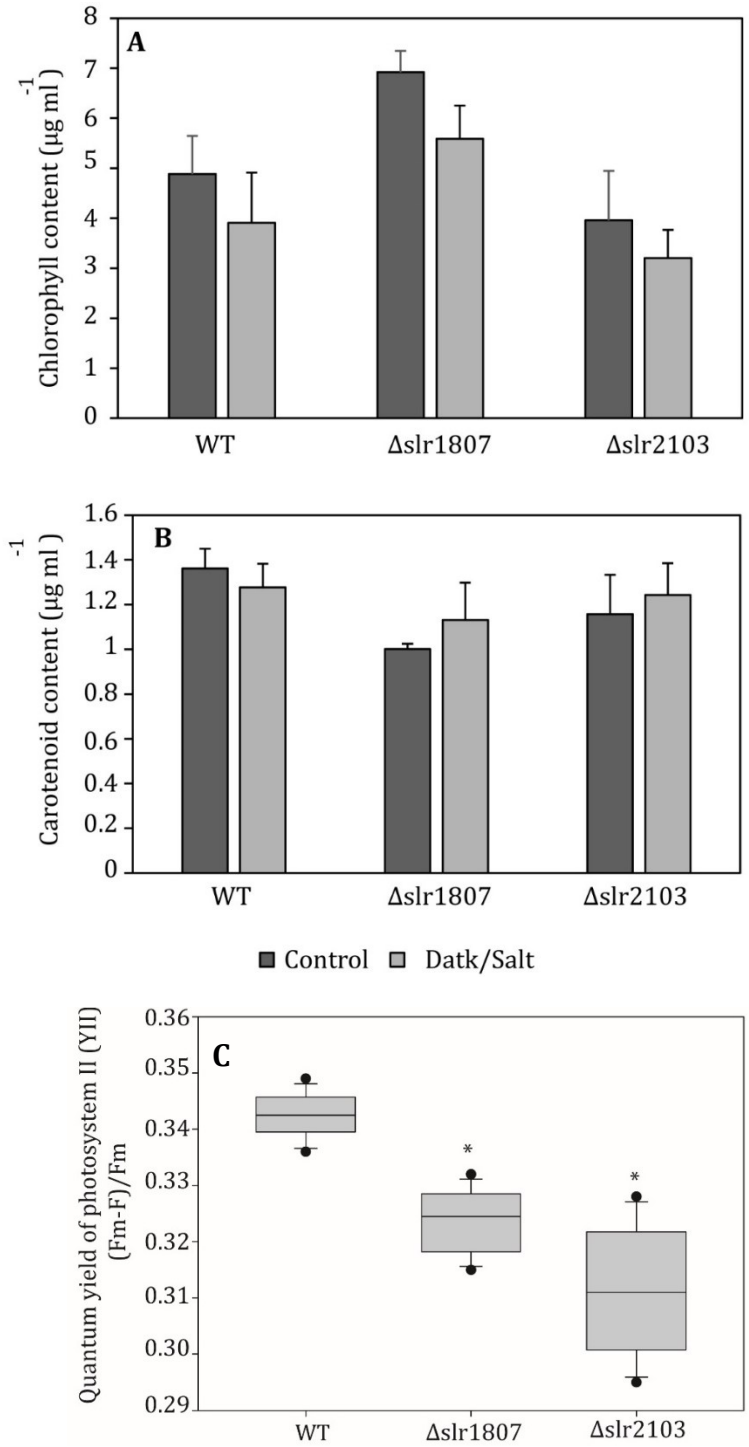

Figure 3. 7: **Photosynthetic pigments and quantum yield of WT, *Δslr807*, *Δslr2103* mutant cells.**
(A and B) Chlorophyll and total carotenoid contents, respectively. Both pigments were measured photometrically. *Synechocystis* cells were grown in BG-11 medium (control, left) or under stress conditions (in darkness and with NaCl, right). **(C)** The boxplot shows the quantum yield of photosystem II YII of *Synechocystis* cells grown in BG-11 medium was recorded by PAM fluorometry. Fv, variable fluorescence under measuring light. Fm, maximal fluorescence after application of a saturating light pulse. Each box ranges from 25 to 75 percentile, the line in the middle of the box indicates the median. The whiskers range to the outliers which are indicated as black dots. Data are means ± SD of 4 or 10 measurements for chlorophyll and carotenoid or YII, respectively. Asterisks indicate significant differences to WT ($p < 0.05$).

3.5. Fatty Acid Phytyl Esters Accumulate in *Synechocystis* WT

In plant chloroplasts, FAPEs accumulate during chlorotic stress for instance during nitrogen starvation, drought, or extended dark stress. This is due to the high rate of chlorophyll degradation under such stresses (Gaude et al. 2007; Ischebeck et al. 2006). In the cyanobacterial world, *Synechococcus* was described to accumulate minor amounts of FAPEs (Lütke-Brinkhaus et al. 1985). To investigate the occurrence of FAPEs in *Synechocystis*, WT cultures were cultivated, lipids were extracted and purified on SPE columns and phytyl esters were analysed by Q-TOF MS/MS. The analysis showed that *Synechocystis* contains low levels of different phytyl esters which were identified by mass spectrometry of their parental ions derived from phytyl ester ammonium adducts. After fragmentation, FAPEs give rises to a mass of a fatty acid ammonia adduct accompanied with a neutral loss of the mass of the phytol moiety lacking H_2O (Figure 7.1 and 7.2.1). The total amount of FAPEs in *Synechocystis* WT growing under normal conditions was calculated as 3.3 nmol OD_{750}^{-1}. To increase the amounts of FAPEs, *Synechocystis* WT cells were grown under two different stress conditions i.e. 3 days of darkness combined with exogenously added 0.5M NaCl, or under nitrogen starvation conditions. The amount of phytyl esters was doubled under dark/salt stress reaching 6.8 nmol OD_{750}^{-1}. Due to structural differences in light harvesting complexes, less chlorophyll is degraded during nitrogen starvation in *Synechocystis* (Li and Sherman 2002; Loura et al. 1987). This fact could explain why the growth of *Synechocystis* cells under N deprivation did not result in the accumulation of phytyl esters (Figure 3.8).

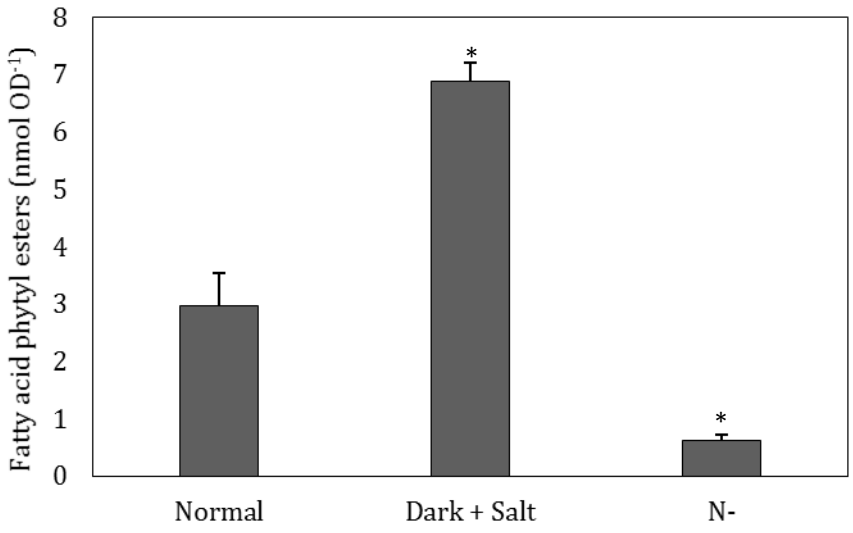

Figure 3. 8: **Quantification of fatty acid phytyl ester content in *Synechocystis* WT cells.**
The cultures were grown under normal or stress conditions (3 days of darkness combined with 0.5 M NaCl, or under nitrogen deprivation). Data represent mean of 3 to 4 replicas. The asterisk (*) indicates significant differences to the wildtype when $P < 0.05$. Error bars in this graph were calculated as the square root of the sum of squares of the individual molecular species.

3.6. Fatty Acid Phytyl Ester Content is Strongly Decreased in *Synechocystis Δslr1807* and *Δslr2103*

To investigate the capability of *slr1807* and *slr2103* to contribute to the phytyl ester synthesis, *Synechocystis* WT, Δ*slr1807* and Δ*slr2103* were grown in BG-11 medium under normal and stress conditions. Phytyl esters were purified by SPE and quantified by Q-TOF MS/MS. The fatty acid phytyl ester levels in *Synechocystis* Δ*slr1807* and Δ*slr2103* were remarkably reduced compared with WT when the cells were grown under normal conditions. This reduction was even more pronounced with over 80% in both mutants compared to the WT when they were grown under dark/salt stress (Figure 3.9).

These results revealed the involvement of slr1807 and slr2103 in the accumulation of phytyl esters in *Synechocystis*. The very low accumulation of FAPEs under nitrogen deprivation did not change in the mutants in comparison to the WT (Figure 3.9).

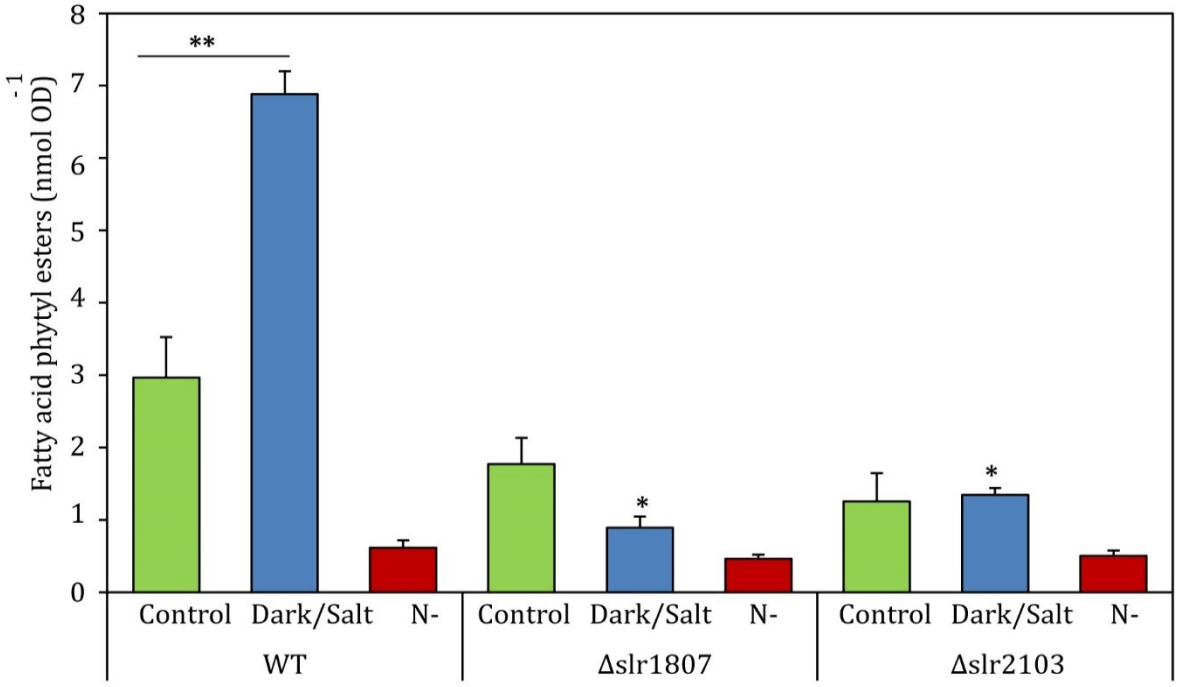

Figure 3. 9: Quantification of fatty acid phytyl ester content in *Synechocystis* WT *Δslr1807* and *Δslr2103*.
The cultures were grown under normal or under stress conditions (3 days of darkness combined with 0.5 M NaCl, or under nitrogen deprivation). Data represent mean of 3 or 4 replicates. Asterisk (*) indicates significant differences to the wildtype under stress when P< 0.05. Error bars in this graph were calculated as the square root of the sum of squares of the individual molecular species.

The relative fatty acid composition in *Synechocystis* slightly changes under certain conditions, for example, temperature or light intensity (Wada and Murata 1990; Cuellar-Bermudez et al. 2015). The *Synechocystis* fatty acid profile determined in this study corresponds

to other studies in which *Synechocystis* cells were cultivated in the same media, under the same temperature and same light intensity (Merritt et al. 1991; Wada and Murata 1990; Cuellar-Bermudez et al. 2015). Total cellular fatty acids were measured as fatty acid methyl esters (FAMEs). Palmitic acid (16:0), α-linolenic acid (18:3), linoleic acid (18:2) and oleic acid (18:1) were the dominant fatty acids with 50%, 27%, 10% and 5%, respectively, of the total fatty acid composition with lower abundance of palmitoleic acid (16:1) and stearic acid (18:0). Nevertheless, the phytyl esters of *Synechocystis* WT show a different fatty acid composition, since the second most abundant phytyl esters is 18:1-phytol with 22% (Figure 3.10). This finding might indicate a substrate specificity of the phytyl ester synthase, or differences in the substrate pool (acyl-CoA) composition, compared with total fatty acid composition. The molecular species of FAPEs accumulating in *Synechocystis* WT did not change after stress (Figure 3.11A and 3.11B).

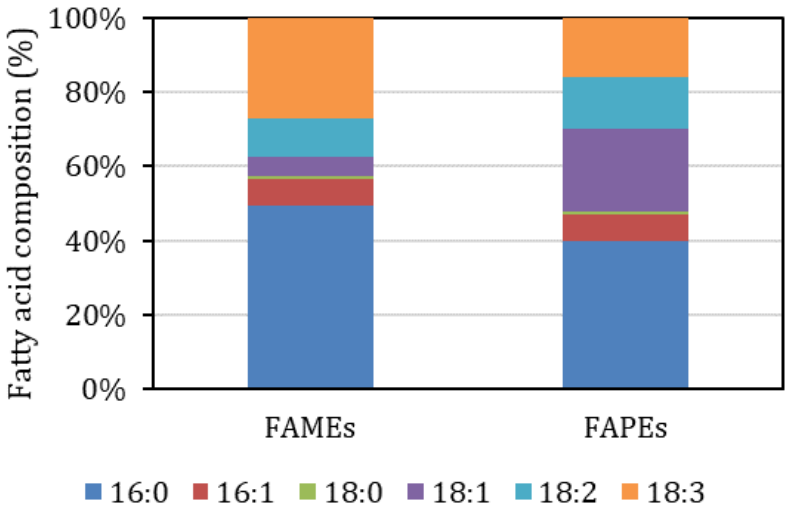

Figure 3. 10: Distribution of total and phytyl ester bound fatty acids in *Synechocystis* WT.
Cells were grown under normal conditions. On the left: fatty acids content in total lipids (FAME) and on the right is the fatty acid content in fatty acid phytyl ester (FAPE). Total fatty acids were measured by GC after methylation, and phytyl ester bound fatty acids were derived from phytyl ester measurement by Q-TOF MS/MS

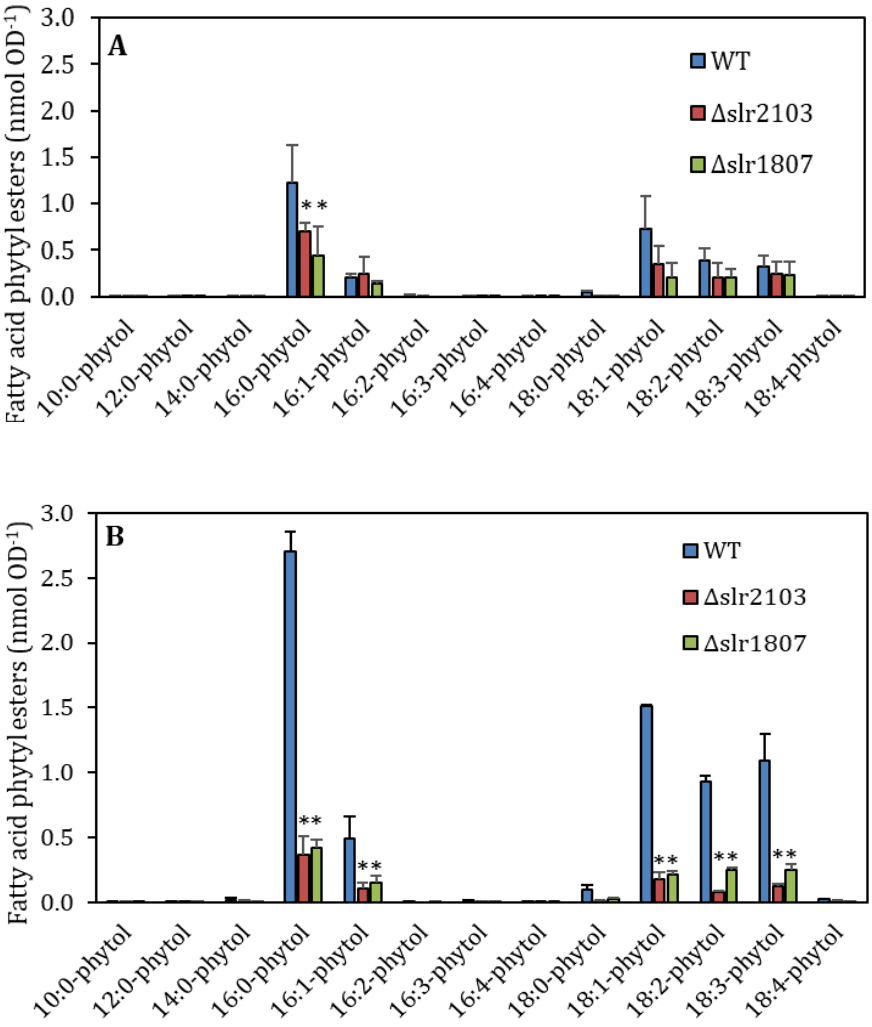

Figure 3. 11: Fatty acid phytyl ester profile in *Synechocystis* WT, *Δslr1807* and *Δslr2103.*
(A) cells were grown under control conditions**. (B) c**ells were grown under darkness/salt stress. Data represent mean and SD of 3 or 4 replicates. Asterisk (*) indicates significant differences to the wildtype under control conditions or under stress when P< 0.05.

3.7. Tocopherol Contents are Slightly Increased in Δ*slr1807* and Δ*slr2103*

Tocopherols (vitamin E) are antioxidants synthesised mainly by plants, algae and some cyanobacteria (Collins and Jones 1981). They are known for their important role in protecting thylakoid membranes from oxidative stress. They are also essential for low temperature-high light tolerance in *Synechocystis* (Yang et al. 2008). In plants, FAPEs and tocopherol biosynthesis is important to remove free phytol and free fatty acids from the thylakoid membrane. A similar function is expected for *Synechocystis*. Phytol is a precursor for the biosynthesis of both FAPEs and tocopherols. Therefore, it was reasonable to assume that blocking the synthesis of FAPEs in *Synechocystis* might lead to an increase in the tocopherol content. Therefore, the tocopherol content was measured in the WT, Δ*slr1807* and Δ*slr2103*. In line with this hypothesis, the

tocopherol level showed a small increase in the two mutants compared to the WT when grown under control conditions (Figure 3.12). However, stressing the cells with salt/darkness did not stimulate any increase in the tocopherol levels compared to control conditions. On the contrary, the tocopherol contents in the three lines grown under stress conditions were lower than when grown under control conditions (Figure 3.12).

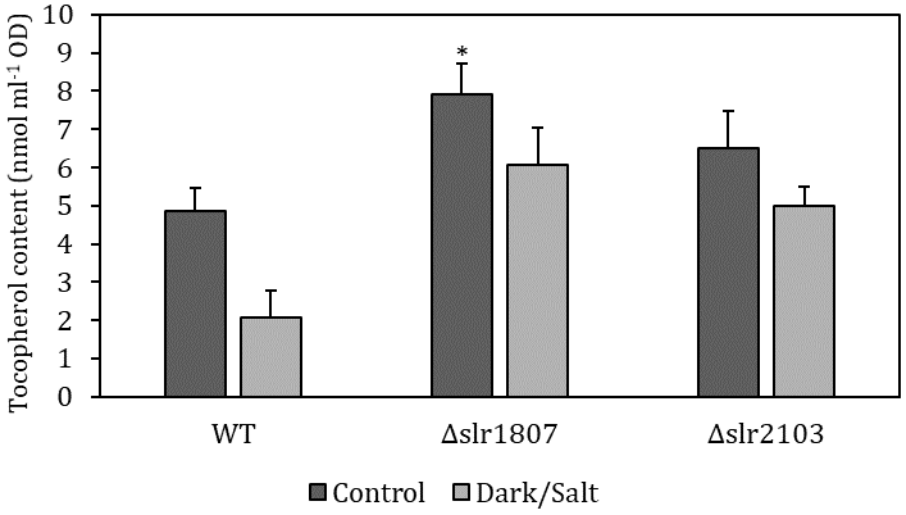

Figure 3. 12: Tocopherol content in the WT, slr1807 and slr2103.
Cells were grown in BG-11 medium under control (dark grey) or stress conditions (light grey). Tocopherols were extracted and analysed by HPLC. Data are means ± SD of 3 or 4 measurements. The asterisks (*) indicate significant differences to WT ($p < 0.05$).

3.8. Feeding Phytol to *Synechocystis* Strains

It was shown before that *Synechocystis* WT cells accumulate more FAPEs when they are grown under stress conditions than when they are grown under normal conditions (3.5). To enhance the accumulation of fatty acid phytyl ester even more, the WT, *Δslr1807* and *Δslr2103* strains were fed with phytol. To this end, WT, *Δslr1807* and *Δslr2103* were grown in 100 ml BG-11 medium under control conditions until OD_{750} of ~1. Then, 0.1% (v/v) phytol was added and the cultures were incubated under the same conditions for 12h. The 12 hours incubation time was chosen because longer incubations with phytol proved to be toxic to the cells. Cell growth was affected after 12h of the addition of phytol, as the growth curves show in Figure 3.13 After the feeding experiment, cells were harvested by centrifugation, cell pellets were washed several times with fresh BG-11 medium to reduce the excess phytol, and lipids were extracted from the cells. The results show that *Synechocystis* cells are able to uptake free phytol from the medium and redirect it into FAPEs without adding any detergent. The added amount of phytol enhanced the accumulation of FAPEs in the WT compared to the control samples (WT without phytol feeding) (Figurer 3.14). FAPE content increased in *Synechocystis* WT about fourfold after feeding with phytol. The fatty acid

composition of FAPEs in the WT after phytol feeding differed from that in the WT without phytol feeding under normal conditions. 18:1-phytol was the dominant fatty acid in the WT FAPEs after phytol feeding instead of 16:0-phytol in the WT samples without phytol feeding. However, the phytol feeding process did not lead to any increase in fatty acid phytyl ester levels in the two mutants *Δslr1807* and *Δslr2103* (Figure 3.15).

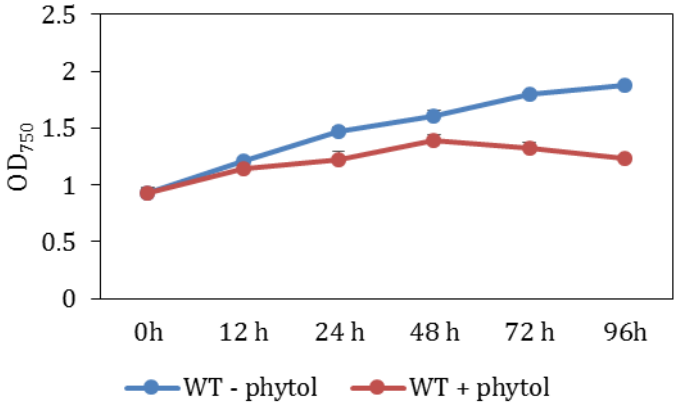

Figure 3. 13: Growth curves of *Synechocystis* sp. PCC 6803 WT in the presence of 1% of phytol.
Mean and SD values were calculated from three independent experiments.

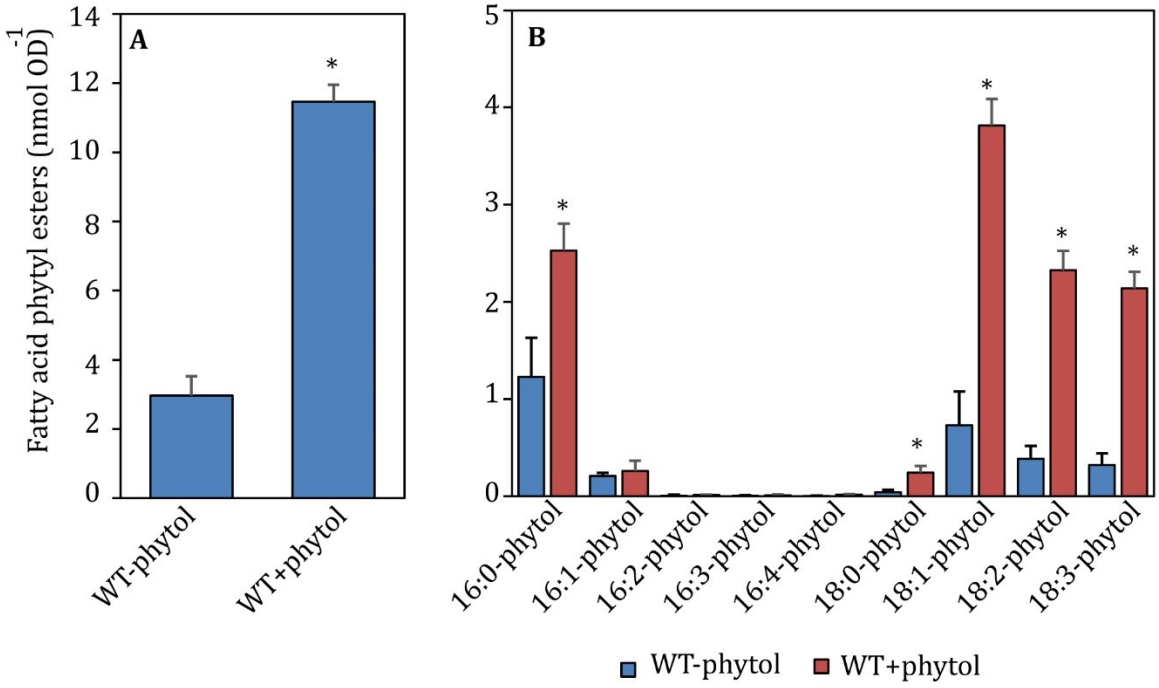

Figure 3. 14: Fatty acids phytyl ester content in *Synechocystis* sp. PCC 6803 WT.
(A) Total FAPEs content with or without feeding of 0.1% of phytol. **(B)** Fatty acid distribution of FAPEs with and without phytol feeding. Mean and SD values were calculated from three or four independent replicates. Error bars in graph (A) were calculated as the square root of the sum of squares of the individual molecular species. Asterisk (*) indicates significant differences to the wildtype when P< 0.05.

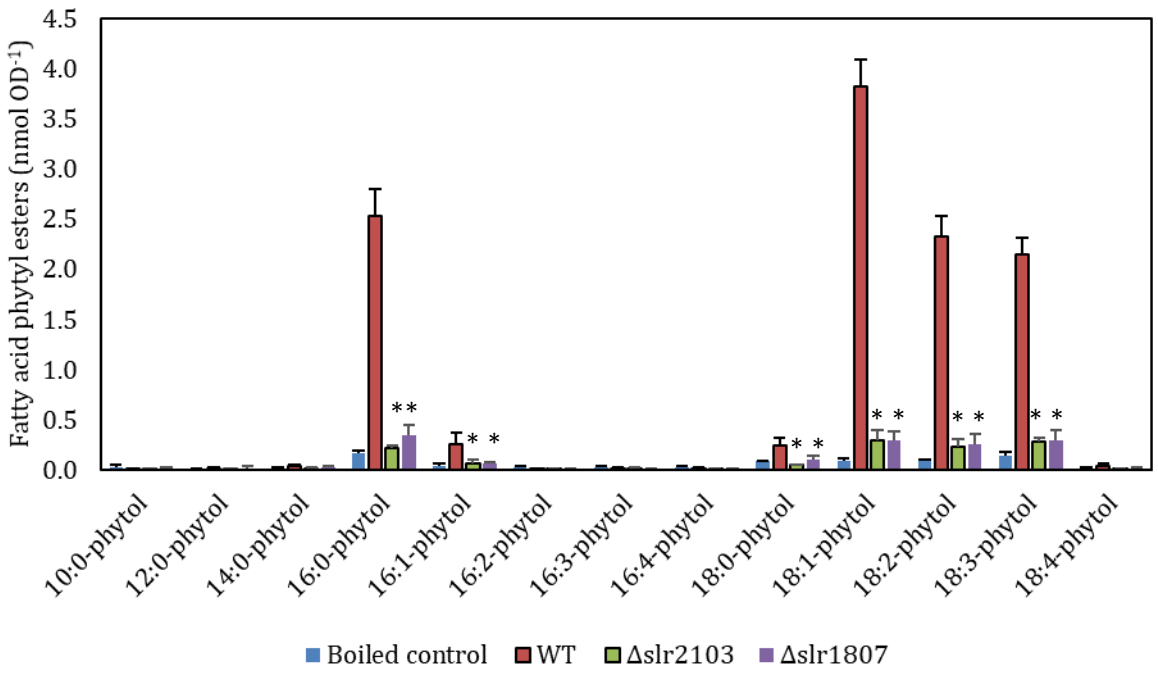

Figure 3. 15: Fatty acids phytyl ester content in *Synechocystis* WT, Δ*slr1807* and Δ*slr2103.*
Cultures were grown in BG-11 medium until OD_{750} of 1. Then 0.1% phytol was added and the cultures were incubated for 6h. FAPEs were measured by direct infusion Q-TOF MS/MS. A boiled culture was used as negative control. Mean and SD values were calculated from three or four independent replicates. Asterisk (*) indicates significant differences to the wildtype when $P < 0.05$.

3.9. Characterization of an Additional slr2103-dependent Lipid

The separation of the neutral lipids, which were extracted from the *Synechocystis* lines, by TLC, reveals two bands representing two unknown lipids (U1 and U2) which co-migrate with the triacylglycerol (TAG) standard (Figure 3.16 left). U1 and U2 appear in the WT and the hydrolase mutant (Δ*slr1807*). Only U1 but not U2 is detectable in the acyltransferase mutant (Δ*slr2103*) (Figure 3.16 left). To enhance the accumulation of the unknown lipids on the TLC plate, lipids were extracted from 200 ml cultures of the three *Synechocystis* lines. The lipid extract was applied to a silica SPE column in chloroform. Then, a second SPE separation on another silica column was performed to further separate the lipid classes (see 2.3.3.2). After that, the lipids from the two fractions of hexane/diethyl ether (99:1) and (92:8) (v/v) collected from the second column were separated again on a TLC plate which was developed with hexane/diethyl ether/acetic acid 70:30:1 (v/v/v). Interestingly, the unknown lipid (U2) was found in the fraction hexane/diethyl ether 92:8 (v/v) where the TAGs are normally found. To identify the neutral lipid which accumulates in *Synechocystis* WT and is absent from the *slr2103* mutant, the band was scrapped from the TLC plate. Lipids were extracted from the silica material with 2 ml chloroform/methanol 2:1 (v/v). Thereafter, the extract was washed with ammonium acetate and phase separation was obtained by centrifugation. The organic phase was collected, dried and analysed by Q-TOF auto MS/MS. The Q-TOF MS/MS analysis did not provide any clear results on the nature of this lipid. It

is possible that the lipid was sticking to the silica material during the exposure to the air (about an hour) that was required to visualize the lipids on the TLC plate after staining with primuline. However, finding U2 in the hexane/diethyl ether 92:8 (v/v) fraction of the second SPE column suggested that it might be TAG.

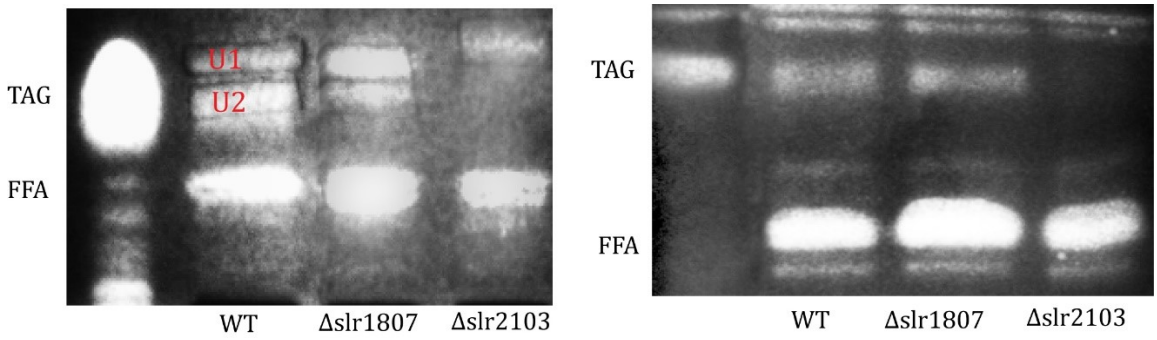

Figure 3. 16: One dimensional TLC of non-polar lipids from *Synechocystis* WT, Δslr1807 and Δslr2103.
Cells were grown in BG-11 and lipids were extracted and separated by TLC. **Left:** total lipid extracts were separated by TLC with hexane/diethyl ether/acetic acid 90:10:1 (v/v/v). **Right**: the SPE fraction of hexane/diethyl ether 92:8 (v/v) where TAGs usually elute was separated by TLC with hexane/diethyl ether/acetic acid 70:30:1 (v/v/v). Lipids were stained with primuline. FFA, free fatty acids; TAG, triacylglycerol. U1, U2, unknown lipids 1 and 2, WT, wild type.

3.9.1. Identification of Lipids Differentially Accumulating in *Synechocystis* WT and *Δslr2103* by Untargeted LC-MS

Untargeted LC-MS analysis was performed with lipid extracts from five biological replicas from each *Synechocystis* WT and the acyltransferase mutant *Δslr2103*. Analysing the raw data files obtained from LC-MS with the metabolomic and lipidomic platform (XCMS), allows to gain information about the metabolites which are up or down regulated in the *Δslr2103* mutant compared to the WT. The untargeted metabolomics resulted in hundreds of peaks in each LC-MS run. These peaks are defined by their mass to charge ratio (*m/z*) and retention time (r). Many peaks can be derived from the same metabolite due to the presence of adducts, the in- source fragmentation or degradation of the ions (Varghese et al. 2012; Wang et al. 2019). To minimize this problem, XCMS provides a filtering system which allows to combine the different peaks into a so-called feature. Some of the features that are dysregulated (*P*-value ≤0.01 and with a fold change greater than 3folds) are displayed in Table 10. The (*m/z*) values of the downregulated features (decreased in the *Δslr2103* samples) 825.7091, 827.7239, 833.7527, 849.7076, 851.7230, 853.7312 could represent the masses of protonated TAG molecular species (Table 10).

Table. 10: (*m/z*) values of the downregulated features in Δ*slr2103.*
All features with *P*-value ≤ 0.01 and fold change greater than 3fold are shown. The masses could represent protonated triacylglycerol species.

TAG species	$(m/z) + H^+$ Calculated	$(m/z) + H^+$ Measured	rt	Up/down	Fold-change	*P*-value
50:5	825.6972	825.7091	48.30	DOWN	31.42	0.00624
50:4	827.7128	827.7239	50.08	DOWN	63.20	0.00176
50:1	833.7598	833.7527	53.85	DOWN	3	0.00003
52:7	849.6972	849.7076	46.05	DOWN	153.3	0.00187
52:6	851.7128	851.7230	49.21	DOWN	41.47	0.00338
52:5	853.7285	853.7312	49.21	DOWN	35	0.00785

The features corresponding to these masses accumulate in the five WT samples and they are strongly reduced in the five *Δslr2103* mutant samples. They have different intensities and similar retention times ranging between 46 and 53 minutes (Figure 3.17). This finding represents first evidence that *Synechocystis* WT might accumulate TAGs.

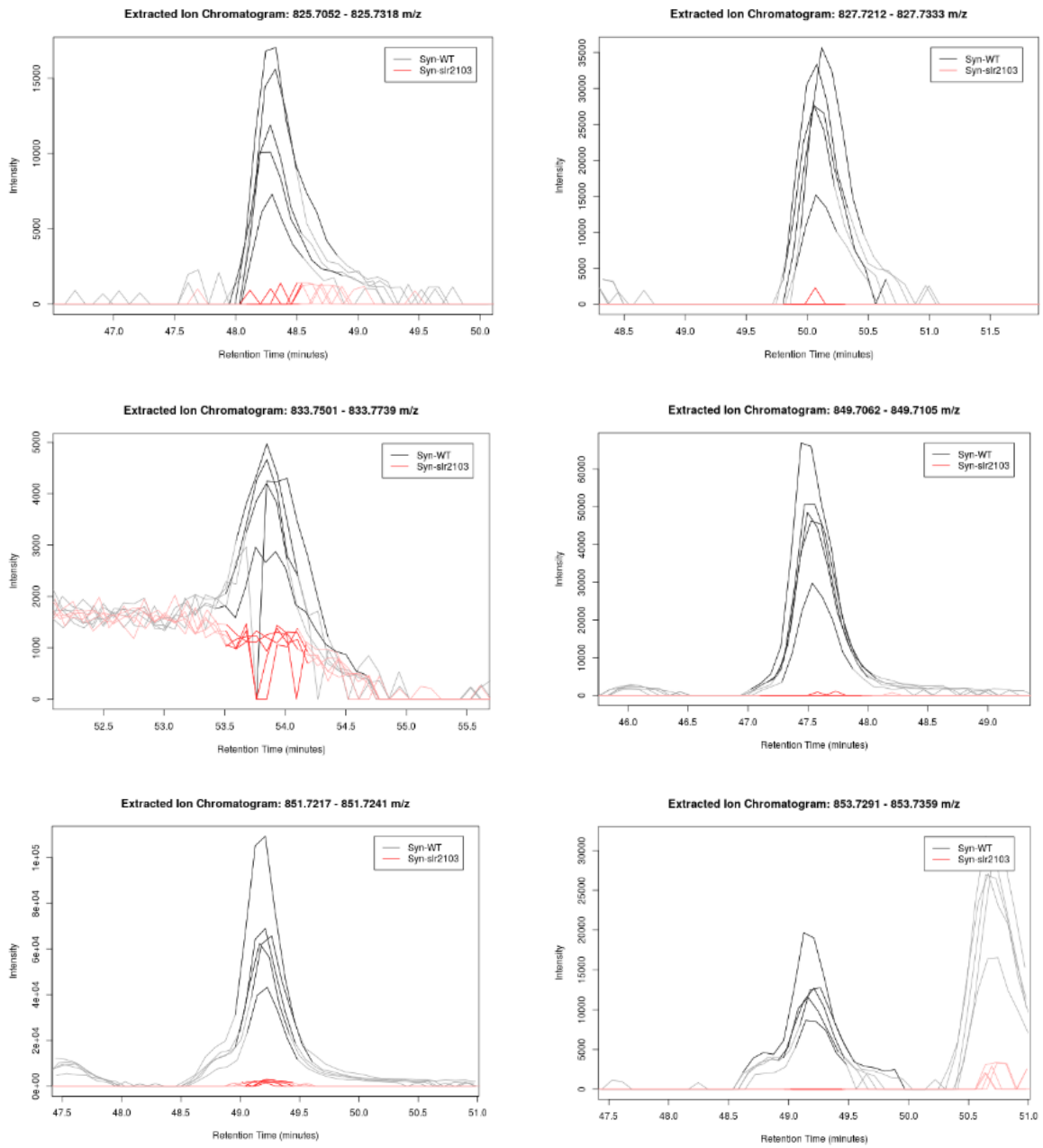

Figure 3. 17: Extracted Ion Chromatograms for selected features that are downregulated in *Δslr2103*. Features with *P*-value ≤ 0.01 and fold change greater than 3 folds are shown. All the presented features accumulate in the wild type samples (black) but not in the mutant Δ*slr2103* (red). These graphs were produced with the XCMS online software.

3.9.2. Triacylglycerol (TAG) is Synthesised in *Synechocystis* in an slr2103 Dependent Manner

TAGs were found in the filamentous and the thermophilic cyanobacteria which belong to the order Nostocales (Hu et al. 2008; Tarante et al. 1993; Peramuna and Summers 2014; Řezanka et al. 2012). To confirm the existence of TAG accumulation, lipids were extracted from *Synechocystis* cultures (WT and Δ*slr2103*) grown in BG-11 medium. Non-polar lipids were isolated by SPE and analysed by Q-TOF MS/MS in the positive mode. The analysis revealed the presence of about 14

different peaks presumably derived from ammonium adducts of TAGs in the WT. After MS/MS fragmentation, protonated diacylglycerol ions were formed with a neutral loss of fatty acid ammonia adducts (Figure Appendix 7.2.2). The MS/MS analyses for the WT samples confirmed the presence of TAG with a total amount of ~5 nmol OD_{750}^{-1}. The dominant molecular species were 48:0 (tri-16:0 TAG) and 50:3 (di16:0-18:3 TAG) (Figure 3.18). However, the total amount of TAGs in the Δ*slr2103* was almost 15fold decreased, and all the molecular species found in the WT were reduced to background levels (Figure 3.18). This leads to the conclusion that *Synechocystis* accumulates TAG in an slr2103-dependent manner.

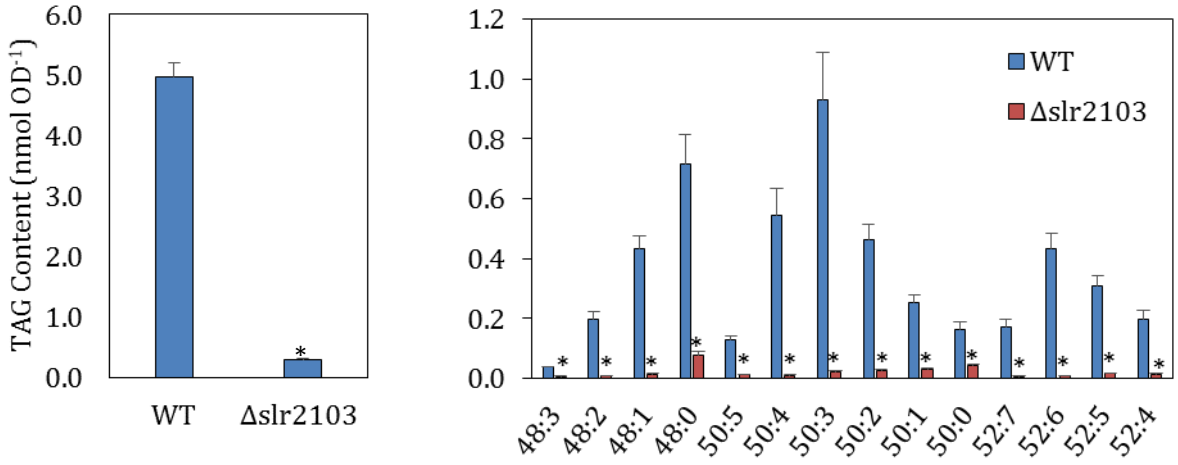

Figure 3. 18 Triacylglycerol accumulation in *Synechocystis.*
The cultures were grown in BG-11 medium. Lipids were extracted, triacylglycerol was purified and analysed by Q-TOF MS/MS. Total amount of TAGs (left) and the molecular species composition of TAGs (right). Mean and SD values were calculated from 4 independent replicates. Error bars for the total TAG amount were calculated as the square root of the sum of squares of the individual molecular species. Asterisk (*) indicates significantly differences to the wildtype when $P < 0.05$.

3.10. The Number of Lipid Droplets is Reduced in *Δslr2103* Cells

The chloroplasts of plants contain plastoglobules which are lipid droplets. They are associated with the thylakoid membrane and they are believed to serve as storage for neutral lipids like tocopherol, phytyl esters and TAGs (Besagni and Kessler 2013; Lippold et al. 2012). Such lipid droplets were also described to accumulate TAGs, tocopherol, alkanes and minor amounts of phytol acetate in the cyanobacterium *Nostoc punctiforme* (Peramuna and Summers 2014). To determine whether the reduction in FAPEs and TAGs is accompanied with a reduction in the number of the lipid droplets, WT and Δslr2103 cells were studied by transmission electron microscopy. Lipid droplets as well as other subcellular structures like thylakoids, carboxysomes and cell membranes were clearly observed (Figure 3.20A). Lipid droplets were counted per cell

cross section in 50 cells each of WT and Δslr2103. Interestingly the number of the lipid droplets per cell in *Δslr2103* decreased to about 50% of the number in the WT (Figure 3.19B, C and 3.20).

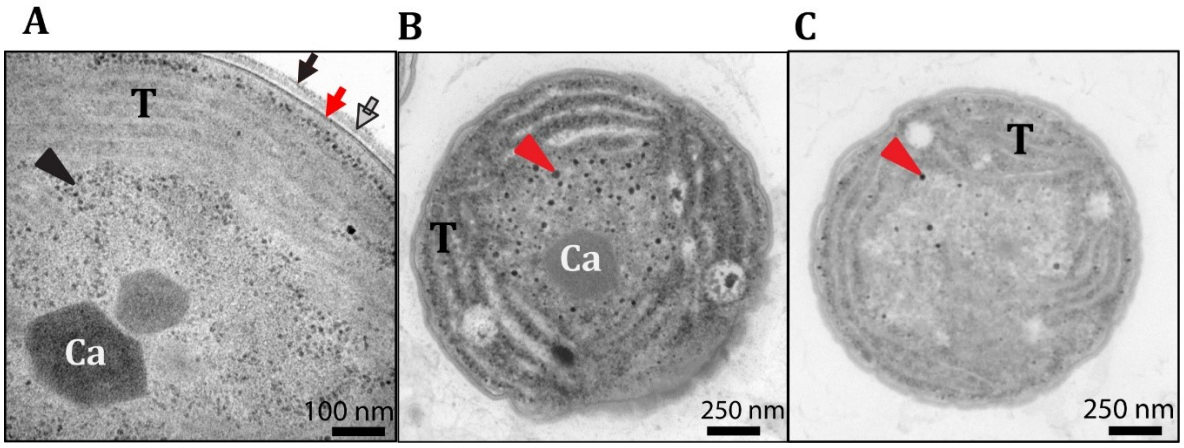

Figure 3. 19: Ultrastructure of a *Synechocystis* cell.
The photos were taken with the transmission electron microscope. **(A)** The WT cell displays the outer membrane (black arrow), the plasma membrane (red arrow) and the periplasmic space (grey arrow) in between. The thylakoid membranes (T) are visible in the cytoplasm. The photo also shows a carboxysome (Ca) and ribosomes (black arrowhead). **(B and C)** WT and Δslr2103 cells, respectively, show the lipid droplets with a reduced number of lipid droplets in the mutant (red arrowheads).

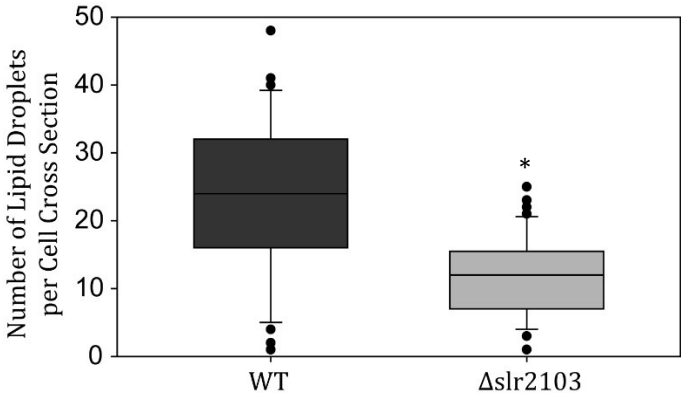

Figure 3. 20: Box plot indicates the number of lipid droplets per cell cross section was counted in 50 cells.
The box plot shows the median, the upper and lower quartile, the 10th and 90th percentile and outliers (dots). Asterisk (*) indicates significant differences to the wildtype when P< 0.05.

3.11. Heterologous Expression of slr1807 and slr2103 in *E. coli*

In this study, the fatty acid phytyl ester and the triacylglycerol biosynthesis pathways from *Synechocystis* were expressed in *E. coli* BL21 (AI) in a functional active state. To this end, slr1807 was cloned in the expression vector pACYC-31, and slr2103 was cloned in the expression vector pQ-80L. *E. coli* cultures containing pACYC-slr1807, pQ-80L-2103 or both plasmids for co-expression as well as *E. coli* cells harbouring the empty vector, were grown to the logarithmic phase. Protein expression in the cultures was induced with 0.5 mM IPTG and 0.1% arabinose at an OD_{600} of 0.6, and the cells grown at 16°C overnight. The expression efficiency was determined via SDS-PAGE and western blot. The Coomassie stained gel showed a strong expression of slr2103.

The slr2103 protein from the single and co-expression cells accumulated on SDS gels showing a strong band at ~32 kDa, which is close to the calculated weight of slr2103 (with His_6 tag, 34.0 kDa). This band is absent in the empty vector cells (Figure 3.21). On the other hand, the band of slr1807 protein (~29 kDa) was not visible on the SDS gel, but it showed a clear band after immunoblot analysis with anti-His tag detection kit (Figure 3.21). The activity of slr1807 and slr2103 in *E. coli* as phytyl ester and TAG synthase was determined by performing phytol or diacylglycerol feeding assays as well as an *invitro* enzyme assays.

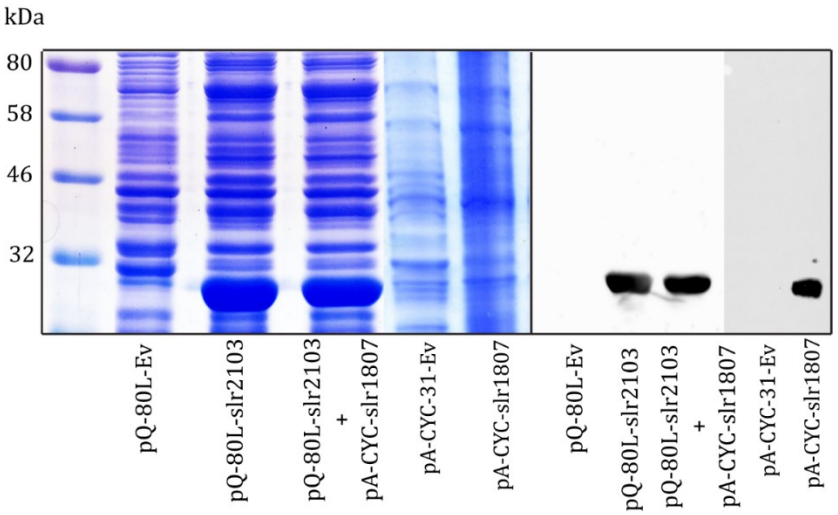

Figure 3. 21: Expression of slr2103 and slr1807 in *E. coli.*
SDS-PAGE stained with Coomassie (left) and western blot (right). slr1807 and slr2103 with an N-terminal His tag were expressed in *E. coli*. Total protein was extracted from *E. coli* cells containing either the empty vectors (EV), single expression (pQ-80L-slr2103, pA-CYC-slr1807) or the co-expression (pQ-80L-slr2103 + pA-CYC-slr1807) vectors.

3.11.1. Feeding Phytol to *E. coli*

For phytol feeding assays, 0.1% (v/v) phytol was incubated for three hours with *E. coli* cultures expressing slr2103, slr1807, or the co-expression of both proteins in addition to cells harbouring the empty vectors. Thereafter, lipids were extracted, purified and analysed by Q-TOF MS/MS. The phytol feeding assay shows five and four times more FAPEs accumulation in the co-expression and the single expression of slr2103, respectively compared to the empty vector (Figure 3.22 left). However, there is no FAPEs accumulation in the single expression of the hydrolase slr1807 (data not shown).

The feeding assay was performed with or without adding a detergent (CHAPS). The result shows an at least 3fold higher FAPE accumulation when CHAPS was added at the same time with phytol (only data after adding CHAPs are shown here). The fatty acid composition of FAPEs showed that 18:1-phytol is the most abundant phytyl ester with 12 nmol per OD (Figure 3.22 right) although 18:1 constitutes only 3.4% of total fatty acid composition in *E. coli* when grown at 30°C (Marr and Ingraham 1962).

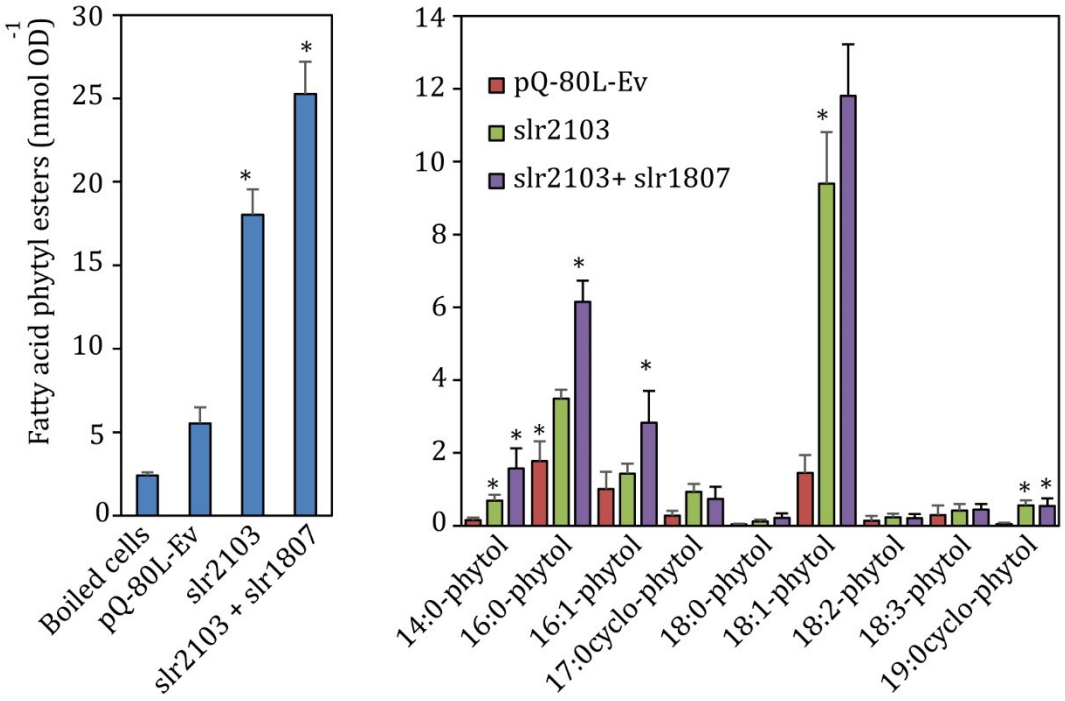

Figure 3. 22: Fatty acid phytyl ester accumulation after the expression of slr2103 and the co-expression with slr1807 in *E. coli.*
Protein expression of the cultures was induced with IPTG and arabinose. The cells were incubated with phytol for 3 h. Lipids were extracted, purified and analysed by Q-TOF MS/MS. Total fatty acid phytyl esters in the boiled cell control, the empty vector, the single expression of slr2103 and the co-expressing with slr1807 are shown (left). The molecular species composition of FAPEs (right) were measured. Mean and SD values were calculated from 3-4 independent replicates. Error bars for the total amounts of FAPEs were calculated as the square root of the sum of squares of the individual molecular species. Asterisk (*) indicates significant differences to the wildtype when $P < 0.05$.

3.11.2. Feeding Diacylglycerols to *E. coli* cells expressing slr2103

In the same manner, a mixture of 30 µM of each of the two DAGs, i.e. the short-chain DAG, dioctanoin (di8:0-DAG) and the long-chain DAG dipalmitin (di16:0 DAG) were incubated with *E. coli* cultures expressing the acyltransferase slr2103, in the presence of CHAPS. The *E. coli* strains do not accumulate any TAG. The results show that the *E.coli* cells expressing slr2103 were able to uptake the DAG molecules and use them as substrate to produce TAGs. The total amount of TAGs in the empty vector cells, the media control and the boiled cells expressing slr2103 were very low (~3 nmol per OD). The low amounts of TAGs in these controls could be derived from the LB medium. However, the amount of TAGs accumulated in the cells expressing slr2103 and was significantly higher with a value of ~20 nmol per OD (Figure 3.23).

Due to its higher solubility in water, di-8:0 DAG was used by the cells faster than di-16:0 DAG. Therefore, most of the accumulated TAGs originate from acylation of di-8:0 DAG rather than di-16:0 DAG. The acyltransferase slr2103 was able to esterify the bacterial fatty acids 14:0, 16:1, 18:0

and predominantly 16:0 and 18:1. Less TAG was detected originating from the di-16:0 DAG. In fact, only tri-16:0 and a low amount of 18:0 di-16:0 TAG were detected (Figure 3.23 right).

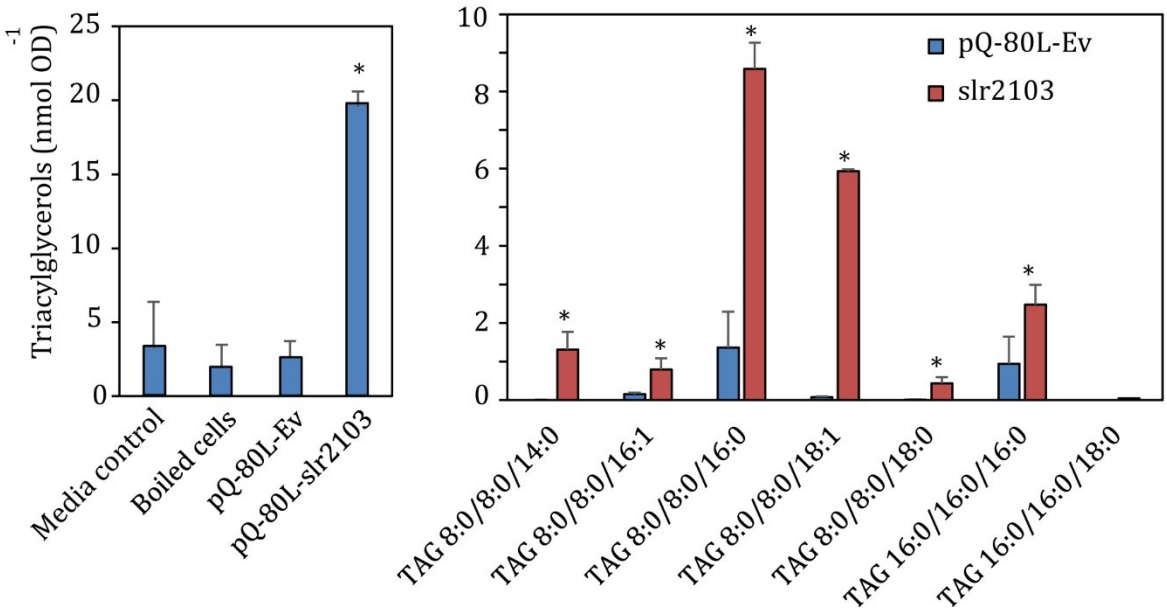

Figure 3. 23: Triacylglycerol accumulation in *E. coli* after the expression of slr2103.
Protein expression was induced with IPTG and arabinose and incubated with diacylglycerols for 3 h. Lipids were extracted, purified and analysed by Q-TOF MS/MS. The left panel shows the total TAG. The molecular species composition of TAGs is shown in the right panel. Mean and SD values were calculated from 3 independent replicates. Error bars in the graph (left) were calculated as the square root of the sum of squares of the individual molecular species. Asterisk (*) indicates significantly differences to the wildtype when $P< 0.05$.

3.11.3. *In vitro* Enzyme Assay with the Recombinant slr2103 Acyltransferase

An *in vitro* enzyme assay was performed to test the fatty acid phytyl ester and TAG synthase activities of slr2103. To this end, the microsomal membrane proteins of *E. coli* cells expressing slr2103 were isolated and supplied with phytol or di-8:0 DAG and an acyl donor (16:0-CoA, 18:0-CoA, 16:0-ACP, 16:0 free fatty acid). Moreover, the ability to transfer the fatty acids derived from the spinach MGDG (16:3 and 18:3) to phytol or DAG was also tested (Figure 3.24A and 3.24B).

The phytyl ester synthesis activity of slr2103 was in general low. However, 16:0-phytyl ester production with 16:0-CoA was significantly higher than with protein from an empty vector control with an activity of 1.9 pmol min^{-1} mg^{-1} protein. The activity with 16:0-ACP or 16:0 free fatty acid was very low and similar to the empty vector levels. The activity of slr2103 with MGDG was very low.

Next, *in vitro* DAG acyltransferase activity (TAG synthesis) was measured with microsomal membrane proteins isolated from *E. coli* cells expressing slr2103. 18:0-CoA and 16:0-CoA were the preferred acyl donors of slr2103 for esterification of di8:0-DAG with activities of 44.4 pmol min^{-1} mg^{-1} protein and up to 300 pmol min^{-1} mg^{-1} protein, respectively. The other acyl donors

(16:0-ACP, 16:0 free fatty acid or fatty acids derived from MGDG) showed similar, low activity as the empty vector control.

It was expected that the slr1807 might hydrolyse the fatty acids from MGDG when MGDG was used as a fatty acid donor in the enzyme assay. Consequently, more substrate would be available to be esterified by slr2103. Unfortunately, the combination of slr2103 and the hydrolase slr1807 did not result in an increase neither in the phytyl ester nor TAG synthesis activity (Figure 3.24C).

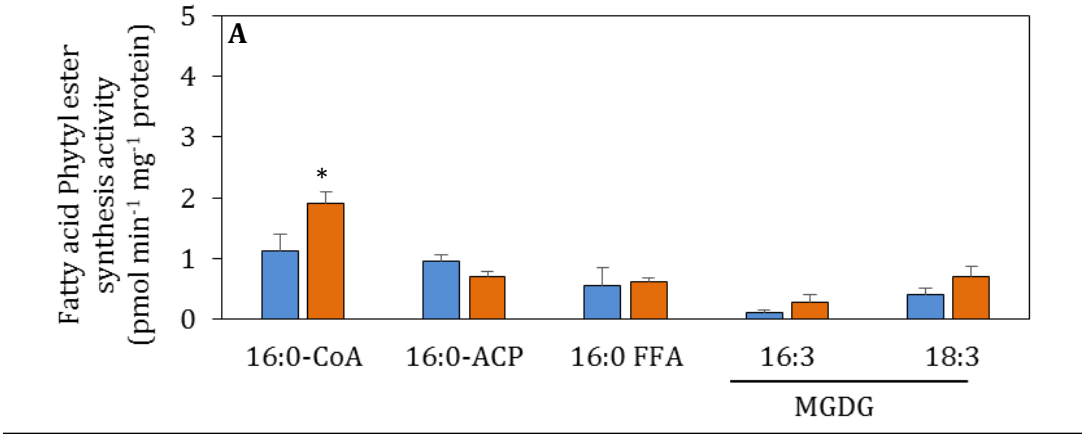

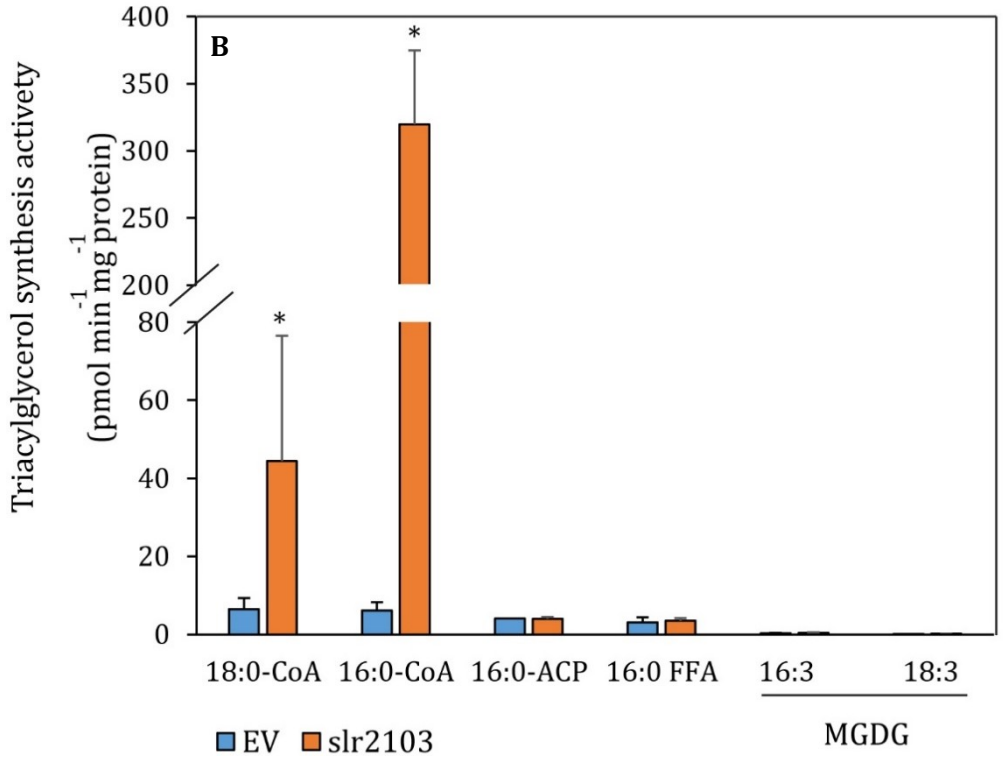

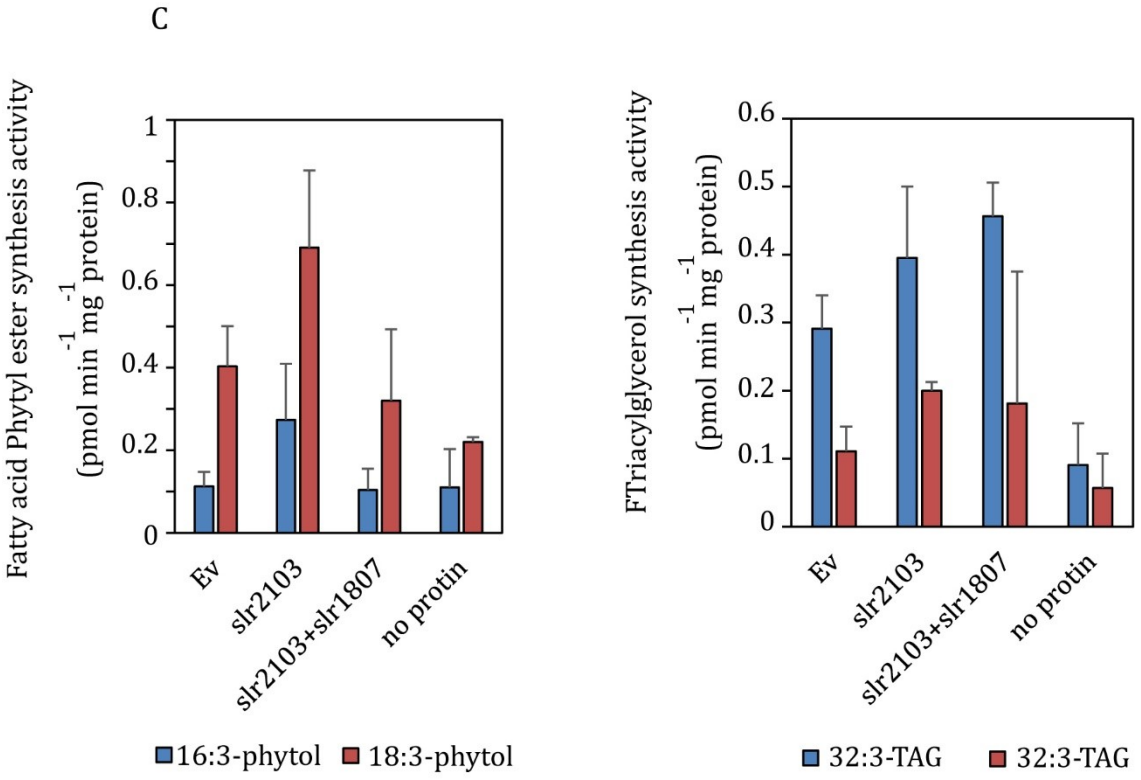

Figure 3. 24: Enzyme assay with recombinant protein from *E. coli* expressing slr2103 or slr1807. The slr2103 protein harbours fatty acid phytyl ester and diacylglycerol acyltransferase synthase activity**.** Membrane proteins were isolated from *E. coli* cells expressing slr2103 and employed for: **(A)** acyltransferase assays with phytol and different acyl donors. **(B)** diacylglycerol acyltransferase (DGAT) assays with dioctanoin and different acyl donors. **(C)** acyltransferase assays with phytol (left) and dioctanoin (right) MGDG from spinach was used as an acyl donor, the co-expression with slr1807 is also included here.

3.12. A Processive Galactosyltransferase from *Blastochloris viridis* Related to Plant-like MGDG Synthase

Chloroplasts of plants harbour several proteins whose genes are originally derived from the cyanobacterial progenitor. This set of proteins includes the phytyl ester synthase PES2 and the orthologous acyltransferase slr2103 from *Synechocystis*. As shown above, slr2103 is involved in TAG and phytyl ester synthesis. Similarly, previous searches for bacterial sequences with similarity to the plant MGDG synthase MGD1 revealed sequences, e.g. BviMgdP and BviMgdN from the purple bacterium *B. viridis* (Hölzl unpublished). BviMgdP harbours a processive glycosyltransferase activity because it can perform serial galcatolysation steps with DAG as the primary acceptor. For further characterisation, BviMgdP was introduced in *A. thaliana* plants lacking galactolipids.

3.12.1. The Processivity of the Bacterial Galactosyltransferase BviMgdP

Expressing BviMgdP in *E. coli* shows that it synthesizes ββDGDG without releasing βMGDG (Hölzl, unpublished). The BviMgdP enzyme is capable of adding two galactose units in series to DAG as the primary acceptor with β-anomeric configuration of the two galactose units to produce ββDGDG (Hölzl, unpublished) (Figure. 1.7). To confirm this hypothesis, the processive activity of the BviMgdP was verified by an *in vitro* enzyme assay (2.3.2.1.3). The crude protein was used for a glycolipid glycosyltransferase assay with UDP-Gal and di18:2 DAG as a sugar donor and acceptor, respectively. The galactolipid lipid production was recorded by direct infusion Q-TOF MS/MS. The results demonstrated a high production of DGDG and a minor amount of MGDG by the enzyme BviMgdP (Figure 3.25). This assay was performed as preliminary work only once with one replica.

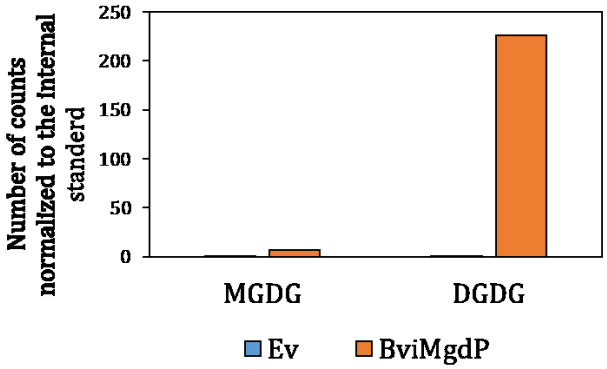

Figure 3. 25: Glycosyltransferase enzyme assay with recombinant protein from *E. coli* cells expressing BviMgdP.
Crude proteins were isolated from *E. coli* cells expressing BviMgdP and employed for glycosyltransferase assays with UDP-Gal and di18:2-DAG as substrates. The assay shows that BviMgdP produces DGDG, and only low a very amount of MGDG when UDP-Gal and di18:2 DAG are used as substrates. The results are shown as number of counts normalized to the internal standards. The assay was performed as preliminary work with only one replica.

3.13. Introduction of Bacterial ββDGDG Results in Complementation of Growth Deficiency of the *Arabidopsis dgd1* Mutant

The production of ββDGDG in *E. coli* expressing the BviMgdP enzyme was confirmed by NMR to have two β anomeric linkages (Hölzl, unpublished). Therefore, the expression of the bacterial MGDG synthase BviMgdP is expected also to accumulate ββDGDG in other *in vivo* systems like plants. To determine the ability of the bacterial ββDGDG to substitute the plant αβDGDG *in vivo*, the BviMgdP ORF sequence was fused behind an N-terminal chloroplast targeting sequence to ensure that the protein would be active in the inner envelope of the chloroplast (Hölzl et al. 2006a).

In *Arabidopsis*, MGD1 and DGD1 are located in the inner and the outer envelope of the chloroplast, respectively. The lipid trafficking between the inner and the outer envelope includes the transfer of MGDG produced by MGD1 to the outer envelope where DGD1 is located. The N-terminal domain of DGD1 is involved in this lipid transfer, especially in the translocation of αβDGDG from the outer to the inner envelope. This transport of αβDGDG back to the inner envelope is important, because only lipids from the inner envelope can be transferred to the thylakoids (Kelly et al. 2016). BviMgdP was targeted to the inner chloroplast envelope where the produced ββDGDG could accumulate in the thylakoids (Figure 3.26).

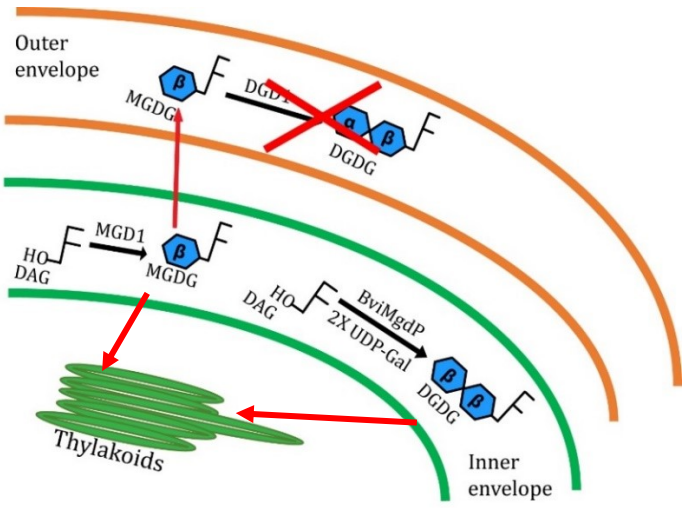

Figure 3. 26: Simplified scheme representing the localisation of the bacterial BviMgdP and DGDG synthesis pathway in the transgenic Arabidopsis *dgd1* plants.
The red X indicates the blocked αβDGDG synthesis pathway in the Arabidopsis *dgd1* mutant. Arrows indicate the MGDG and DGDG trafficking between the inner and the outer envelope or the thylakoid.

The bacterial BviMgdP was introduced into the *dgd1* mutant by floral dipping with *Agrobacterium tumefaciens* (2.3.2.5.3). The DsRed fluorescent protein from *Discosoma* sp. was used as a positive selection marker. Cells expressing DsRed emitted a red bright fluorescence

when illuminated with green light (Jach et al. 2001). The resulting transgenic seeds were selected by DsRed fluorescence under a binocular fluorescence microscope. Previous results demonstrated that the *dgd1* mutant plants of *Arabidopsis* showed an up to 90% reduction of the DGDG content when grown under full nutrition. Furthermore, *dgd1* plants show dwarfed growth, reduction of the chlorophyll content and loss in photosynthetic activity (Dörmann et al. 1995; Dörmann et al. 1999). The transformed *dgd1*-BviMgdP plants accumulated DGDG (four different transgenic lines; only line number 2 is shown in Figure 3.27). The accumulation of sufficient amounts of DGDG in the thylakoids is demonstrated by the WT-like appearance of the trans formed *dgd1*-BviMgdP plants (Figure 3.27). Simultaneously, the chlorophyll content was restored in *dgd1* plants expressing BviMgdP, and the Chl *a*/*b* ratio was altered such that it was nearly at WT levels (Figure 3.28).

Total lipids were extracted from at least three different leaves belonging to three different *Arabidopsis* plants of each line. Lipids were separated on by TLC and visualised by α-naphthol-sulfuric acid staining (2.3.3.3) (Figure 3.29).

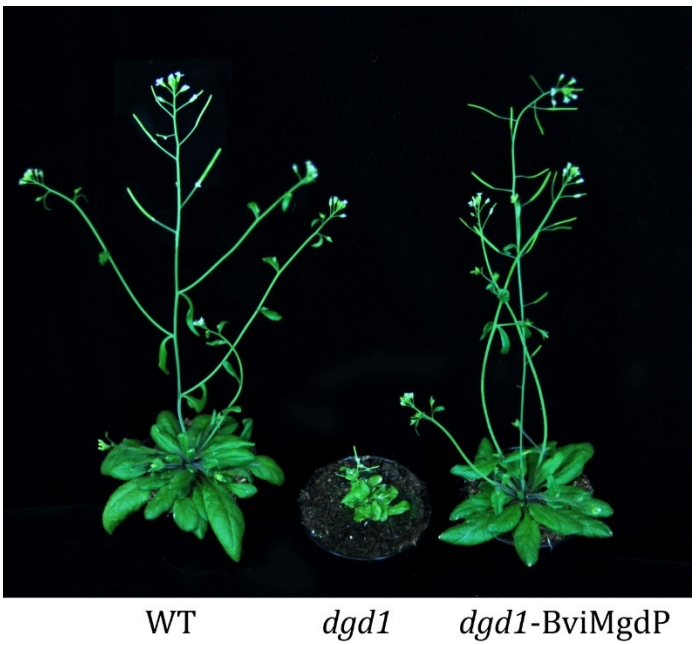

Figure 3. 27: Complementation of the growth deficiency of the *Arabidopsis dgd1* mutant by expression of the processive glycosyltransferase BviMgdP from *Blastochloris viridis*.
Plants were grown for 6 weeks. Expression of BviMgdP in *dgd1* (*dgd1*-BviMgdP) led to the complementation of the *dgd1* growth phenotype.

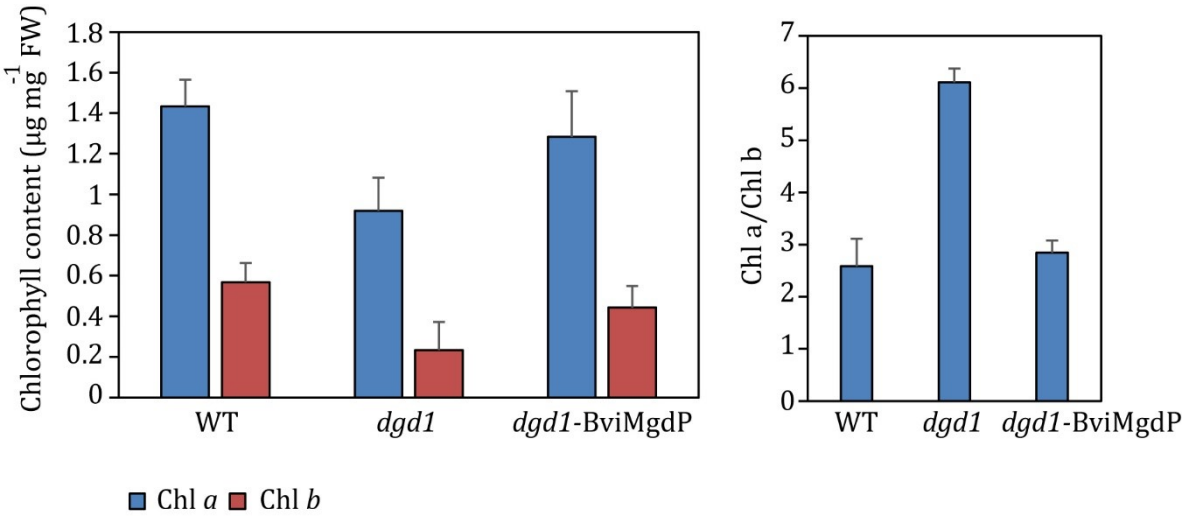

Figure 3. 28: Chlorophyll contents of leaves of wild type, *dgd1*, and *dgd1*-BviMgdP.
The left panel shows chlorophyll *a* and *b* contents, and the right panel the chlorophyll *a*/*b* ratio. Mean and SD values were calculated from 3 independent replicates.

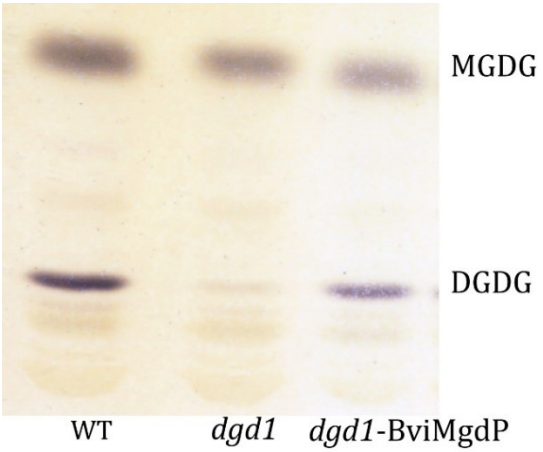

Figure 3. 29: One dimensional TLC of leaf lipid extracts from *Arabidopsis* wild type and mutant lines.
Expression of the processive glycosyltransferase BviMgdP in *dgd1* leads to the accumulation of a glycolipid co-migrating with DGDG from WT, while DGDG in *dgd1* is hardly detectable. The glycolipids were stained with α-naphthol sulfuric acid.

For a closer look on the lipid profile, the extracted lipids were also analysed with Q-TOF MS/MS. Different galactolipids, phospholipids, and sulfolipids were identified according to their fragmentation patterns resulting from ionisation of the molecules in a targeted approach. The fragment ions and neutral losses are characteristic for the respective lipids. In the case of glycolipids they are characterized by a neutral loss (difference of *m/z* of DAG and parent ion) representing the mass of the sugar head group as an ammonium adduct (Appendix 7.2.3).

While the absolute amounts of MGDG were similar in the WT and the transformed lines ~70 nmol per mg dry weight (DW), the amount of MGDG in *dgd1* plants was about 40 nmol per mg DW (Figure 3.30A). This reduction in the absolute amount of βMGDG can be due to the decrease in thylakoid membrane abundance of *dgd1* plants. However, the mol% βMGDG content was reduced by almost 7% in the transformed plants compared to the WT and the *dgd1* plants. This can be explained by the competition between MGD1 and BviMgdP enzymes for DAG as a substrate to produce βMGDG and ββDGDG, respectively (Appendix Figure 7.6). Blocking the αβDGDG pathway in the chloroplasts of the *dgd1* plants led to the accumulation of the 36:6-βMGDG which is the preferred substrate for DGD1 (Klaus et al. 2002; Kelly et al. 2003). This increase in the 36:6-βMGDG in *dgd1* is accompanied with a reduction in the 34:6-βMGDG content such that the total amount of βMGDG remains constant and similar to the WT levels (Kelly et al. 2003). The absolute amounts of the βMGDG were increased after expressing the bacterial BviMgdP in the *dgd1* plants (Figure 3.30A and 3.30B). The increased βMGDG synthesis presumably leads to improved thylakoid membrane production in the complemented plant.

Interestingly, ββDGDG accumulated in the *dgd1*-BviMgdP line with higher amounts than in the WT (Figure 3.30A). This high accumulation rate of ββDGDG could be due to the expression of BviMgdP under the constitutive promoter 35S. Independently from the higher amounts of DGDG in *dgd1*-BviMgdP these plants also differ in molecular species composition of MGDG and DGDG, with a strong increase in 34:6-ββDGDG compared to the WT (Figure 3.30C). This accumulation in ββDGDG in *dgd1*-BviMgdP plants can be explained by the substrate specificity of BviMgdP which does not discriminate towards the different DAG species, while DGD1 in WT exhibits a high preference for MGDG with C18 at *sn*1 and *sn*2 to produce 36:6-αβDGDG. No significant changes were detected for the other measured lipids (Figure 3.30A).

.

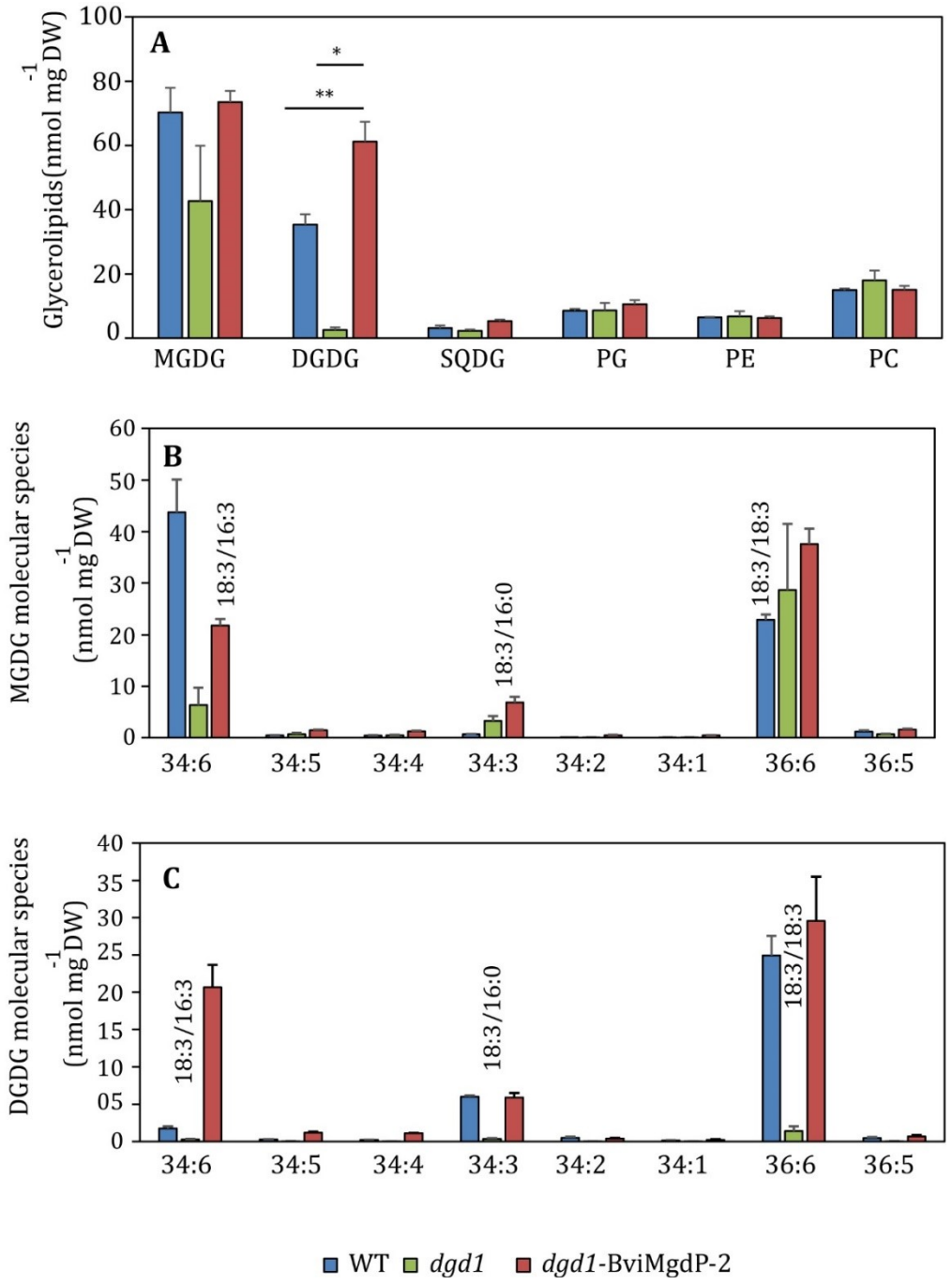

Figure 3. 30: Contents of membrane glycerolipids and the molecular species of MGDG and DGDG in Arabidopsis WT, *dgd1* and *dgd1*-BviMgdP.
(A) Glycerolipids were quantified in leaves of wild type, *dgd1*, and one line of *dgd1*-BviMgdP using direct infusion Q-TOF MS/MS. Data are shown in nmol per mg dry weight (DW). **(B)** The molecular species of MGDG in nmol per mg DW **(C)** The molecular species of DGDG in nmol per mg DW. The numbers over the bars indicate the fatty acid composition with *sn*1/*sn*2. Mean and SD values were calculated from 3 independent replicates.

3.13.1. The ββDGDG Content is Increased in the *dgd1*-BviMgdP Plants Growing under Phosphate Limitation

Phosphate deficiency is a major stress of plants. The role of αβDGDG as a surrogate lipid for phospholipids when phosphate is limited has previously been described (Härtel and Benning 2000). The phosphate limitation induces the expression of the two enzymes DGD1 and DGD2 and accordingly increases the synthesis of αβDGDG in wild type, and also the amount of αβDGDG is increased in *dgd1* produced by DGD2 (Kelly et al. 2003).

To study the response of *dgd1*-BviMgdP plants to phosphate starvation, the plants from the three lines WT, *dgd1* and *dgd1*-BviMgdP were grown firstly under normal conditions. Then they were transferred and grown on synthetic medium that either lacked or contained phosphate (control). The results showed that the transformed plants showed many yellow leaves compared to the wild type, indicating that they suffered more than the wild type. In fact, the complemented plants showed even more yellow leaves than the *dgd1* plants (Figure 3.31). Under phosphate replete conditions *dgd1*-BviMgdP plants grew like WT while *dgd1* mutants exhibited the stunted phenotype as described (Dörmann et al. 1995).

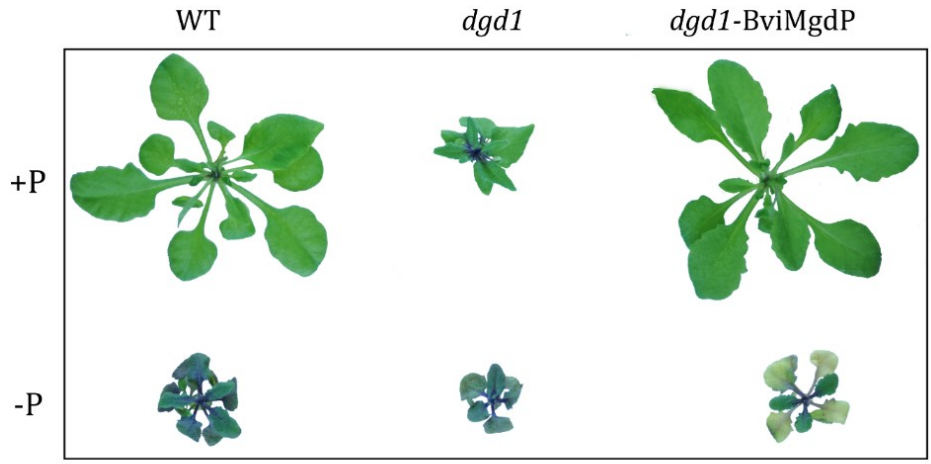

Figure 3. 31: *Arabidopsis* WT, *dgd1*, and *dgd1*-BviMgdP growing under normal conditions and under phosphate limitation.
The phenotype of *dgd1*-BviMgdP is similar to wild type under phosphate replete conditions, but *dgd1*-BviMgdP plants show severe stress symptoms (yellow leaves) compared with WT and even with *dgd1* when grow under phosphate limitation.

To show the relative changes in the lipid compositions between the WT, *dgd1* and *dgd1*-MgdP plants, lipids were extracted and quantified by Q-TOF MS/MS and data is shown here in mol% (Figure 3.32). The mol% of the total MGDG content in the transformed *dgd1* plants was similar to the WT with 50 and 40% under phosphate replete (P+) and phosphate starvation (P-), respectively (Figure 3.32A and C). The amount of 34:6-MGDG in *dgd1*-BviMgdP plants was reduced from 30 to 13% of the total MGDG when growing under P+ or P- conditions (Figure

3.32D). This reduction in 34:6-MGDG could be the plant's response to the increase in the 34:3-MGDG produced by MGD2 and MGD3 which are activated under phosphate limitation.

The observed increase in the αβDGDG and ββDGDG amount in the transformed plants growing under phosphate limitation is presumably derived from DGD2 (which is more highly expressed) and from BviMgdP which has more substrate available under phosphate deprivation because of the extra DAG released via phospholipid degradation (Figure 3.32A and 3.32C). The expression of BviMgdP cannot be induced during phosphate deprivation because it was cloned in the plant expression vector pBin-35S-Lnt-DsRed under the control of the constitutive 35S promoter which is not regulated by phosphate. This scenario is supported by another study where the bacterial lipid glucosylgalactosyldiacylglycerol (βGlcβGalDG) was introduced into *dgd1* plants by ectopic expressing a glucosyltransferase (CaGlcT) from *Chloroflexus aurantiacus* (Hölzl et al. 2009a). In that study, αβDGDG in the WT and the sum of αβDGDG and βGlcβGalDG in the *dgd1*-CaGlcT lines were similarly regulated when the plants were growing under phosphate limitation (Hölzl et al. 2009a).

The molecular species of αβDGDG and ββDGDG in the transformed lines also showed almost 10% reduction in the 36:4-αβDGDG accompanied by an increase in the 34:3-αβDGDG resulting in a αβDGDG accumulation rate close to the WT when growing under phosphate limitation (Figure 3.32A, C and E).

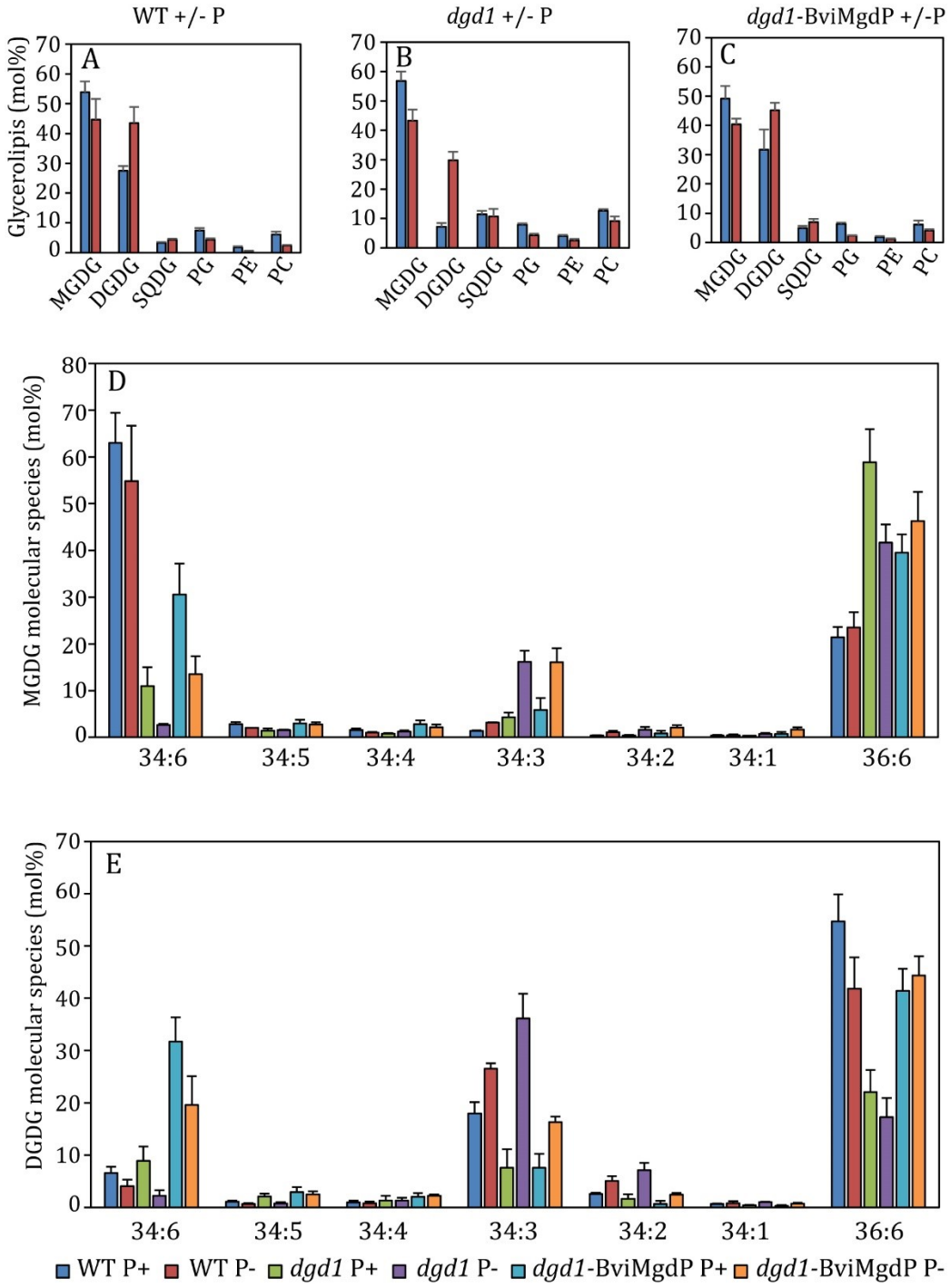

Figure 3. 32: Membrane glycerolipid composition and molecular species of MGDG and DGDG in mol% of WT, *dgd1* and *dgd1*-BviMgdP grown under phosphate replete and depleted conditions. **(A, B and C)** leaf glycerolipids from wild type, *dgd1*, and of *dgd1*-BviMgdP (line 2). The αβDGDG content is strongly increased in *dgd1*-BviMgdP and exceeds the αβDGDG level of the WT. Phosphate deprivation leads to increased αβDGDG contents in all three lines. **(D)** βMGDG with intermediate levels of 34:6 and 36:6 species in *dgd1*-BviMgdP compared to WT (high levels of 34:6; lower levels of 36:6) and *dgd1* (lower levels of 34:6; higher levels 36:6). **(E)** αβDGDG from *dgd1*-BviMgdP with increased levels of 34:6 compared to WT and *dgd1*, reduced levels of 34:3, and higher levels of 36:6 levels of DGDG compared to *dgd1*. DGDG in *dgd1*-BviMgdP is a mixture of αβDGDG and ββDGDG. The lipids were analysed by direct infusion Q-TOF MS/MS, and the data are shown in mol%. Mean and SD values of at least 3 replicas.

3.13.2. The Photosynthetic Activity in *Arabidopsis dgd1* Plants Accumulating Bacterial ββDGDG

To address the question whether the photosynthesis activity is fully complemented in the transgenic *dgd1*-BviMgdP lines which exhibit a WT-like growth under full nutrition, pulse amplified modulation (PAM) chlorophyll fluorescence was measured. PAM measurements allow to quantify the fluorescence emission from chlorophyll in photosystem II after light excitation and therefore to determine the quantum yield of PSII. The plants were dark adapted for 60 min before exposure to different light intensities (150, 500, 1000 and 1500 $\mu mol.m^{-2}.s^{-1}$).

As shown in Figure 3.33, the quantum yield of *dgd1* leaves was reduced at the all light intensities compared to the WT. This reduction of YII in *dgd1* was described before (Dörmann et al. 1995). αβDGDG is an integral component of the structure and directly involved in the function of the photosystem II. The absence of αβDGDG modifies the electron transfer by altering the oxidation reaction between the primary and the secondary plastoquinone of PS II (Reifarth et al. 1997; Steffen et al. 2005). The quantum yield of *dgd1*-BviMgdP is similar to WT under low light conditions up to 150 $\mu mol.m^{-2}.s^{-1}$, and drops under high light to intermediate levels between WT and *dgd1*. Therefore, the bacterial ββDGDG is able to complement for the loss of αβDGDG under low light conditions, but under high light, αβDGDG is the preferred lipid. Similar results were obtained from transgenic *dgd1* lines complemented with a bacterial glucosyltransferase synthesizing βGlcβGalDG (Hölzl et al. 2006a).

Therefore, the epimeric and the anomeric configurations as shown in the present work are important factors for the function of DGDG in photosynthesis.

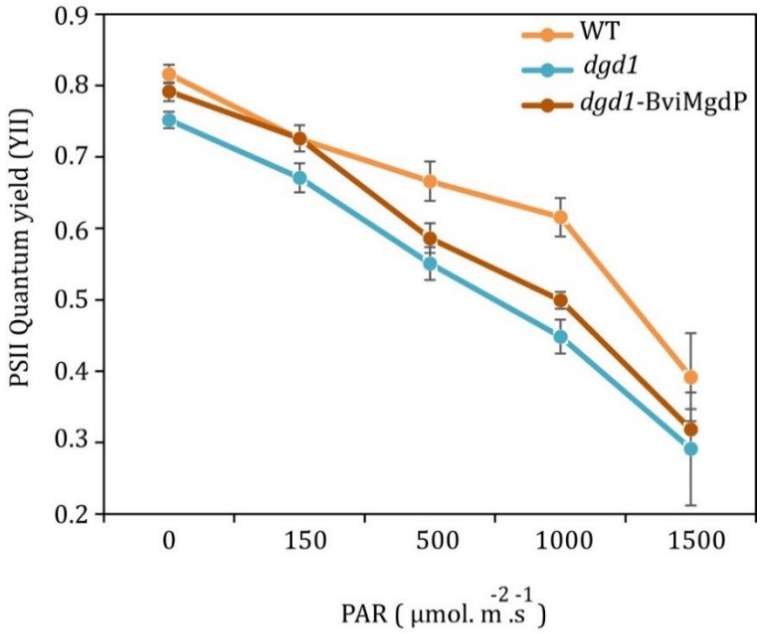

Figure 3. 33: Light-response curves of PSII quantum yield.
Arabidopsis WT, *dgd1*, and complemented plants *dgd1*-BviP. Plants were dark adapted and then exposed to different light intensities 150 (normal light), 500, 1000 and 1500 µmol.m^{-2}.s^{-1}. Chlorophyll fluorescence was measured using the Pulse-amplitude modulated (PAM) fluorometer (Junior PAM) to determine the effective PSII quantum yield. PAR: photosynthetically active radiation. Data represent means and SD of three groups of ten measurements of each line. Asterisks indicate significant difference to WT (Student T-test, $P < 0.05$).

3.14. Strategy for the Generation of βMGDG-free *Arabidopsis* Plants Accumulating ββDGDG via Expression of BviMgdP in *mgd1-3*

βMGDG and αβDGDG are essential for the synthesis of thylakoid membrane and accordingly, for the production of chloroplasts. In *mgd1*, DGD1 is not able to produce αβDGDG because its substrate, MGDG, is missing. The new approach is to create plants producing only αβDGDG by expressing BviMgdP in *mgd1-3* plants without accumulating βMGDG. To address the question whether the presence of ββDGDG in the absence of βMGDG is sufficient for the growth and photosynthesis in plants, BviMgdP was expressed in the *Arabidopsis* null mutant *mgd1-3* (GABI-kat 080C05) (Hölzl, Georg, unpublished). The T-DNA insertion line *mgd1-3* is also a null mutant like the published allele *mgd1-2* (Kobayashi et al. 2007). The position of the T-DNA insertion, the structure of the introns and exons of the *mgd1-3* and the primer positions are shown in Figure 3.34A. The mutant allele *mgd1-3* completely lacks βMGDG and accordingly αβDGDG, it is dwarfed and reveals an albino phenotype without development of a thylakoid membrane. For this reason, the homozygous *mgd1-3* plants are infertile and cannot be transformed (Hölzl, unpublished). Therefore, the heterozygous plants were transformed by floral dipping and red seeds (DsRed marker) were selected. Homozygous *mgd1-3* plants were identified by genotyping of genomic DNA using two PCR reactions with two primers each. The first PCR was conducted with

the primer pair PD661/PD660 amplifying the WT allele of *MGD1*. The second PCR was done with the primer pair PD394/PD660 with PD394 is binding specifically in the T-DNA insertion (Figure 3.34A). The transformation of *mgd1*-3 with BviMgdP led to the identification of several lines homozygous for the T-DNA insertion in *MGD1*. Two lines (*mgd1*-BviMgdP7, *mgd1*-BviMgdP-K) were selected for further experiments (Figure 3.34B).

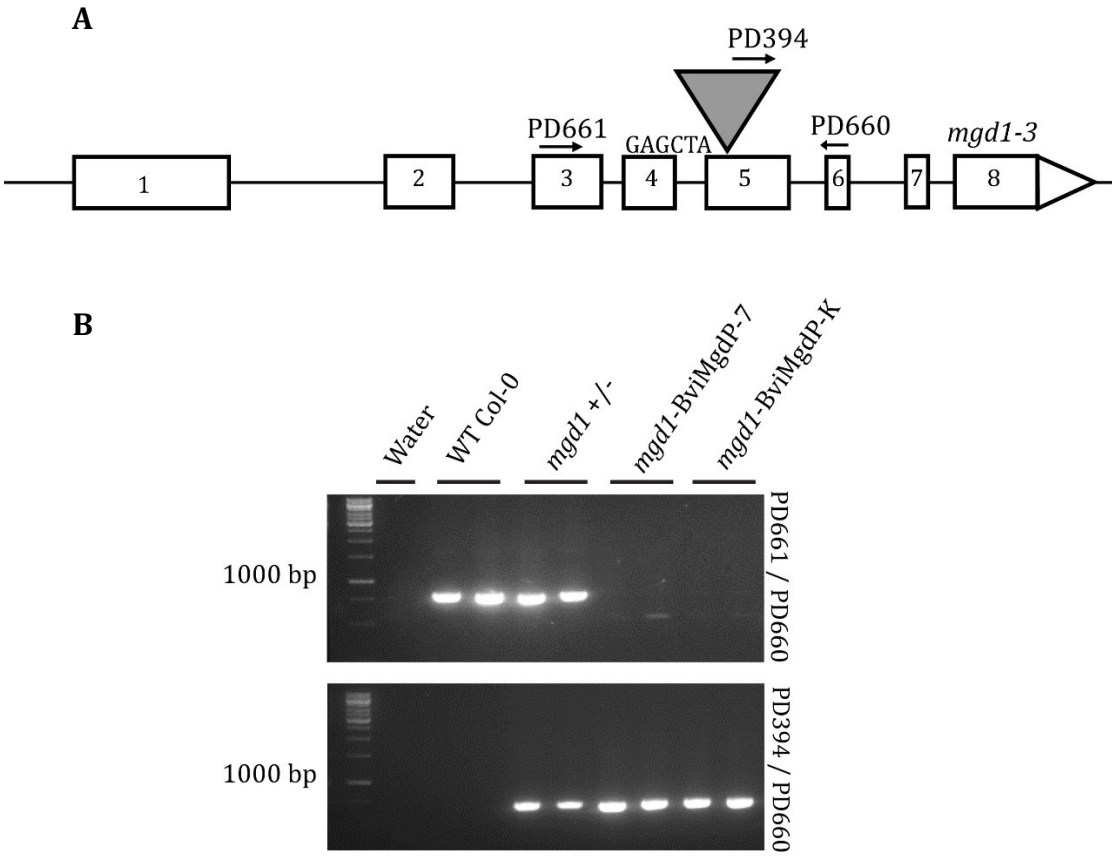

Figure 3. 34: Genotyping of *mgd1-3* mutant plants transformed with BviMgdP.
(A) The *mgd1-3* intron/exon gene structure shows the position of the T-DNA insertion in the fifth exon represented by grey triangle. The primers that were used for genotyping are also shown. **(B)** Agarose gel with the separated PCR products obtained from genotyping of WT, *mgd1* heterozygous (+/-) and 2 lines of *mgd1-3* plants transformed with BviMgdP (*mgd1*-BviMgdP-7 and *mgd1*-BviMgdP-k). The absence of PCR products using the primer pair PD660/PD661 and the presence of PCR products by use of the primer pair PD394/PD660 confirm the homozygous mutation of MGD1 in *mgd1*-BviMgdP-7 and *mgd1*-BviMgdP-K. The expected sizes of the PCR products are ~800bp (PD660/PD661) and ~700bp (PD394/PD660), respectively.

The transgenic *Arabidopsis mgd1*-3 plants expressing BviMgdP were still dwarfed although they showed larger size than the homozygous *mgd1*-3 plants lacking BviMgdP (Figure 3.35). All the transformed homozygous *mgd1*-BviMgdP plants have a yellow-green to green colour. The green colour of the plant could indicate their ability to develop a thylakoid membrane and chloroplasts. All the obtained *mgd1*-BviMgdP plants were infertile, only few of them developed empty siliques. Most of the *mgd1*-BviMgdP plants were not able to flower or to grow

on soil. Due to the difficulties of measuring the dry weight of the rather small leaf material of *mgd1*-BviMgdP plants, the lipid content was measured and calculated in nmol per fresh weight.

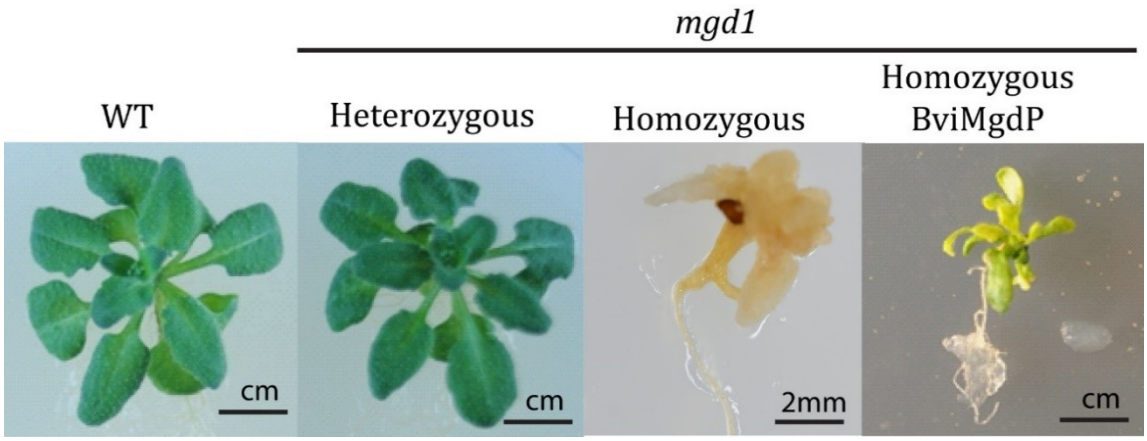

Figure 3. 35: Partial complementation of *mgd1-3* plant growth with the BviMgdP gene.
Heterozygous *mgd1-3* plants show a WT similar phenotype while homozygous lines are albono and not able of photoautotrophic growth. Homozygous *mgd1-3* mutants expressing BviMgdP are partially complemented with stunted growth and yellowish leaves. The plants were grown on MS medium with sucrose.

3.14.1. The *mgd1*-BviMgdP Plants Accumulate ββDGDG and a Low Amount of βMGDG

Analysis the lipid content of the *dgd1* plants expressing the bacterial glycosyltransferase BviMgdP reveals an accumulation of ββDGDG nearly to the WT levels in 8 different plants that are derived from 4 independently transformed lines (only two are shown here i.e. *mgd1*-BviMgdP-7 and *mgd1*-BviMgdP-K) (Figure 3.36A). Lipid analysis showed that the selected transgenic plants accumulate also βMGDG. A clear statement of the anomeric configuration of the DGDG is not possible. If DGDG is exclusively produced by BviMgdP then the anomeric configuration of the two galactoses is β. However, the presence of βMGDG in the transgenic lines allow to speculate that DGD1 may be active and use this βMGDG as substrate for the production of αβDGDG.

Nevertheless, the amount of βMGDG is considerably lower (~1.5 nmol. mg^{-1} FW) compared to the WT (6.2 nmol. mg^{-1} FW), whereas the transgenic lines produce levels of DGDG similar to WT (Figure 3.36A). This causes a changed ratio of βMGDG to DGDG. While this ratio is 2:1 in WT, it is nearly 1:2 in the complemented mutant lines. As a certain ratio of bilayer (such as DGDG) and non-bilayer (βMGDG) forming lipids is crucial in the membranes for optimal function (Rocha et al. 2018), considerable disturbances of the membrane functions of the thylakoids may be expected. Other membrane lipids are hardly affected (SQDG, phospholipids)

Furthermore, not only the ratio of βMGDG and DGDG is changed, the complemented mutant lines differ also in their molecular species composition regarding βMGDG and DGDG. Interestingly, βMGDG in the transgenic *mgd1*-BviMgdP lines is mainly of 36:6-βMGDG and to a minor extent of 34:6-βMGDG origin, while the latter is the dominant form in the WT (Figure 3.36B). Deviations in

the species composition were also observed for DGDG. The main species 36:6-DGDG was reduced in *mgd1*-BviMgdP compared to the WT (Figure 3.36C), and a minor species 34:3-DGDG was increased. A further DGDG species 34:6 was low in all lines.

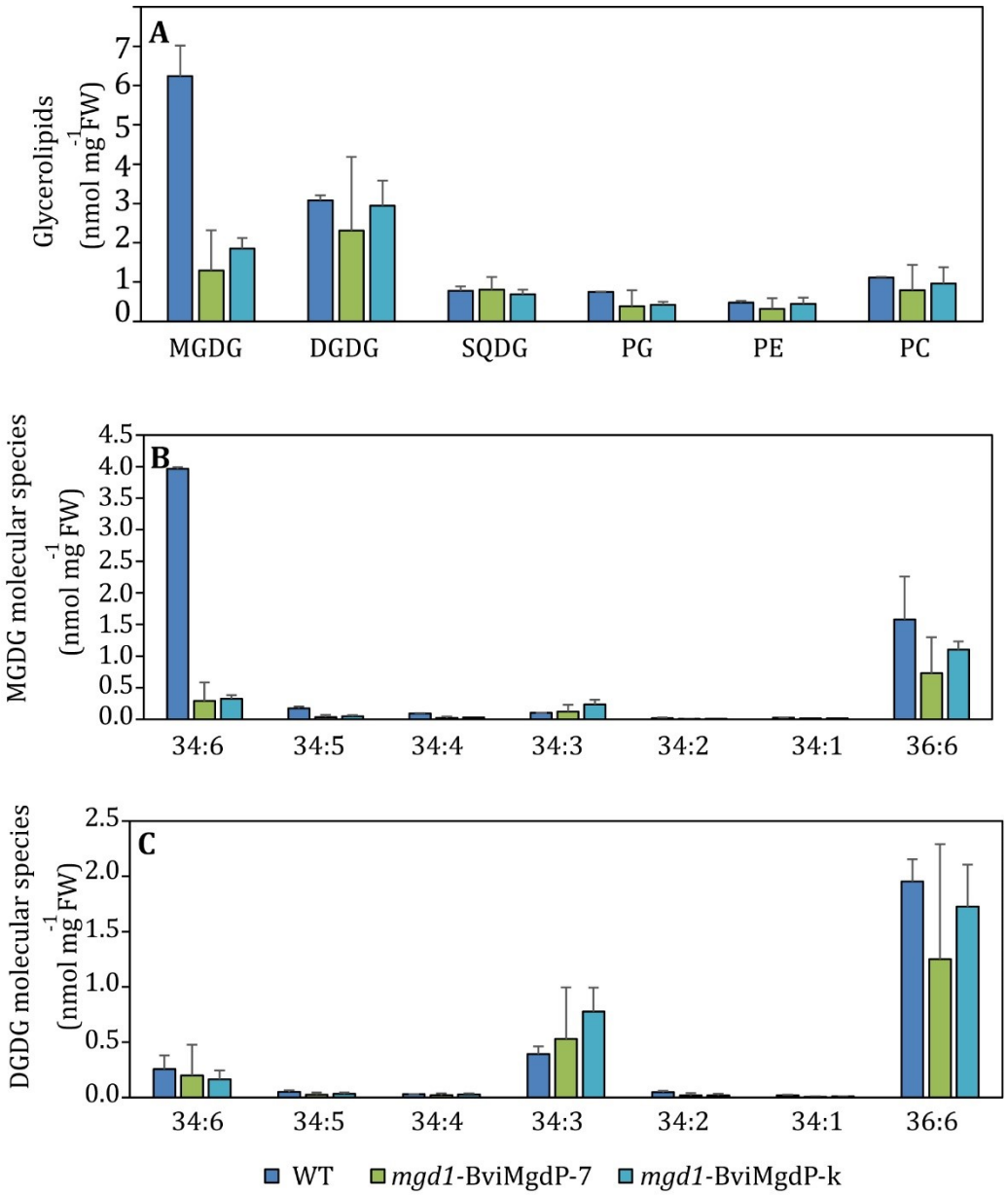

Figure 3. 36: Membrane glycerolipid composition and molecular species of MGDG and DGDG in nmol per mg FW of WT and *mgd1*-BviMgdP grown under control conditions.
(A) leaf glycerolipids from wild type, *mgd1*-BviMgdP-7 and of *mgd1*-BviMgdP-k. The transformed plants accumulate both DGDG and MGDG. Unlike the WT, the transformed plants accumulated more DGDG than MGDG **(**B**)** The molecular species of MGDG are shown in nmol per mg FW. **(C)** The molecular species of ββDGDG in nmol per mg per FW. Glycerolipids were quantified using direct infusion Q-TOF MS/MS. Mean and SD values were calculated from 3 independent replicates.

3.15. A glucuronosyldiacylglycerol Synthase from *Blastochloris viridis*

Glucuronosyldiacylglycerol (GlcADG) is an anionic glycolipid. This lipid is synthesised mainly under phosphate deprivation in several organisms like plants, the plant pathogenic bacterium *Agrobacterium tumefaciens* , in the nodule bacterium *Mesorhizobium loti,* and in the anoxygenic photosynthetic bacterium *Blastochloris viridis* (Hölzl and Dörmann 2007; Diercks et al. 2015; Siebers et al. 2015; Linscheid et al. 1997). GlcADG is synthesised in *A. tumefaciens* by the enzyme Agt (α-glycosyltransfease) with UDP-glucuronic acid as sugar donor and diacylglycerol as sugar acceptor (Semeniuk et al. 2014). A BLAST search with the agrobacterial Agt protein sequence in the NCBI database reveals an ORF in the *B. viridis* genome (BV133_371) for a putative Agt-like enzyme. The ORF was amplified via PCR and expressed in *E. coli*. Analysis of the lipids from the expression culture with TLC (data not shown) and Q-TOF MS/MS led to the detection of a new glycolipid co-migrating with and showing a fragmentation pattern of GlcADG. Characteristic for GlcADG is a neutral loss of 210.9878 indicating the presence of hexuronic acid in the head group (Figure 3.37) (Semeniuk et al. 2014).

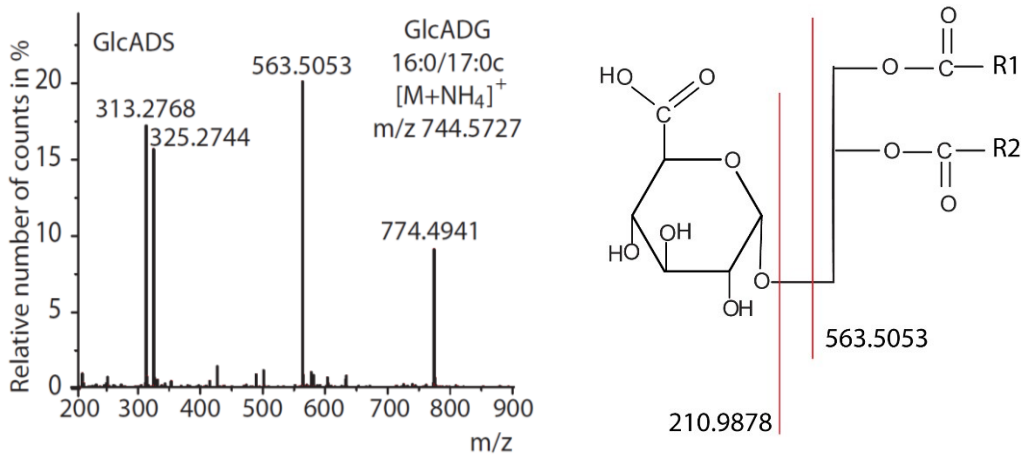

Figure 3. 37: Q-TOF MS/MS spectrum of monohexuronosyl diacylglycerol.
The ammonium adduct ion of the main molecular species of the novel glycolipid synthesized in *E. coli* after expression of BV133_371 (HexADS) from *B. viridis* was fragmented. The neutral loss of 210.9878 (*m/z* 774.4941 minus 563.5053) is derived from hexuronic acid, and the fragment with *m/z* 563.5053 represents diacylglycerol with 16:0 (COO-R1) and 17:0 cyclo (COO-R2) fatty acids. The ions *m/z* 325.2744 and 313.2768 represent monoacylglycerol with 17:0 cyclo and 16:0, respectively.

3.16. MGDG and DGDG Synthase from *Caldilinea aerophila*

Further BLAST searches for plant-like proteins revealed the presence of another galactosyltransferase in the thermophilic bacteria *Caldilinea aerophila* i.e. CaeMgdS (Hölzl, unpublished), which shows high similarity to the plant's MGDG synthase. The filamentous, anaerobic, thermophilic, bacterium *Caldilinea aerophila* (strain DSM 14525T) was previously isolated from hot spring sulfur-turf in Japan (Sekiguchi et al. 2003). In addition, *C. aerophila* contains another sequence related to the bacterial glucosylgalactosyldiacylglycerol (GlcGalDG) synthase from *Chloroflexus* aurantiacus. This second gene was designated CaeDgdS (Hölzl, unpublished). The lipid composition of *C. aerophila* was not analysed in this study due to the difficulties in growing this species. However, the two genes of CaeMgdS and CaeDgdS were amplified by PCR from genomic *C. aerophila* DNA and cloned into a vector for heterologous expression in *E. coli*. After induction of protein expression in *E. coli* harbouring the CaeMgdS gene, MGDG accumulated, while no glycolipid was detected after the single expression of CaeDgdS. Nonetheless, DGDG accumulated after co-expression of CaeMgdS and CaeDgdS in *E. coli* cells (Figure 3.38). This indicates that CaeDgdS utilises the MGDG produced by CaeMgdS as a substrate for DGDG synthesis. In addition, low amounts of lysoMGDG were detected on the TLC plate which is derived from MGDG via degradation in *E. coli*.

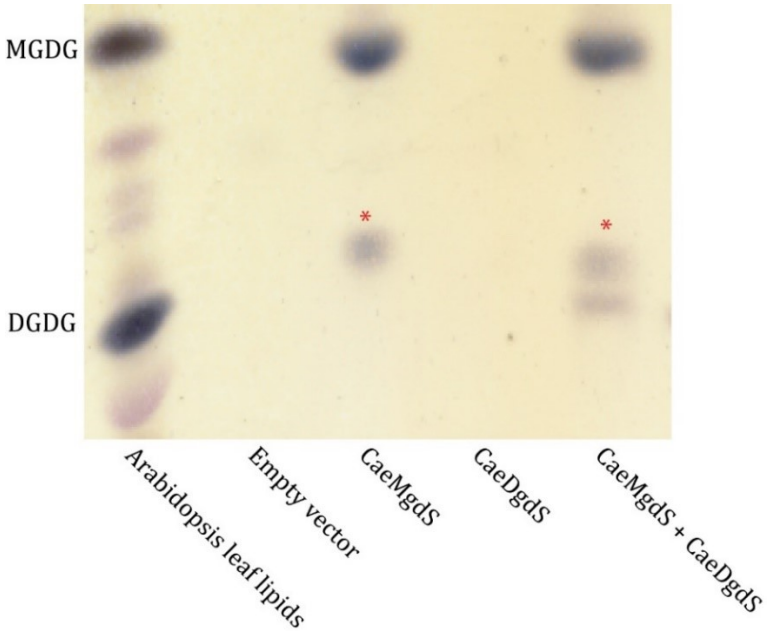

Figure 3. 38: Separation of glycerolipids from *E. coli* cells expressing MGDG synthases from *Caldilinea aerophila* (CaeMgdS, CaeDgdS) by TLC.
Lipids were extracted from *E. coli* expressing different constructs and separated by thin layer chromatography. Glycolipids were stained with α-naphthol sulfuric acid. An *Arabidopsis* total leaf lipid extract was used as standard. *E. coli* harbouring an empty vector was used as a negative control. Lipids which are marked with red asterisks are lysoMGDG derived from MGDG via degradation in *E. coli*.

4. Discussion

4.1. Characterisation of the Acyltransferase slr2103 from *Synechocystis*

The cyanobacterial ORF, slr2103, encoding an acyltransferase-like sequence, is related to plant ELT enzymes. Plant PES enzymes, which belong to the ELT family of acyltransferases, synthesize FAPEs and xanthophyll esters in the chloroplast (Lippold et al. 2012; Ariizumi et al., 2104). The acyltransferase slr2103 is capable of synthesizing phytyl esters and TAG. The ORF slr2103 shows DGAT activity although it is not related neither to the plant DGAT1, PDAT1, DGAT2 nor to the bacterial AtfA-type acyltransferases. The AtfA acyltransferase belongs to the only described family involved in the TAG synthesis in bacteria. Therefore, slr2103 establishes a new bacterial acyltransferase family that is involved in the synthesis of FAPEs and TAG. The cyanobacterial gene slr2103 presumably is the evolutionary origin of the acyltransferase domain of the plant ELT enzymes.

4.1.1. Phytyl esters and Triacylglycerols are Synthesised in *Synechocystis*

In green plant leaves, phytyl esters and TAGs accumulate in small amounts when grown under normal conditions and in large amounts during chlorotic stress including nitrogen deprivation (Lippold et al. 2012; Moellering et al., 2010). Phytyl ester synthesis helps the plant cell to re-direct the toxic phytol derived from the degradation of chlorophyll from the photosystems and the light-harvesting complexes. Phytyl ester synthesis also is advantageous to remove the excess of free fatty acids derived from membrane lipid degradation. Another way to preserve energy and fatty acids is to deposit fatty acids as triacylglycerols in the cytosol and the chloroplast.

In this thesis, the cyanobacterium *Synechocystis* was found to accumulate both phytyl esters and TAG in low amounts. Due to the different architecture in the light harvesting complexes, nitrogen deprivation does not lead to an accumulation of free phytol in *Synechocystis*, which contains chlorophyll-free light harvesting complexes (Li and Sherman 2002; Loura et al. 1987). On the contrary, *Synechocystis* accumulates phytyl esters during high salt/darkness. Darkness terminates the chlorophyll biosynthesis as it is fully light-dependent (Wu and Vermaas 1995). Furthermore, salt stress led to the accumulation of glucosylglycerol in the cells (Marin et al. 2006), and consequently disturbs the ability to uptake carbon sources from the medium. This forces the cells to metabolize the intracellular carbon.

No changes in the fatty acid composition of the phytyl esters before and after stress were observed. However, after supplying the cyanobacterial cultures with phytol, the most abundant phytyl ester changed from 16:0-phytol to 18:1-phytol. The 18:1-phytol was also the dominant molecular species when phytol was added to *E. coli* cultures expressing slr2103. The fatty acid

18:1 could be the preferred fatty acid for the fatty acid phytyl ester synthesised by slr2103. The position of the double band seemed to be irrelevant because it is $18:1^{\Delta 9}$ in *Synechocystis* and it is $18:1^{\Delta 11}$ in *E. coli*.

Plants are the main source of TAGs that humans need for nutritional, industrial applications and for animal feeding. The eukaryotic microalgae harbour a cytosolic TAG synthesis pathway similar to plants, and TAG accumulation is most often dependent on chlorotic stress conditions like nitrogen deprivation. The identification of the TAG synthesis pathway in *Synechocystis* provides the means for a novel strategy of employing prokaryotic photosynthetic organisms for oil synthesis. The pathway of TAG synthesis in cyanobacteria is different from plants and eukaryotic algae. In addition, cyanobacteria are prokaryotic cells which can easily be grown and are easily amenable to genetic engineering to increase the capacity for oil production in future applications.

4.1.2. Characterisation of the Mutant Δ*slr2103* in *Synechocystis*

To understand the function of slr2103, a deletion mutant (Δ*slr2103*) was generated. Growth of *Δslr2103* mutant cells on BG-11 medium as well as on nitrogen deficient medium was not compromised. The chlorophyll *a* content of *Δslr2103* cells was slightly reduced when grown in liquid BG-11 medium under control or stress conditions (darkness/salt), while the amounts of carotenoids remained similar to WT. The quantum yield of photosystem II determined by fluorescence measurements was decreased compared with the WT. Therefore, the deletion of the gene slr2103 has only minor consequences for growth and photosynthesis in *Synechocystis*. The amount of phytyl esters in the mutant Δ*slr2103* is reduced to about 50% compared to the WT growing under control conditions. The remaining amount of phytyl esters in the *Δslr2103* could be synthesised by one or more of the other acyltransferase contained in *Synechocystis*. In contrast to the WT, no increase was detected in the phytyl ester content when the mutant Δslr2103 was grown under stress conditions (darkness/salt). Moreover, the increase of the phytyl esters content in the WT cultures supplied with exogenous phytol was not detected in the Δ*slr2103* cultures.

Another neutral lipid from the WT that was highly reduced in the Δ*slr2103* mutant was identified as triacylglycerol. The disrupting of slr2103 also altered the number of the lipid droplets per cell in *Δslr2103* where it decreased to about 50% of the number in the WT.

4.1.3. PES/DGAT Activity of slr2103 from *Synechocystis*

In Arabidopsis, TAGs accumulate mainly in the seeds. Under stress conditions, TAGs also accumulates in the leaves (Moellering et al., 2010). It was shown before that both PES and WSD enzymes harbour wax/phytyl ester synthesis, while the evidence that they also harbour DGAT activity is weak (Lippold et al. 2012; Patwari 2019). Heterologous expression of slr2103 in *E. coli*

showed that slr2103 was capable to esterify fatty acids from *E. coli* to the supplied phytol or diacylglycerol producing phytyl esters or triacylglycerol, respectively. Moreover, *in vitro* acyltransferase assays of recombinant slr2103 protein with diocatanoin (di8:0 DAG), dipalmitin (di-16:0 DAG) or with phytol were performed. Although a detergent (CHAPS) was added to the enzyme assays to facilitate the solubility of lipids containing long chain acyl groups like dipalmitin (di-16:0 DAG) or the phytol, the activity with di-8:0 DAG was much higher compared to di-16:0 DAG or phytol. It is still possible that phytol was poorly dissolved in the assay buffer. Therefore, it is difficult to determine whether phytol or diacylglycerol is the preferred substrate of slr2103. Although the other cyanobacterial acyltransferases like slr2080 were described to show higher *in vitro* activities with acyl-acyl carrier protein (acyl-ACP) as acyl donor than with acyl-CoA (Weier et al. 2005), the enzyme assay with slr2103 showed that acyl-CoA was the preferred substrate. Therefore, the *in vivo* acyl donor for slr2103, like the other TAG synthases DGAT1, DGAT2 or AtfA, is most likely acyl-CoA.

The finding that the gene slr2103 involved in phytyl ester and TAG ester synthesis in *Synechocystis* is related to PES1/PES2 of plants, indicates that the pathway of conversion of lipid and chlorophyll breakdown products into non-polar lipids with subsequent storage in plastoglobules/lipid droplets is presumably derived from the cyanobacterial progenitor of chloroplasts.

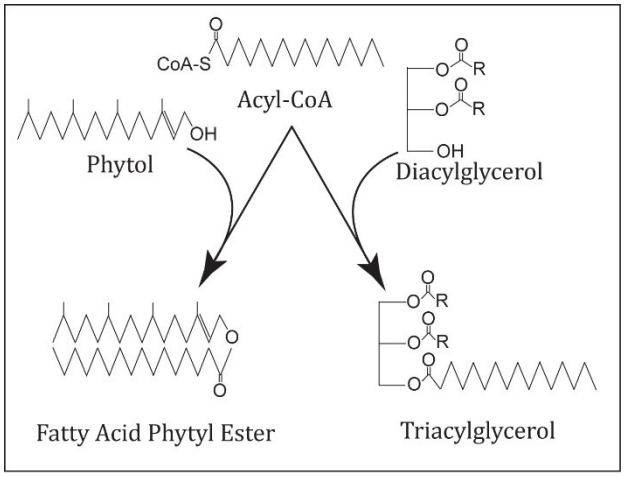

Figure 4. 1: Acyltransferase reactions for phytyl ester and triacylglycerol synthesis by *Synechocystis* slr2103.

4.1.4. The Hydrolase slr1807 is not Essential for Phytyl Ester Synthesis

The plants ELT family of enzymes consists of a C-terminal acyltransferase domain and an N-terminal hydrolase domain. The function of the hydrolase domain in the ELT protein is unknown. This study shows that the cyanobacterial hydrolase slr1807 could be involved in the accumulation of the FAPEs in *Synechocystis*. The phytyl ester content was reduced 50% in the Δ*slr1807* mutant compared to the WT. Furthermore, phytol feeding of *E. coli* cells expressing both

slr1807 and slr2103 showed a higher accumulation of phytyl esters than the single expression of slr2103. It is possible that slr1807 might be necessary to cleave the fatty acid from other acyl donors like phospholipids. If this is true, it might provide more fatty acids as substrates to slr2103 in addition to the acyl-CoA substrates from in *E. coli* used by slr2103. However, an enzyme assay with the combination of slr1807 and slr2103 recombinant enzymes did not lead to any increase in FAPEs accumulation when phytol was added and MGDG was used as an acyl donor. No evidences in this thesis whether or not phospholipids can be used as an acyl donor. However, this could be possible. On the other hand, the hydrolase slr1807 is not involved in the accumulation of TAGs in *Synechocystis*. The accumulation of TAGs in the Δ*slr1807* mutant was confirmed by TLC.

Finally, the hydrolase slr1807 is not absolutely required for the phytyl ester synthesis or TAG synthesis activity of slr2103, because expression of slr2103 in *E. coli* is sufficient to establish phytyl ester and TAG production.

4.2. Plant MGD1-like, Processive Galactosyltransferase from *Blastochloris viridis*

The role of the two galactolipids βMGDG and αβDGDG in the synthesis and the organisation of the thylakoid membrane of the chloroplasts has been studied previously. These two lipids play an important role in the chloroplast biogenesis, in the function of photosynthesis and under phosphate deprivation (Fujii et al. 2019; Hölzl and Dörmann 2007).

4.2.1. The role of αβDGDG for growth and photosynthesis revealed by its replacement with ββDGDG by expression of BviMgdP in *dgd1*

In a previous study, the plant αβDGDG was replaced by the glucose containing βGlcβGalDG with expressing the bacterial glucosyltransferase from *Chloroflexus aurantiacus* in *dgd1* mutant of *Arabidopsis* (Hölzl et al. 2006a). The growth defect of the transformed plants was fully complemented by the accumulation of the bacterial βGlcβGalDG. However, photosynthesis was still affected, indicating that galactose in αβDGDG and the α anomeric structure could be required for maximal photosynthetic activity (Hölzl et al. 2006a). In the same manner, the expression of the BviMgdP in *dgd1* and the accumulation of ββDGDG provides the means to study the importance of the anomeric configuration of the terminal galactose (α vs β). The results in this thesis demonstrate, that the anomeric configuration of the terminal galactose does not play a role for the plant growth, but it is required for optimal photosynthesis.

The contents of the two lipids βMGDG and αβDGDG are strictly regulated in the plant chloroplast, because a certain ratio of the non-bilayer forming βMGDG and the bilayer forming αβDGDG is crucial for optimal membrane functions. In this case, the anomeric configuration plays obviously a negligible role as shown before for βGlcβGalDG which differs also in its epimeric configuration at C-4 compared to αβDGDG (Hölzl et al. 2006a), i.e. irrespective of their anomeric

and epimeric configurations the different glycolipids have similar physico-chemical functions provided that they contain two sugars. This explains why the transgenic plants form normal thylakoids and chloroplasts and show a growth similar to WT.

Unlike to the complementation of growth, the photosynthetic deficiency of *dgd1* was not fully complemented in *dgd1*-BviMgdP. αβDGDG contributes to the assembly of the photosystem II and the light harvesting complexes in cyanobacteria and plants (Sheng et al. 2018). αβDGDG is also required for the stabilization of the light harvesting complexes and the formation and the stabilization of the thylakoid membrane (Hölzl and Dörmann 2007; Lee 2000). As shown in (3.4.4) the bacterial ββDGDG can only complement the photosynthetic deficiency when the plants are exposed to low light, but under high light stress the complementation is insufficient. This indicates that the α-anomeric configuration is important. As DGDG is an integral component of PSII (Dörmann et al. 1995) and of the light harvesting complexes, and possibly plays a role in dissipation of excess light energy, the binding capacity or the interactions with the different photosynthetic protein complexes may be unsatisfactory or disturbed. This would especially explain the susceptibility of the complemented mutants for high light stress.

A further function of DGDG is to replace phospholipids under phosphate deprivation. For this purpose, DGDG is exported to extraplastidial membranes where it accumulates. The lipid measurements indicate that the synthesis of ββDGDG is increased under phosphate deprivation. This was also shown in the previous study for βGlcβGalDG (Hölzl et al. 2006). Furthermore, this study revealed that the complemented *dgd1*-CaGlcT plants were able to export βGlcβGalDG to extraplastidial membranes. The export of ββDGDG was not analysed in the present study, but its accumulation indicates that *dgd1*-BviMgdP plants are able to export also this lipid to replace extraplastidial phospholipids. In contrast to the expression of DGD1 and DGD2, which is driven by the endogenous promoter and induced under phosphate deprivation, BviMgdP is constitutively expressed in *dgd1*-BviMgdP under the 35S promoter independent of phosphate supply. Therefore, export mechanisms may exist which do not dependent of expression of DGD1, DGD2 or BviMgdP, and of the anomeric sugar conformation, and these mechanisms may allow the increased synthesis of ββDGDG by removing this lipid from the chloroplasts. However, the transformed *dgd1*-BviMgdP plants suffered more under phosphate deprivation compared to *dgd1* or wild type. The explanation may be that the fine tuning of expression and export may not be optimal in such an artificial expression system in *dgd1*-BviMgdP.

4.2.2. Expression of BviMgdP in the *mgd1* Mutant of *Arabidopsis*

The motivation of expressing the bacterial enzyme BviMgdP in the *Arabidopsis mgd1* mutant was to generate βMGDG-free *Arabidopsis* plants that accumulate only ββDGDG. Unlike expected, the transformed plants accumulate βMGDG in addition to DGDG. The consequence of accumulation of βMGDG is that the complemented plants probably synthesise a mixture of

ββDGDG and αβDGDG, the latter produced by DGD1. Besides, two scenarios could possibly explain the accumulation of βMGDG.

(i) BviMgdP was able to produce certain amounts of βMGDG in the plant, though the synthesis of βMGDG could not be observed after expression in *E. coli*. In this scenario, the enzymatic conditions BviMgdP in the transgenic plants where it localizes to the inner envelope and has access to the substrates DAG, MGDG and UDP-Gal (whose exact local concentrations are unknown), might be very different from the conditions in bacteria like *B. viridis* or *E. coli*.

(ii) βMGDG was produced by MGD2 and MGD3. Although they are mainly expressed under phosphate deprivation, MGD2 and MGD3 are also slightly expressed in different tissues and certain developmental stages (Awai et al. 2001). MGD2 was described to have a very low expression in all the plant development stages (Awai et al. 2001). MGD3 was expressed to a similar extent as MGD1 in the seedlings (3 to 5 days old plants) under normal conditions (Kobayashi et al. 2004).

MGD1 is the major producer of MGDG that is required for chloroplast biogenesis including the formation of the outer envelope where MGD2 and MGD3 are located (Hölzl and Dörmann 2019; Fujii et al. 2019a). As mentioned above, MGD2 and MGD3 are expressed under certain developmental stages, but in the *mgd1* background they may not be active because of the lack of functional plastids. It could be possible that the amounts of galactolipids (ββDGDG) and βMGDG synthesised by BviMgdP or MGD2/3 was sufficient to form rudimentary plastids. Such rudimentary plastids may be sufficient to allow MGDG2/3 to associate with such plastids to synthesize βMGDG which further stabilizes these organelles.

4.3. Possible Glycolipid Biosynthesis Pathways in *Blastochloris viridis*

The role of the two galactolipids MGDG and DGDG is well known for the structure and the function of the bio-membrane in plants and some bacteria. Furthermore, they play a role in substituting phospholipids when grown under phosphate limitation. A further lipid, which also accumulates in plants and some bacteria like *A. tumefaciens* under phosphate limitation is the anionic glycolipid GlcADG (Okazaki et al. 2013; Semeniuk et al. 2014). Some plants, for example soybean, and some bacteria like *B. viridis* synthesise GlcADG under normal conditions (Okazaki et al. 2015; Linscheid et al. 1997). Together with SQDG, GlcADG plays an important role to replace phospholipids especially phosphatidylglycerol (PG) to maintain the negative charge of the thylakoid membrane (Yu et al. 2002). A similar function of GlcADG is expected for bacteria which are able to synthesize this lipid. While GlcADG is synthesised by SQD2 in plants, in bacteria (*A. tumefaciens*, *Mesorhizobium loti*) a different enzyme (Agt) is responsible for the synthesis of

GlcADG (Diercks et al. 2015; Semeniuk et al. 2014). SQD2 and Agt use UDP-glucuronic acid (UDP-GlcA) as sugar donor and DAG as sugar acceptor. The presence of GlcADG in *Blastochloris*, indicates that BV133_371 is a possible candidate for the synthesis of GlcADG in *Blastochloris* (GlcADG synthase, BviGlcADS). Finally, a possible pathway for glycolipid biosynthesis in *B. viridis* including MGDG, DGDG and GlcADG as deduced from the results of this thesis is shown in Figure 4. 2.

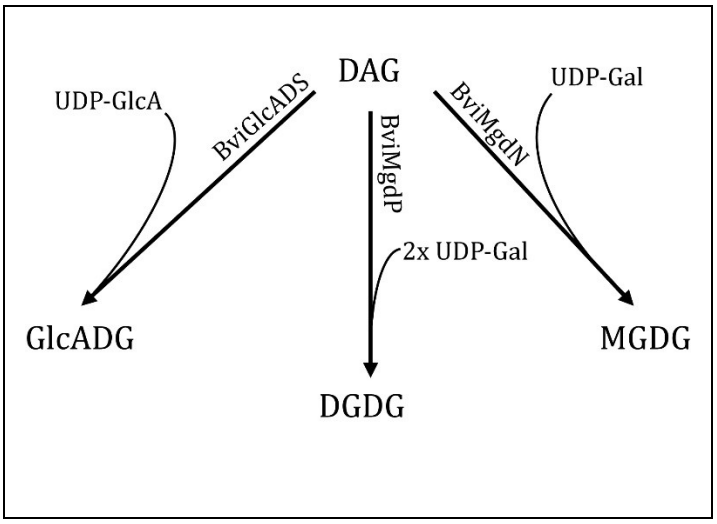

Figure 4. 2: Simplified scheme representing glycolipid biosynthesis in *Blastochloris viridis.*

5. Summary

Cyanobacteria are unicellular prokaryotic algae that perform oxidative photosynthesis similar to plants. The cells harbour thylakoid membranes composed of lipids related to those of chloroplasts in plants, to accommodate the complexes of photosynthesis. The occurrence of storage lipids, including TAG or wax esters, which are found in plants, animals and some bacteria, nevertheless remained unclear in cyanobacteria. This thesis shows that the cyanobacterium *Synechocystis* sp. PCC6803 accumulates both TAG and wax esters (fatty acid phytyl esters). Phytyl esters accumulate in higher levels under abiotic stress conditions. The analysis of an insertional mutant revealed that the acyltransferase slr2103, with sequence similarity to the acyltransferase domain of plant esterase/lipase/thioesterase (ELT) proteins, is essential for TAG and phytyl ester synthesis in *Synechocystis*. The recombinant slr2103 enzyme showed acyltransferase activity with phytol and diacylglycerol, thus producing phytyl esters and triacylglycerol. Acyl-CoA thioesters were the preferred acyl donors, while acyl-ACP (acyl carrier protein), free fatty acids or galactolipid-bound fatty acids were poor substrates. The slr2103 protein sequence is unrelated to acyltransferases from bacteria (AtfA) or plants (DGAT1, DGAT2, PDAT), and therefore establishes an independent group of bacterial acyltransferases involved in TAG and wax ester synthesis.

Synechocystis harbours a second ORF (slr1807) with sequence similarity to the hydrolase domain of plant ELT proteins. Analysis of the *Synechocystis* slr1807 mutant reveals that slr1807 is involved in the accumulation of phytyl esters. However, the recombinant slr1807 enzyme did not enhance the triacylglycerol or phytyl ester synthesis activity when it was combined with the recombinant slr2103 enzyme in *in vitro* enzyme assays.

The galactolipids digalactosyldiacylglycerol (αβDGDG) and monogalactosyldiacylglycerol (βMGDG) are the most abundant membrane lipids in photosynthetic organisms including plants, green algae and cyanobacteria. Different organisms employ different pathways with different galactosyltransferases to synthesize βMGDG and αβDGDG. In plants and green algae, βMGDG is produced by MGD1, and βMGDG is the substrate for αβDGDG synthesis by the DGDG synthase DGD1. The photosynthetic purple bacterium *Blastochloris viridis* contains a plant MGD1-type processive galactosyltransferase (BviMgdP) which converts diacylglycerol directly to ββDGDG, without accumulating βMGDG as intermediate, when expressed in *E. coli*. In this thesis, BviMgdP, was introduced into the *Arabidopsis* galactolipid-deficient *mgd1* and *dgd1* mutants to study its activity *in planta* and its capacity to complement lipid and photosynthetic deficiency of the plant mutants. The introduction of BviMgdP in *dgd1* plants resulted in the accumulation of ββDGDG instead of the plant-type αβDGDG. While growth, chlorophyll content and DGDG amount were similar to WT, photosynthesis was only partially complemented presumably due to different anomeric configurations of the outermost galactose in DGDG (β vs. α). Transfer of BviMgdP into the *Arabidopsis mgd1* null mutant resulted in partial complementation with dwarfed, but green,

transgenic plants. Interestingly, most *mgd1*-BviMgdP lines contained higher amounts of ββDGDG than MGDG in the leaves, in contrast to *Arabidopsis* and other plants, where MGDG is ~2fold more abundant than DGDG. The accumulation of small amounts of MGDG in *mgd1*-BviMgdP plants might be due to low MGDG synthase activity of BviMgdP in the plant environment, or to MGD2/MGD3 from *Arabidopsis* which could contribute to MGDG synthesis in the transgenic plants.

In addition to MGDG and DGDG, *B. viridis* accumulates an anionic glycolipid, i.e glucuronosyldiacylglycerol (GlcADG). The GlcADG synthase (BviGlcADS) from *B. viridis* shows high similarity to the agrobacterial Agt. Therefore, *B. viridis* contains three pathways for the synthesis of MGDG (BviMgdN), DGDG (BviMgdP) and GlcADG (BviGlcADS).

The bacterial enzymes involved in lipid synthesis reported in this thesis show sequence similarity to plant lipid enzymes found in chloroplasts. These results emphasize the importance of the cyanobacterial progenitor (slr2103, slr1807) or lateral gene transfer from bacteria, i.e. the presence of MGD1-related (BviMgdP, BviMgdN), and SQD2-related sequences (BviGlcADS) indicate, that bacteria represent the origin of chloroplast enzymes.

Keywords: Triacylglycerol, Fatty acid phytyl ester, Cyanobacteria, wax, acyltransferase, Processive galactosyltransferase.

6. References

Alvarez, H. M.; Kalscheuer, R.; Steinbüchel, A. (2000): Accumulation and mobilization of storage lipids by *Rhodococcus opacus* PD630 and *Rhodococcus ruber* NCIMB 40126. *Applied Microbiology and Biotechnology* 54, 218–223.

Alvarez, H. M.; Steinbüchel, A. (2002): Triacylglycerols in prokaryotic microorganisms. *Applied Microbiology and Biotechnology* 60, 367–376.

Alvarez, H. M.; Mayer, F.; Fabritius, D.; Steinbüchel, A. (1996): Formation of intracytoplasmic lipid inclusions by *Rhodococcus opacus* strain PD630. *Archives of Microbiology* 165, 377–386.

Anderson, A. J.; Dawes, E. A. (1990): Occurrence, metabolism, metabolic role, and industrial uses of bacterial polyhydroxyalkanoates. *Microbiological Reviews* 54, 450–472.

Ariizumi, T.; Kishimoto, S.; Kakami, R.; Maoka, T.; Hirakawa, H.; Suzuki, Y.; Ozeki, Y.; Shirasawa, K.; Bernillon, S.; Okabe, Y.; Moing, A.; Asamizu, E.; Rothan, C.; Ohmiya, A.; Ezura, H. (2014) Identification of the carotenoid modifying gene *Pale Yellow Petal 1* as an essential factor in xanthophyll esterification and yellow flower pigmentation in tomato (*Solanum lycopersicum*). *Plant Journal* 79, 453-465.

Awai, K.; Kakimoto, T.; Awai, C.; Kaneko, T.; Nakamura, Y.; Takamiya, K. (2006): Comparative genomic analysis revealed a gene for monoglucosyldiacylglycerol synthase, an enzyme for photosynthetic membrane lipid synthesis in cyanobacteria. *Plant Physiology* 141, 1120–1127.

Awai, K.; Maréchal, E.; Block, M. A.; Brun, D.; Masuda, T.; Shimada, H. (2001): Two types of MGDG synthase genes, found widely in both 16:3 and 18:3 plants, differentially mediate galactolipid syntheses in photosynthetic and nonphotosynthetic tissues in *Arabidopsis thaliana*. *Proceedings of the National Academy of Sciences of the United States of America* 98, 10960–10965.

Awai, K.; Ohta, H.; Sato, N. (2014): Oxygenic photosynthesis without galactolipids. *Proceedings of the National Academy of Sciences of the United States of America* 111, 13571–13575.

Awai, K.; Watanabe, H.; Benning, C.; Nishida, I. (2007): Digalactosyldiacylglycerol is required for better photosynthetic growth of *Synechocystis* sp. PCC6803 under phosphate limitation. *Plant and Cell Physiology* 48, 1517–1523.

Backasch, N.; Schulz-Friedrich, R.; Appel, J. (2005): Influences on tocopherol biosynthesis in the cyanobacterium *Synechocystis* sp. PCC 6803. *Plant Physiology* 162, 758–766.

Barksdale, L.; Kim, K. (1977): Mycobacterium. *Bacteriological Reviews* 41, 217–372.

Besagni, C.; Kessler, F. (2013): A mechanism implicating plastoglobules in thylakoid disassembly during senescence and nitrogen starvation. *Planta* 237, 463–470.

Bhaya, D.; Takahashi, A.; Grossman, A. R. (2001): Light regulation of type IV pilus-dependent motility by chemosensor-like elements in *Synechocystis* PCC6803. *Proceedings of the National Academy of Sciences of the United States of America* 98, 7540–7545.

Blankenship, R. E. (1995): Anoxygenic photosynthetic bacteria. Dordrecht: *Kluwer Academic* (Advances in photosynthesis, 2).

Bligh, E. G.; Dyer, W. J. (1959): A rapid method of total lipid extraction and purification. *Canadian Journal of Biochemistry and Physiology* 37, 911–917.

Bouvier, Florence; Rahier, Alain; Camara, Bilal (2005): Biogenesis, molecular regulation and function of plant isoprenoids. *Progress in Lipid Research* 44, 357–429.

Cahoon, E. B.; Shockey, J. M.; Dietrich, C. R.; Gidda, S. K.; Mullen, R. T.; Dyer, J. M. (2007): Engineering oilseeds for sustainable production of industrial and nutritional feedstocks: solving bottlenecks in fatty acid flux. *Current Opinion in Plant Biology* 10, 236–244.

Catling, D.; Zahnle, K. James R. H., Judith A. C.; John A. P. (2002): Evolution of atmospheric oxygen. *Encyclopaedia of Atmospheric Sciences*. Academic Press, 754–761.

Chang, L.; Liu, X.; Li, Y.; Liu, C.; Yang, F.; Zhao, J.; Sui, S. (2015): Structural organization of an intact phycobilisome and its association with photosystem II. *Cell Research* 25, 726–737.

Collins, M. D.; Jones, D. (1981): Distribution of isoprenoid quinone structural types in bacteria and their taxonomic implication. *Microbiology and Molecular Biology Reviews* 45, 316–354.

Cornah, E.; Terry, J.; Smith, G. (2003): Green or red: what stops the traffic in the tetrapyrrole pathway?. *Trends in Plant Science* 8, 224–230.

Coutinho, P. M.; Deleury, E.; Davies, G. J.; Henrissat, B. (2003): An evolving hierarchical family classification for glycosyltransferases. *Journal of Molecular Biology* 328, 307–317.

Cuellar-Bermudez, S. P.; Romero-Ogawa, M. A.; Vannela, R.; Lai, Y. S.; Rittmann, B. E.; Parra-Saldivar, R. (2015): Effects of light intensity and carbon dioxide on lipids and fatty acids produced by *Synechocystis* sp. PCC6803 during continuous flow. *Algal Research* 12, 10–16.

Daghma, D. S.; Kumlehn, J.; Melzer, M. (2011): The use of cyanobacteria as filler in nitrocellulose capillaries improves ultrastructural preservation of immature barley pollen upon high pressure freezing. *Journal of Microscopy* 244, 79–84.

Dahlqvist, A.; Ståhl, U.; Lenman, M.; Banas, A.; Lee, M.; Sandager, L. (2000): Phospholipid. diacylglycerol acyltransferase: an enzyme that catalyzes the acyl-CoA-independent formation of triacylglycerol in yeast and plants. *Proceedings of the National Academy of Sciences of the United States of America* 97, 6487–6492.

Darcy D. L. (2006): Optimization and characterization of the growth of the photosynthetic bacterium *Blastochloris viridis* And a brief survey of its potential as a remediative tool. Dissertation. University of Notre Dame, Notre Dame. Graduate School. Available online at https://curate.nd.edu/show/ks65h992130.

Deisenhofer, J.; Michel, H. (1989): The photosynthetic reaction center from the purple bacterium *Rhodopseudomonas viridis*. *Science* 245, 1463–1473.

Diercks, H.; Semeniuk, A.; Gisch, N.; Moll, H.; Duda, K. A.; Holzl, G. (2015): Accumulation of novel glycolipids and ornithine lipids in *Mesorhizobium loti* under phosphate deprivation. *Journal of Bacteriology* 197, 497–509.

Diezel, W.; Kopperschläger, G.; Hofmann, E. (1972): An improved procedure for protein staining in polyacrylamide gels with a new type of Coomassie Brilliant Blue. *Analytical Biochemistry*. 48, 617–620.

Dörmann, P.; Balbo, I.; Benning, C. (1999): *Arabidopsis* galactolipid biosynthesis and lipid trafficking mediated by DGD1. *Science* 284 , 2181–2184.

Dörmann, P.; Hoffmann-Benning, S.; Balbo, I.; Benning, C. (1995): Isolation and characterization of an *Arabidopsis* mutant deficient in the thylakoid lipid digalactosyl diacylglycerol. *Plant Cell* 7, 1801–1810.

Dörmann, P.; Hölzl, G.; H. Wada; N. Murata (2009): The role of glycolipids in photosynthesis. Lipids in photosynthesis, Dordrecht: Springer 30, 265–282.

Eckhardt, U.; Grimm, B.; Hörtensteiner, (2004): Recent advances in chlorophyll biosynthesis and breakdown in higher plants. *Plant Molecular Biology* 56, 1–14.

Feige, G. B.; Heinz, E.; Wrage, K.; Cochems, N.; Ponzelar, E.; Mazliak, P.; Benveniste, C. C.; Douce, R. (1980): Discovery of a new glyceroglycolipid in blue-green algae and its role in galactolipid synthesis.: Biogenesis and Function of Plant Lipids. Amsterdam: Elsevier/North-Holland Biochemical Press 6, 135–140.

Fujii, S.; Nagata, N.; Masuda, T.; Wada, H.; Kobayashi, K. (2019a): Galactolipids are essential for internal membrane transformation during etioplast-to-chloroplast differentiation. *Plant and Cell Physiology* 60, 1224–1238.

Fujii, S.; Wada, H.; Kobayashi, K. (2019b): Role of galactolipids in plastid differentiation before and after light exposure. *Plants* 8, 357.

Gao, Y.; Xiong, W.; Li, X.; Gao, C.; Zhang, Y.; Li, H.; Wu, Q. (2009): Identification of the proteomic changes in *Synechocystis* sp. PCC 6803 following prolonged UV-B irradiation. *Journal of Experimental Botany* 60, 1141–1154.

Gaude, N.; Brehelin, C.; Tischendorf, G.; Kessler, F.; Dörmann, P. (2007): Nitrogen deficiency in *Arabidopsis* affects galactolipid composition and gene expression and results in accumulation of fatty acid phytyl esters. *The Plant Journal* 49, 729–739.

Gowda, H.; Ivanisevic, J.; Johnson, C. H.; Kurczy, M. E.; Benton, H. Paul; Rinehart, D. (2014): Interactive XCMS online: simplifying advanced metabolomic data processing and subsequent statistical analyses. *Analytical Chemistry* 86, 6931–6939.

Griese, M.; Lange, C.; Soppa, J. (2011): Ploidy in cyanobacteria. *FEMS Microbiology Letters* 323, 124–131.

Güler, S.; Seeliger, A.; Härtel, H.; Renger, G.; Benning, C. (1996): A null mutant of *Synechococcus* sp. PCC7942 deficient in the sulfolipid sulfoquinovosyl diacylglycerol. *Journal of Biological Chemistry* 271, 7501–7507.

Gutthann, F.; Egert, M.; Marques, A.; Appel, J. (2007): Inhibition of respiration and nitrate assimilation enhances photohydrogen evolution under low oxygen concentrations in *Synechocystis* sp. PCC 6803. *Biochimica et Biophysica Acta* 1767, 161–169.

Hanada, S.; Hiraishi, A.; Shimada, K.; Matsuura, K. (1995): Chloroflexus aggregans sp. nov., a filamentous phototrophic bacterium which forms dense cell aggregates by active gliding movement. *International Journal of Systematic Bacteriology* 45, 676–681.

Härtel, H.; Benning, C. (2000): Can digalactosyldiacylglycerol substitute for phosphatidylcholine upon phosphate deprivation in leaves and roots of *Arabidopsis*? *Biochemical Society transactions* 28, 729–732.

Heinz, S.; Rast, A.; Shao, L.; Gutu, A.; Gügel, I. L.; Heyno, E. (2016): Thylakoid membrane architecture in *Synechocystis* depends on CurT, a homolog of the granal curvature thylakoid1 proteins. *Plant Cell* 28, 2238–2260.

Hiraishi, A. (1997): Transfer of the bacteriochlorophyll b-containing phototrophic bacteria *Rhodopseudomonas viridis* and *Rhodopseudomonas sulfoviridis* to the genus *Blastochloris* gen. nov. *International Journal of Systematic Bacteriology* 47, 217–219.

Hobbs, Douglas H.; Lu, Chaofu; Hills, Matthew J. (1999): Cloning of a cDNA encoding diacylglycerol acyltransferase from *Arabidopsis thaliana* and its functional expression. *FEBS Letters* 452, 145–149.

Hölzl, G.; Dörmann, P. (2007): Structure and function of glycoglycerolipids in plants and bacteria. *Progress in Lipid Research* 46, 225–243.

Hölzl, G.; Leipelt, M.; Ott, C.; Zähringer, U.; Lindner, B.; Warnecke, D.; Heinz, E. (2005a): Processive lipid galactosyl/glucosyltransferases from *Agrobacterium tumefaciens* and *Mesorhizobium loti* display multiple specificities. *Glycobiology* 15, 874–886.

Hölzl, G.; Witt, S.; Gaude, N.; Melzer, M.; Schöttler, M. A.; Dörmann, P. (2009): The role of diglycosyl lipids in photosynthesis and membrane lipid homeostasis in *Arabidopsis*. *Plant Physiology* 150, 1147–1159.

Hölzl, G.; Witt, S.; Kelly, A. A.; Zähringer, U.; Warnecke, D.; Dörmann, P.; Heinz, E. (2006): Functional differences between galactolipids and glucolipids revealed in photosynthesis of higher plants. *Proceedings of the National Academy of Sciences of the United States of America* 103, 7512–7517.

Hölzl, G.; Dörmann, P. (2019): Chloroplast lipids and their biosynthesis. *Annual Review of Plant Biology* 70, 51–81.

Hölzl, G.; Zähringer, U.; Warnecke, D.; Heinz, E. (2005b): Glycoengineering of cyanobacterial thylakoid membranes for future studies on the role of glycolipids in photosynthesis. *Plant and Cell Physiology* 46, 1766–1778.

Hu, Q.; Sommerfeld, M.; Jarvis, E.; Ghirardi, M.; Posewitz, M.; Seibert, M.; Darzins, A. (2008): Microalgal triacylglycerols as feedstocks for biofuel production: perspectives and advances. *The Plant Journal* 54, 621–639.

Ischebeck, T.; Zbierzak, A. M.; Kanwischer, M.; Dormann, P. (2006): A salvage pathway for phytol metabolism in *Arabidopsis*. *Journal of Biological Chemistry* 281, 2470–2477.

Jach, G.; Binot, E.; Frings, S.; Luxa, K.; Schell, J. (2001): Use of red fluorescent protein from *Discosoma* sp. (dsRED) as a reporter for plant gene expression. *The Plant Journal* 28, 483–491.

Jarvis, P.; Dörmann, P.; Peto, C. A.; Lutes, J.; Benning, C.; Chory, J. (2000): Galactolipid deficiency and abnormal chloroplast development in the *Arabidopsis* MGD synthase 1 mutant. *Proceedings of the National Academy of Sciences of the United States of America* 97, 8175–8179.

Jones, M. R. (2007): Lipids in photosynthetic reaction centres. Structural roles and functional holes. *Progress in Lipid Research* 46, 56–87.

Joyard, J.; Douce, R. (1987): Galactolipid synthesis. P. K. Stumpf (Hg.): The biochemistry of plants. Lipids: Structure and function, New York: Academic Press, 215–274.

Kalscheuer, R.; Steinbüchel, A. (2003): A novel bifunctional wax ester synthase/acyl-CoA:diacylglycerol acyltransferase mediates wax ester and triacylglycerol biosynthesis in *Acinetobacter calcoaceticus* ADP1. *Journal of Biological Chemistry*. 278, 8075–8082.

Kalscheuer, R.; Stöveken, T.; Malkus, U.; Reichelt, R.; Golyshin, P. N.; Sabirova, J. (2007): Analysis of storage lipid accumulation in *Alcanivorax borkumensis*: Evidence for alternative triacylglycerol biosynthesis routes in bacteria. *Journal of Bacteriology* 189, 918–928.

Kaneko, T.; Tabata, (1997): Complete genome structure of the unicellular cyanobacterium *Synechocystis* sp. PCC6803. *Plant and Cell Physiology* 38, 1171–1176.

Kaneko, T.; Nakamura, Y.; Sasamoto, S.; Watanabe, A.; Kohara, M.; Matsumoto, M. (2003): Structural analysis of four large plasmids harboring in a unicellular cyanobacterium, *Synechocystis* sp. PCC 6803. *DNA Research* 10, 221–228.

Kanwischer, M.; Porfirova, S.; Bergmuller, E.; Dörmann, P. (2005): Alterations in tocopherol cyclase activity in transgenic and mutant plants of *Arabidopsis* affect tocopherol content, tocopherol composition, and oxidative stress. *Plant Physiology* 137, 713–723.

Kelly, A. A.; Froehlich, J. E.; Dörmann, P. (2003): Disruption of the two digalactosyldiacylglycerol synthase genes DGD1 and DGD2 in *Arabidopsis* reveals the existence of an additional enzyme of galactolipid synthesis. *Plant Cell* 15, 2694–2706.

Kelly, A. A.; Kalisch, B.; Hölzl, G.; Schulze, S.; Thiele, J.; Melzer, M. (2016): Synthesis and transfer of galactolipids in the chloroplast envelope membranes of *Arabidopsis thaliana*. *Proceedings of the National Academy of Sciences of the United States of America*113, 10714–10719.

Kessler, F.; Vidi, P. (2007): Plastoglobule lipid bodies: their functions in chloroplasts and their potential for applications. *Advances in Biochemical Engineering/Biotechnology* 107, 153–172.

Klaus, D.; Härtel, H.; Fitzpatrick, L. M.; Froehlich, J. E.; Hubert, J.; Benning, C.; Dörmann, P. (2002): Digalactosyldiacylglycerol synthesis in chloroplasts of the *Arabidopsis dgd1* mutant. *Plant Physiology* 128, 885–895.

Kobayashi, K.; Awai, K.; Nakamura, M.; Nagatani, A.; T, Masuda; Ohta, H. (2009): Type-B monogalactosyldiacylglycerol synthases are involved in phosphate starvation-induced lipid remodeling, and are crucial for low-phosphate adaptation. *The Plant Journal* 57, 322–331.

Kobayashi, K.; Awai, K.; Takamiya, K.; Ohta, H. (2004): *Arabidopsis* type B monogalactosyldiacylglycerol synthase genes are expressed during pollen tube growth and induced by phosphate starvation. *Plant Physiology* 134, 640–648.

Kobayashi, K.; Kondo, M.; Fukuda, H.; Nishimura, M.; Ohta, H. (2007): Galactolipid synthesis in chloroplast inner envelope is essential for proper thylakoid biogenesis, photosynthesis, and embryogenesis. *Proceedings of the National Academy of Sciences of the United States of America* 104, 17216–17221.

Koblížek, M. (2015): Ecology of aerobic anoxygenic phototrophs in aquatic environments. *FEMS Microbiology Reviews* 39, 854–870.

Kopečná, J.; Komenda, J.; Bučinská, L.; Sobotka, R. (2012): Long-term acclimation of the cyanobacterium *Synechocystis* sp. pcc 6803 to high light is accompanied by an enhanced production of chlorophyll that is preferentially channeled to trimeric photosystem I1W. *Plant Physiology* 160, 2239–2250.

Kopfmann, S.; Hess, W. R. (2013): Toxin-antitoxin systems on the large defense plasmid pSYSA of *Synechocystis* sp. PCC 6803. *Journal of Biological Chemistry* 288, 7399–7409.

Laemmli, U. K. (1970): Cleavage of structural proteins during the assembly of the head of bacteriophage T4. *Nature* 227, 680–685.

Lang, F. S.; Oesterhelt, D. (1989): Microaerophilic growth and induction of the photosynthetic reaction center in *Rhodopseudomonas viridis*. *Journal of Bacteriology* 171, 2827–2834.

Lardizabal, K. D.; Mai, J. T.; Wagner, N. W.; Wyrick, A.; Voelker, T.; Hawkins, D. J. (2001): DGAT2 is a new diacylglycerol acyltransferase gene family. purification, cloning, and expression in insect cells of two polypeptides from *Mortierella ramanniana* with diacylglycerol acyltransferase activity. *Journal of Biological Chemistry* 276, 38862–38869.

Lee, A. G. (2000): Membrane lipids: It's only a phase. *Current Biology* 10, 377-380.

Li, F.; Wu, X.; Lam, P.; Bird, D.; Zheng, H.; Samuels, L. (2008): Identification of the wax ester synthase/acyl-coenzyme A. diacylglycerol acyltransferase WSD1 required for stem wax ester biosynthesis in *Arabidopsis*. *Plant Physiology* 148, 97–107.

Li, H.; Sherman, L. A. (2002): Characterization of *Synechocystis* sp. strain PCC 6803 and Δnbl mutants under nitrogen-deficient conditions. *Archives of Microbiology* 178, 256–266.

Liberton, M.; Howard B., R.; Heuser, J.; Roth, R.; Pakrasi, H. B. (2006): Ultrastructure of the membrane systems in the unicellular cyanobacterium *Synechocystis* sp. strain PCC 6803. *Protoplasma* 227, 129–138.

Line, M. A. (2002): The enigma of the origin of life and its timing. *Microbiology* 148, 21–27.

Linscheid, M.; Diehl, B. W.; Övermöhle, M.; Riedl, I.; Heinz, E. (1997): Membrane lipids of *Rhodopseudomonas viridis*. *Biochimica et Biophysica Acta* 1347, 151–163.

Lippold, F.; vom Dorp, K.; Abraham, M.; Holzl, G.; Wewer, V.; Yilmaz, J. L. (2012): Fatty acid phytyl ester synthesis in chloroplasts of *Arabidopsis*. *Plant Cell* 24, 2001–2014.

Los, D. A.; Mironov, K. (2015): Modes of fatty acid desaturation in Cyanobacteria: An update. *Life* 5, 554–567.

Loura, I. C.; Dubacq, J. Thomas, J. C. (1987): The effects of nitrogen deficiency on pigments and lipids of cyanobacteria. *Plant Physiology* 83, 838–843.

Lütke-Brinkhaus, F.; Weiss, G.; Kleinig, H. (1985): Prenyl lipid formation in spinach chloroplasts and in a cell-free system of *Synechococcus* (Cyanobacteria): polyprenols, chlorophylls, and fatty acid prenyl esters. *Planta* 163, 68–74.

Maeda, H.; Sakuragi, Y.; Bryant, D. A.; DellaPenna, D. (2005): Tocopherols protect *Synechocystis* sp. strain PCC 6803 from lipid peroxidation. *Plant Physiology* 138, 1422–1435.

Makula, R. A.; Lockwood, P. J.; Finnerty, W. R. (1975): Comparative analysis of the lipids of *Acinetobacter* species grown on hexadecane. *Journal of Bacteriology* 121, 250–258.

Malcolm S. B. (1996): Phytyl esters and phaeophytins from the hornwort *Megaceros flagellaris*. *Phytochemistry* 41, 1373–1376.

Margaria, T.; Kubczak, C.; Steffen, B. (2008): Bio-jETI: a service integration, design, and provisioning platform for orchestrated bioinformatics processes. *BMC Bioinformatics* 9, 12.

Marin, Kay; Stirnberg, Marit; Eisenhut, Marion; Krämer, Reinhard; Hagemann, Martin (2006): Osmotic stress in *Synechocystis* sp. PCC 6803: low tolerance towards nonionic osmotic stress results from lacking activation of glucosylglycerol accumulation. *Microbiology* 152, 2023–2030.

Marr, A. G.; Ingraham, J. L. (1962): Effect of temperature on the composition of fatty acids in *Escherichia coli*. *Journal of Bacteriology* 84, 1260–1267.

Martin, S.; Parton, R. G. (2006): Lipid droplets: a unified view of a dynamic organelle. *Nature Reviews Molecular cell biology* 7, 373–378.

Masuda, T. (2008): Recent overview of the Mg branch of the tetrapyrrole biosynthesis leading to chlorophylls. *Photosynth Research* 96, 121–143.

Méheust, R.; Zelzion, E.; Bhattacharya, D.; Lopez, P.; Bapteste, E. (2016): Protein networks identify novel symbiogenetic genes resulting from plastid endosymbiosis. *Proceedings of the National Academy of Sciences of the United States of America* 113, 3579–3584.

Merritt, M. V.; Rosenstein, S. P.; Rachel, C. Loh; Chou, H.; Allen, M. M. (1991): A comparison of the major lipid classes and fatty acid composition of marine unicellular cyanobacteria with freshwater species. *Archives of Microbiology* 155, 107–113.

Miller, S.l I.; Salama, N. R. (2018): The gram-negative bacterial periplasm: Size matters. *PLOS Biology* 16, e2004935.

Minnikin, D. E.; Abdolrahimzadeh, H. (1974): The replacement of phosphatidylethanolamine and acidic phospholipids by an ornithine-amide lipid and a minor phosphorus-free lipid in *Pseudomonas fluorescens* NCMB 129. *FEBS Letters* 43, 257–260.

Moellering, E.R.; Muthan, B.; Benning, C. (2010). Freezing tolerance in plants requires lipid remodeling at the outer chloroplast membrane. *Science* 330, 226–228.

Murata, N.; Wada, H.; Gombos, Z. (1992): Modes of Fatty-acid desaturation in cyanobacteria. *Plant Cell Physiol* 3, 933–941.

Nacir, H.; Bréhélin, C. (2013): When proteomics reveals unsuspected roles: the plastoglobule example. *Frontiers in Plant Science* 4.

Narayanan, A.; Ridilla, M.; Yernool, D. A. (2011): Restrained expression, a method to overproduce toxic membrane proteins by exploiting operator-repressor interactions. *Protein Science* 20, 51–61.

Nelson, N.; Yocum, C. F. (2006): Structure and function of photosystems I and II. *Annual Review of Plant Biology* 57, 521–565.

Nickelsen, J.; Rengstl, B. (2013): Photosystem II assembly: from cyanobacteria to plants. *Annual Review of Plant Biology* 64, 609–635.

Okazaki, K.; Sato, N.; Tsuji, N.; Tsuzuki, M.; Nishida, I. (2006): The significance of C16 fatty acids in the sn-2 positions of glycerolipids in the photosynthetic growth of *Synechocystis* sp. PCC6803. *Plant Physiology* 141, 546–556.

Okazaki, Y.; Otsuki, H.; Narisawa, T.; Kobayashi, M.; Sawai, S.; Kamide, Y. (2013): A new class of plant lipid is essential for protection against phosphorus depletion. *Nature Communications* 4, 1510.

Okazaki, Y.; Nishizawa, T.; Takano, K.; Ohnishi, M.; Mimura, T.; Saito, K. (2015): Induced accumulation of glucuronosyldiacylglycerol in tomato and soybean under phosphorus deprivation. *Physiologia Plantarum* 155, 33–42.

Olukoshi, E. R.; Packter, N. M. (1994): Importance of stored triacylglycerols in *Streptomyces*: possible carbon source for antibiotics. *Microbiology* 140, 931–943.

Oster, U.; Bauer, C. E.; Rüdiger, W. (1997): Characterization of chlorophyll a and bacteriochlorophyll a synthases by heterologous expression in *Escherichia coli*. *Journal of Biological Chemistry* 272, 9671–9676.

Pattanaik, B.; Lindberg, P. (2015): Terpenoids and Their Biosynthesis in Cyanobacteria. *Life* 5, 269–293.

Patwari P. (2019): Cuticular waxes contribute to drought tolerance in *Arabidopsis* and Barley. Doctoral dissertation PhD. Bonn University, Germany - Bonn. Institute of Molecular physiology and Biotechnology of Plants (IMBIO).

Peramuna, A.; Summers, Mi. L. (2014): Composition and occurrence of lipid droplets in the cyanobacterium *Nostoc punctiforme*. *Archives of Microbiology* 196, 881–890.

Porra, R. J.; Thompson, W. A.; Kriedemann, P. E. (1989): Determination of accurate extinction coefficients and simultaneous equations for assaying chlorophylls a and b extracted with four different solvents. Verification of the concentration of chlorophyll standards by atomic absorption spectroscopy. *Biochimica et Biophysica Acta* 975, 384–394.

Proels, R. (2014): Stable Transformation of cyanobacterium *Synechocystis* sp. *Bio-protocol* 4.

Reifarth, F.; Christen, G.; Seeliger, A. G.; Dörmann, P.; Benning, C.; Renger, G. (1997): Modification of the water oxidizing complex in leaves of the dgd1 mutant of *Arabidopsis thaliana* deficient in the galactolipid digalactosyldiacylglycerol. *Biochemistry* 36, 11769–11776.

Reyes-Prieto, A.; Weber, A. P. M.; Bhattacharya, D. (2007): The origin and establishment of the plastid in algae and plants. *Annual Review of Genetics* 41, 147–168.

Řezanka, T.; Lukavský, J.; Siristova, L.; Sigler, K. (2012): Regioisomer separation and identification of triacylglycerols containing vaccenic and oleic acids, and α- and γ-linolenic acids, in thermophilic cyanobacteria *Mastigocladus laminosus* and *Tolypothrix* sp. *Phytochemistry* 78, 147–155.

Rocha, J.; Nitenberg, M.; Girard-Egrot, A.; Jouhet, J.; Maréchal, E.; Block, A.; Breton, C. (2018): Do galactolipid synthases play a key role in the biogenesis of chloroplast membranes of higher plants?, *Frontiers in Plant Science* 9, 126.

Rontani, J.; Bonin, P. C.; Volkman, J. K. (1999): Production of wax esters during aerobic growth of marine bacteria on isoprenoid compounds. *Applied and Environmental Microbiology* 65, 221–230.

Rottet, S.h; Besagni, C.; Kessler, F. (2015): The role of plastoglobules in thylakoid lipid remodeling during plant development. *Biochimica et Biophysica Acta* 1847, 889–899.

Röttig, A.; Steinbüchel, A. (2013): Acyltransferases in bacteria. *Microbiology and Molecular Biology Reviews.* 77, 277–321.

Sakurai, I.; Mizusawa, N.; Wada, H.; Sato, N. (2007): Digalactosyldiacylglycerol Is required for Stabilization of the oxygen-evolving complex in photosystem II. *Plant Physiology* 145, 1361–1370.

Sargent, J. R.; Falk-Petersen, (1981): Ecological investigations on the zooplankton community in Balsfjorden, northern Norway: Lipids and fatty acids in *Meganyctiphanes norvegica*, *Thysanoessa raschi* and T. *inermis* during mid-winter. *Marine Biology* 62, 131–137.

Sato, N.; Murata, N. (1982): Lipid biosynthesis in the blue-green alga, *Anabaena variabilis*. II. Fatty acids and lipid molecular species. *Biochimica et Biophysica Acta* 710, 279–289.

Schledz, M.; Seidler, A.; Beyer, P.; Neuhaus, G. (2001): A novel phytyltransferase from *Synechocystis* sp. PCC 6803 involved in tocopherol biosynthesis. *FEBS Letters* 499, 15–20.

Schopf, J. W. (1993): Microfossils of the early archean apex chert: new evidence of the antiquity of life. *Science* 260, 640–646.

Schopf, J. W. (2006): Fossil evidence of Archaean life. *Philosophical Transactions of the Royal Society of London. Series B*, *Biological sciences* 361, 869–885.

Schreiber, U.; S., U.; Bilger, W. (1986): Continuous recording of photochemical and non-photochemical chlorophyll fluorescence quenching with a new type of modulation fluorometer. *Photosynth Research* 10, 51–62.

Sekiguchi, Y.; Yamada, T.; Hanada, S.; Ohashi, A.; Harada, H.i; Kamagata, Y. (2003): *Anaerolinea thermophila* gen. nov., sp. nov. and *Caldilinea aerophila* gen. nov., sp. nov., novel filamentous thermophiles that represent a previously uncultured lineage of the domain bacteria at the subphylum level. *International Journal of Systematic and Evolutionary Microbiology* 53, 1843–1851.

Semeniuk, A.; Sohlenkamp, C.; Duda, K.; Hölzl, G. (2014): A Bifunctional glycosyltransferase from *Agrobacterium tumefaciens* synthesizes monoglucosyl and glucuronosyl diacylglycerol under phosphate deprivation. *Journal of Biological Chemistry* 289, 10104–10114.

Shahak, Y.; Schütz, M.; Bronstein, M.; Griesbeck, C.; Hauska, G.; Padan, E.; Gunter A.; Peschek, Wolfgang L.; Georg S. (1999): Sulfide-dependent anoxygenic photosynthesis in prokaryotes. *The Phototrophic Prokaryotes* 30, 217–228.

Sheng, X.; Liu, X.; Cao, P.; Li, M.; Liu, Z. (2018): Structural roles of lipid molecules in the assembly of plant PSII–LHCII supercomplex. *Biophysics Reports* 4, 189–203.

Shimojima, M.; Ohta, H.; Iwamatsu, A.; Masuda, T.; Shioi, Y.; Takamiya, K. (1997): Cloning of the gene for monogalactosyldiacylglycerol synthase and its evolutionary origin. *Proceedings of the National Academy of Sciences of the United States of America* 94, 333–337.

Shockey, J. M.; Gidda, S. K.; Chapital, D. C.; Kuan, J.; Dhanoa, P. K.; Bland, John M. . (2006): Tung tree DGAT1 and DGAT2 have nonredundant functions in triacylglycerol biosynthesis and are localized to different subdomains of the endoplasmic reticulum W. *The Plant Cell* 18, 2294–2313.

Shpilyov, A. V.; Zinchenko, V. V.; Shestakov, S. V.; Grimm, B.; Lokstein, H. (2005): Inactivation of the geranylgeranyl reductase (ChlP) gene in the cyanobacterium *Synechocystis* sp. PCC 6803. *Biochimica et Biophysica Acta* 1706, 195–203.

Siebers, M.; Dörmann, P.; Hölzl, G. William C. Plaxton; Lamber H. (2015): Membrane remodelling in phosphorus-deficient plants: *Annual Plant Reviews* 282, 237–263.

Siegenthaler, P.; Murata, N. (1998): Lipids in photosynthesis: structure, function and genetics. Dordrecht: Kluwer Academic Publishers, Advances in Photosynthesis, 1-20.

Singh, A.K.; Sherman, Louis, A. (2006): Iron-independent dynamics of IsiA production during the transition to stationary phase in the cyanobacterium *Synechocystis* sp. PCC 6803. *FEMS Microbiology Letters* 256, 159–164.

Smith, C. A.; Want, Elizabeth J.; O'Maille, G.; Abagyan, R.; Siuzdak, G. (2006): XCMS: processing mass spectrometry data for metabolite profiling using nonlinear peak alignment, matching, and identification. *Analytical Chemistry* 78, 779–787.

Smith, P. K.; Krohn, R. I.; Hermanson, G. T.; Mallia, A. K.; Gartner, F. H.; Provenzano, M. D. (1985): Measurement of protein using bicinchoninic acid. *Analytical Biochemistry* 150, 76–85.

SS. Hasan (2011): Conservation of lipid functions in cytochrome bc complexes. *Journal of Molecular Biology* 414, 145–162.

Stanier, R. Y.; Deruelles, J.; Rippka, R.; Herdman, M.; Waterbury, J. B. (1979): Generic assignments, strain histories and properties of pure cultures of cyanobacteria. *Microbiology* 111, 1–61.

Steffen, R.; Eckert, H. J.; Kelly, A. A.; Dormann, P.; Renger, G. (2005): Investigations on the reaction pattern of photosystem II in leaves from *Arabidopsis thaliana* by time-resolved fluorometric analysis. *Biochemistry* 44, 3123–3133.

Tahara, H.; Matsuhashi, A.; Uchiyama, J.; Ogawa, S.; Ohta, H. (2015): Sll0751 and Sll1041 are involved in acid stress tolerance in *Synechocystis* sp. PCC 6803. *Photosynth Research* 125, 233–242.

Tarante, P.; Keenan, T. W.; Potts, M. (1993): Rehydration induces rapid onset of lipid biosynthesis in desiccated *Nostoc commune* (Cyanobacteria). *Biochimica et Biophysica Acta* 1168, 228–237.

Timmis, J. N.; Ayliffe, Ayliffe, M.; Huang, C. Y.; Martin, W. (2004): Endosymbiotic gene transfer: organelle genomes forge eukaryotic chromosomes. *Nature Reviews Genetics* 5, 123–135.

Towbin, H.; Staehelin, T.; Gordon, J. (1979): Electrophoretic transfer of proteins from polyacrylamide gels to nitrocellulose sheets: procedure and some applications.

Proceedings of the National Academy of Sciences of the United States of America 76, 4350–4354.

Tsukatani, Y.; Hirose, Y.; Harada, J.; Misawa, N.; Mori, K.; Inoue, K.; Tamiaki, H. (2015): Complete genome sequence of the bacteriochlorophyll b-producing photosynthetic bacterium *Blastochloris viridis*. *Genome Announc* 3.

van de Meene, A. M. L.; Hohmann-Marriott, M. F.; Vermaas, Wim F. J.; Roberson, R. W. (2006): The three-dimensional structure of the cyanobacterium *Synechocystis* sp. PCC 6803. *Archives of Microbiology* 184, 259–270.

Varghese, Rency S.; Zhou, B.; N. R. Mohammad; Zhao, Y.; Ressom, W. (2012): Ion annotation-assisted analysis of LC-MS based metabolomic experiment. *Proteome Science* 10, 8.

Vavilin, Dmitrii V.; Vermaas, Wim F. J. (2002): Regulation of the tetrapyrrole biosynthetic pathway leading to heme and chlorophyll in plants and cyanobacteria. *Physiologia Plantarum* 115, 9–24.

vom Dorp, K.; Dombrink, I.; Dörmann, P. (2013): Quantification of diacylglycerol by mass spectrometry. *Methods in Molecular Biology* 1009, 43–54.

vom Dorp, K.; Hölzl, G.; Plohmann, C.; Eisenhut, M.; Abraham, M.; Weber, A. P. M. (2015): Remobilization of phytol from chlorophyll degradation is essential for tocopherol synthesis and growth of *Arabidopsis*. *Plant Cell* 27, 2846–2859.

Wada, H.; Murata, N. (1990): Temperature-induced changes in the fatty acid composition of the cyanobacterium, *Synechocystis* PCC6803 1. *Plant Physiology* 92, 1062–1069.

Wang, L.; Xing, X.; Chen, L.; Yang, L.; Su, X.; Rabinowitz, J. (2019): Peak Annotation and verification engine for untargeted LC-MS metabolomics. *Analytical Chemistry* 91, 1838–1846.

Weier, D.; Müller, C.; Gaspers, C.; Frentzen, M. (2005): Characterisation of acyltransferases from *Synechocystis* sp. PCC6803. *Biochemical and Biophysical Research Communications* 334, 1127–1134.

Welti, R.; Li, W.; Li, M.; Sang, Y.; Biesiada, H.; Zhou, H-E (2002): Profiling membrane lipids in plant stress responses. Role of phospholipase D in freezing-induced lipid changes in *Arabidopsis*. *Journal of Biological Chemistry* 277, 31994–32002.

Wewer, V.; Brands, M.; Dörmann, P. (2014): Fatty acid synthesis and lipid metabolism in the obligate biotrophic fungus *Rhizophagus irregularis* during mycorrhization of *Lotus japonicus*. *The Plant Journal* 79, 398–412.

White, T.; Bursten, S.; Federighi, D.; Lewis, R. A.; Nudelman, E. (1998): High-resolution separation and quantification of neutral lipid and phospholipid species in mammalian cells and sera by multi-one-dimensional thin-layer chromatography. *Analytical Biochemistry* 258, 109–117.

Williams, J. G.K. Lester P.: (1988): 85 Construction of specific mutations in photosystem II photosynthetic reaction center by genetic engineering methods in *Synechocystis* 6803. *Methods in Enzymology* 167, 766–778.

Withers, N. W.; Nevenzel, J. C. (1977): Phytyl esters in a marine dinoflagellate. *Lipids* 12, 989–993.

Wu, Q.; Vermaas, Wim F. J. (1995): Light-dependent chlorophyll a biosynthesis upon chlL deletion in wild-type and photosystem I-less strains of the cyanobacterium *Synechocystis* sp. PCC 6803. *Plant Molecular Biology* 29, 933–945.

Yang, Y.; Yin, Ch.; Li, W.; Xu, X. (2008): Alpha-tocopherol is essential for acquired chill-light tolerance in the cyanobacterium *Synechocystis* sp. strain PCC 6803. *Journal of Bacteriology* 190, 1554–1560.

Yu, B.; Xu, C.; Benning, C. (2002): *Arabidopsis* disrupted in SQD2 encoding sulfolipid synthase is impaired in phosphate-limited growth. In: *Proceedings of the National Academy of Sciences of the United States of America* 99, 5732–5737.

Yuzawa, Y.; Nishihara, H.; Haraguchi, T.; Masuda, S.; Shimojima, M.; Shimoyama, A. (2012): Phylogeny of galactolipid synthase homologs together with their enzymatic analyses revealed a possible origin and divergence time for photosynthetic membrane biogenesis. *DNA Research* 19, 91–102.

Zavrel, T.; Sinetova, M.; Cerven, J. (2015): Measurement of chlorophyll a and carotenoids concentration in cyanobacteria. *Bio-protocol* 5.

Zhang, M.; Fan, J.; Taylor, D. C.; Ohlrogge, J. B. (2009): DGAT1 and PDAT1 acyltransferases have overlapping functions in *Arabidopsis* triacylglycerol biosynthesis and are essential for normal pollen and seed development. *Plant Cell* 21, 3885–3901.

Zou, J.; Wei, Y.; Jako, C.; Kumar, Arvind; Selvaraj, Gopalan; Taylor, David C. (1999): The *Arabidopsis thaliana* TAG1 mutant has a mutation in a diacylglycerol acyltransferase gene. *The Plant Journal* 19, 645–653.

7. Appendix

7.1. Synthetic Oligonucleotides Used in this Study

Target	Primer	Sequence (5'-3')	Product size (bp)	PCR programme Cycles; numbers; Tm°C; extension time sec
slr1807	bn3230 (f)	TTTTCTAGAATGCAGTTAGTTAATCTTCATCC	804	35; 50; 60
	bn3231 (r)	TTTCTCGAGTCATGAATTTTTGTTAAGCAA		
slr2103	bn3268 (f)	TTTGAGCTCGTGCTAAGAGCGACCAGTGATC	903	35; 54; 60
	bn3269 (r)	TTTCTGCAGTCAGAGAAAATTTAATTGAGGC		
BviMgdP	bn2874 (f)	TTTCCCACTAGTATGAGACAGCCGAGTGC	1275	35; 65; 90
	bn2875 (r)	TTTCCCAGTACTTCAGTAAACCCGCGCGGCAA		
CaeMgdS	bn3069 (f)	TTTTCTAGAATGAAACGTATCCTGATTCTAATG	1161	35; 57; 60
	bn2993 (r)	TTTCTCGAGTCATCGACTGTCCTTCATTAAC		
CaeDgdS	bn2994 (f)	TTTTCTAGAATGGCACGCATTCTGATTTTTTA	1159	35; 57; 60
	bn2995 (r)	TTTGGATCCCGGGTCAGGATGCAATGTGTGCAAG		
BviGlcADS	bn2577 (f)	CTT TCTAGA ATGATGAAGTTCAATAACTTGTG	1203	35; 55; 40
	bn2578 (r)	ATG GGATCC CTATCCCGCCCGCCGCACC		
5' slr2103	bn2263 (f)	GGTAGAGGAGATTGAAGCGATTC	976	35; 58; 40
	bn2264 (r)	CAACCATGGAAATAGTATTTGTAAAACCATTC		
3' slr2103	bn2265 (f)	TTAACGCGTGGACCCGGTGGTTTTTCCC	982	35; 58; 40
	bn2266 (r)	TCTTACTTTTCGTCAGTTCCTCTG		
5' slr1807	bn2259 (f)	GGGATCGCTAGGTCGAGAATG	959	35; 58; 40
	bn2260 (r)	TTACCATGGTACAGGGGTAATGTTAATCC		
3' slr1807	bn2261 (f)	TTAACGCGTGAAAATATTGCCCCACAGCG	981	35; 58; 40
	bn2262 (r)	CCGTAAACATATCCGTCAGGG		
nptII (Kan)	bn1116 (f)	ATATACGCGTCACGCTGCCGCAAGCACTCA	1165	35; 55; 60
	bn1117 (r)	ATATCCATGGTCAGAAGAACTCGTCAAGAAG		
Genotyping *Δslr2103*	bn2277 (f)	TGCTCGACGTTGTCACTGAAG	1047	35; 55; 90
	Bn3001 (r)	CAATGGTCTGTTCGTCATCATTG		
Genotyping *Δslr2103*	bn3000 (f)	GTTAACCTAGTCAACCAACTTAA	3152	37; 45; 210
	bn3001 (r)	CAATGGTCTGTTCGTCATCATTG		
Genotyping *Δslr2103*	bn3000 (f)	GTTAACCTAGTCAACCAACTTAA	1545	35; 55; 90
	bn2278 (r)	TGCTCGACGTTGTCACTGAAG		
Genotyping *Δslr1807*	bn2998 (f)	AGTAGGGCTGGTATCTTGGATG	3276	37; 45; 210
	bn2999 (r)	CCTGTTCCATAGCGTGGACATC		
Genotyping *Δslr1807*	bn2277 (f)	GCGGACTGGCTTTCTACGTG	1230	35; 55; 90
	bn2999 (r)	CCTGTTCCATAGCGTGGACATC		
Genotyping *Δslr1807*	bn2998 (f)	AGTAGGGCTGGTATCTTGGATG	1537	35; 55; 90
	bn2278 (r)	TGCTCGACGTTGTCACTGAAG		
Genotyping *mgd1*	PD394 (f)	CCCATTTGGACGTGAATGTAGACAC	~700	35; 58; 60
	PD660 (r)	TCCATTTTCGTTATAAACCCCTTA		
Genotyping *mgd1*	PD661 (f)	AAGGGTTAATGAAATATCAACCAG	~800	35; 58; 60
	PD660 (r)	TCCATTTTCGTTATAAACCCCTTA		

7.2. Targeted Lists for Q-TOF MS/MS Analyses

7.2.1. Targeted List for the Q-TOF MS/MS Analysis of FAPEs

Collision induced dissociation of the parental ions of fatty acid phytyl esters (ammonium adduct; $[M + NH_4]^+$) with a collision energy of 5 V results in the formation of fatty acid ammonia ions combined with a neutral loss of phytol moiety lacking H_2O (278.2974).

FAPE species*	Chemical Formula (M)	Mass (*m/z*) $[M + NH_4]^+$	Neutral loss
6:0 phytol	$C_{26}H_{50}O_2$	412.4155	278.2974
8:0 phytol	$C_{28}H_{54}O_2$	440.4468	
9:0 phytol	$C_{29}H_{56}O_2$	454.4624	
10:0 phytol	$C_{30}H_{58}O_2$	468.4781	
12:0 phytol	$C_{32}H_{62}O_2$	496.5094	
14:0 phytol	$C_{34}H_{66}O_2$	524.5407	
16:4 phytol	$C_{36}H_{62}O_2$	544.5094	
16:3 phytol	$C_{36}H_{64}O_2$	546.5250	
16:2 phytol	$C_{36}H_{66}O_2$	548.5407	
16:1 phytol	$C_{36}H_{68}O_2$	550.5563	
16:0 phytol	$C_{36}H_{70}O_2$	552.5720	
17:0 phytol (I.S.)	$C_{37}H_{72}O_2$	566.5876	
18:4 phytol	$C_{38}H_{66}O_2$	572.5407	
18:3 phytol	$C_{38}H_{68}O_2$	574.5563	
18:2 phytol	$C_{38}H_{70}O_2$	576.5720	
18:1 phytol	$C_{38}H_{72}O_2$	578.5876	
18:0 phytol	$C_{38}H_{74}O_2$	580.6033	

* 17:0cyclo phytol (*m/z*: 564.5719) and 19:0cyclo phytol (*m/z*: 592.6032) were added to the target list for quantifying phytyl esters in *E. coli*.

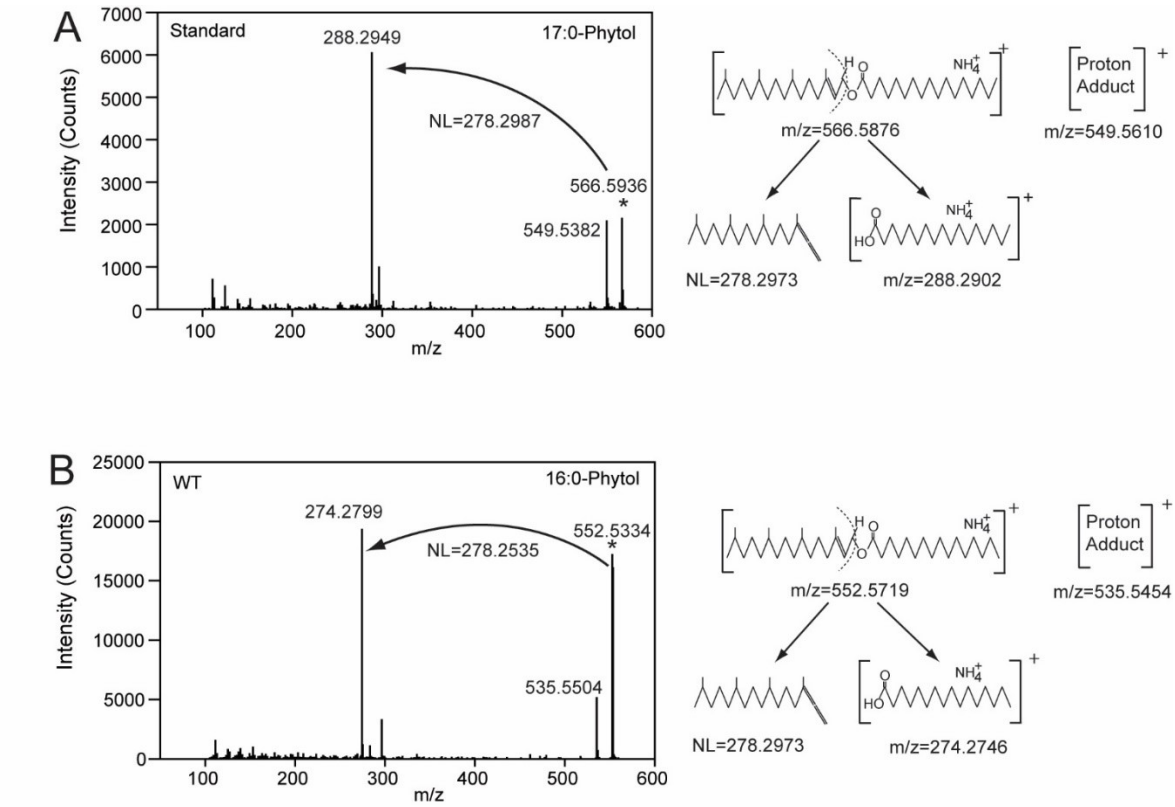

Figure 7. 1: Mass spectra of *Synechocystis* fatty acid phytyl esters and their fragmentation patterns. Fatty acid phytyl esters were isolated from *Synechocystis* cells grown in BG-11 medium and measured by direct infusion Q-TOF MS/MS. (**A**) Internal standard (17:0-Phytol). (**B**) 16:0-Phytol from *Synechocystis* WT. Collision induced dissociation of the parental ions (ammonium adduct, asterisk) results in the formation of fatty acid ammonium ions. The neutral loss (NL) is equivalent to the phytol moiety lacking H_2O. The proton adduct of the parent molecule is also observed in the spectrum. Numbers in the spectra and in the fragmentation pathways represent measured and calculated *m/z*, respectively.

7.2.2. Targeted List for the Q-TOF MS/MS Analysis of TAGs

Collision induced dissociation of the parental ion (ammonium adduct, $[M + NH_4]^+$) with a collision energy of 20 V, results in the formation of diacylglycerol ammonium ions combined with a neutral loss of a fatty acid ammonia adducts $[FA + NH_3]^+$.

Triacylglycerol	(*m/z*) $[M + NH_4]^+$
30:0 TAG	572.4885
32:1 TAG	598.5041
32:0 TAG	600.5198
34:1 TAG	626.5354
34:0 TAG	628.5511
48:6 TAG	812.6765
48:5 TAG	814.6921
48:4 TAG	816.7077
48:3 TAG	818.7233
48:2 TAG	820.7389
48:1 TAG	822.7545
48:0 TAG	824.7702
50:9 TAG	834.6608

Fatty acid	Chemical Formula (M)	Neutral Loss (*m/z*) $[FA + NH_3]^+$
8:0	$C_8H_{19}O_2$	161.1416
10:0	$C_{10}H_{20}O_2$	189.1728
12:0	$C_{12}H_{24}O_2$	217.2041
14:0	$C_{14}H_{28}O_2$	245.2354
16:3	$C_{16}H_{26}O_2$	267.2198
16:2	$C_{16}H_{31}O_2$	269.2355
16:1	$C_{16}H_{33}O_2$	271.2511
16:0	$C_{16}H_{32}O_2$	273.2667
18:3	$C_{18}H_{30}O_2$	295.2511
18:2	$C_{18}H_{32}O_2$	297.2667
18:1	$C_{18}H_{34}O_2$	299.2824
18:0	$C_{18}H_{36}O_2$	301.2980

50:8 TAG	836.6764
50:7 TAG	838.6920
50:6 TAG	840.7076
50:5 TAG	842.7232
50:4 TAG	844.7389
50:3 TAG	846.7545
50:2 TAG	848.7702
50:1 TAG	850.7858
50:0 TAG	852.8015
52:9 TAG	862.6921
52:8 TAG	864.7077
52:7 TAG	866.7233
52:6 TAG	868.7389
52:5 TAG	870.7545
52:4 TAG	872.7702
52:3 TAG	874.7858
52:2 TAG	876.8015
52:1 TAG	878.8171
52:0 TAG	880.8328
54:9 TAG	890.7233
54:8 TAG	892.7389
54:7 TAG	894.7545
54:6 TAG	896.7702
54:5 TAG	898.7858
54:4 TAG	900.8015
54:3 TAG	902.8171

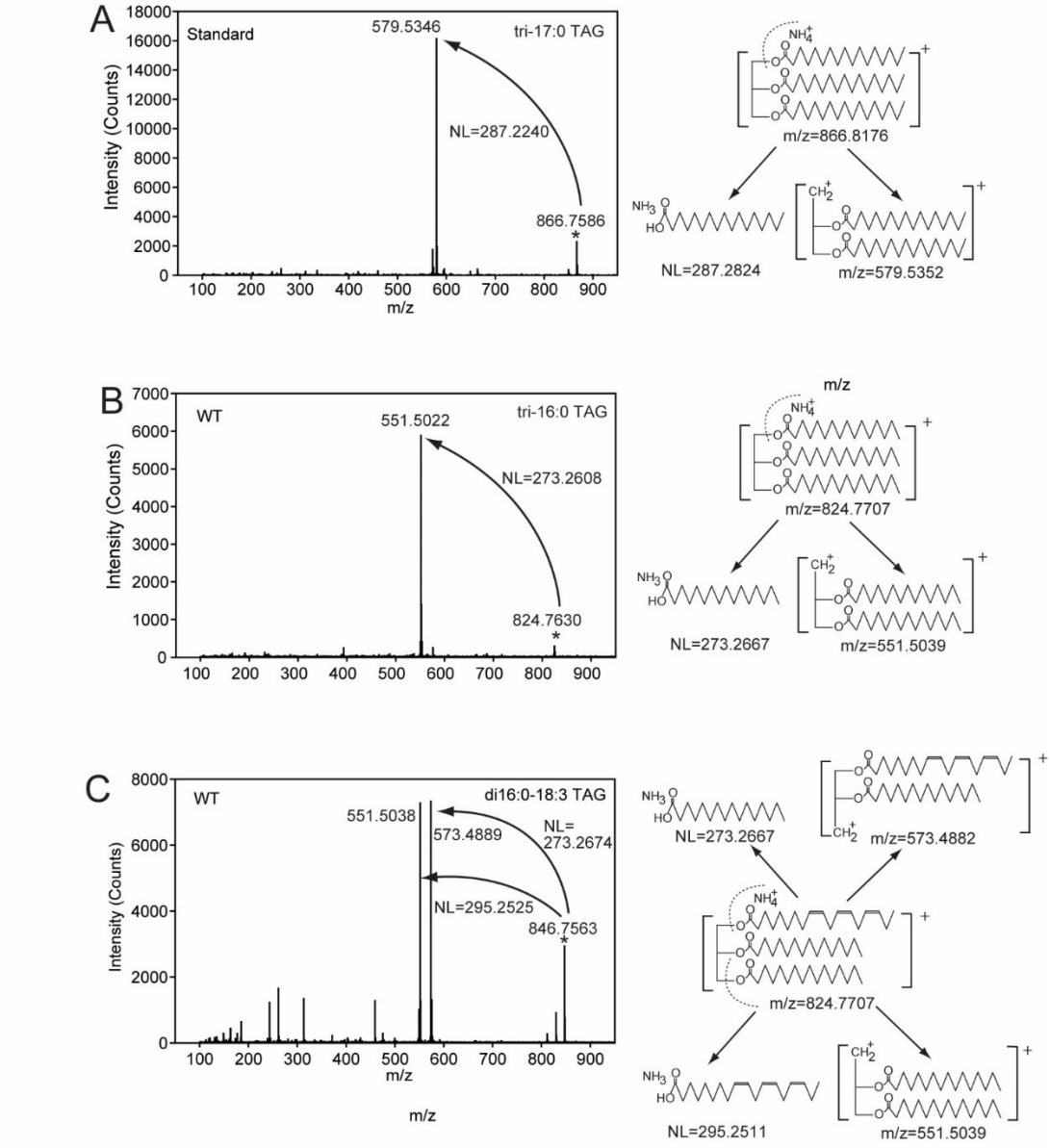

Figure 7. 2: Mass spectra of *Synechocystis* triacylglycerol molecular species.
Triacylglycerols were isolated from *Synechocystis* cells grown in BG-11 medium and measured by Q-TOF MS/MS. (A) Internal standard (tri-17:0 TAG). (B) Tri-16:0 from *Synechocystis* WT. (C) Di16:0-18:3 TAG from *Synechocystis* WT. Collision induced dissociation of the parental ion (ammonium adduct, asterisk) results in the formation of diacylglycerol ions. The neutral loss (NL) is equivalent to the fatty acid ammonia adduct. Numbers in the spectra and in the fragmentation pathways represent measured and calculated *m/z*, respectively. Note that the positional distribution of 16:0 and 18:3 in di16:0-18:3 TAG is unknown. TAG, triacylglycerol.

7.2.3. Targeted List for the Q-TOF Analysis of Membrane Glycerolipids

Collision induced dissociation of the parental ion adducts (ammonium adducts $[M + NH_4]^+$ (MGDG, DGDG, SQDG, PA, PI, PG) or protonated $[M + H]^+$ (PS, PE, PC)) results in the formation of diacylglycerol ions combined with a neutral loss of the head group mass (Table 11). One exception is PC which was identified and quantified based on the product ion scanning with (*m/z*) 184.0739.

Lipid	Mass (*m/z*)	Lipid	Mass (*m/z*)
34:6 MGDG	764.5307	34:4 PI	848.5283
34:5 MGDG	766.5463	34:3 PI	850.5440
34:4 MGDG	768.5620	34:2 PI	852.5597
34:3 MGDG	770.5776	34:1 PI	854.5753
34:2 MGDG	772.5933	34:0 PI (IS)	856.5910
34:1 MGDG	774.6089	36:6 PI	872.5283
34:0 MGDG (IS)	776.6246	36:5 PI	874.5440
36:6 MGDG	792.5620	36:4 PI	876.5596
36:5 MGDG	794.5776	36:3 PI	878.5753
36:4 MGDG	796.5933	36:2 PI	880.5909
36:3 MGDG	798.6089	36:1 PI	882.6066
36:2 MGDG	800.6246	36:0 PI (IS)	884.6223
36:1 MGDG	802.6402	28:0 PE (IS)	636.4604
36:0 MGDG (IS)	804.6559	34:4 PE	712.4912
38:6 MGDG	820.5933	34:3 PE	714.5069
38:5 MGDG	822.6089	34:2 PE	716.5225
38:4 MGDG	824.6246	34:1 PE	718.5382
38:3 MGDG	826.6402	36:6 PE	736.4912
34:6 DGDG	926.5835	36:5 PE	738.5069
34:5 DGDG	928.5992	36:4 PE	740.5225
34:4 DGDG	930.6148	36:3 PE	742.5382
34:3 DGDG	932.6305	36:2 PE	744.5538
34:2 DGDG	934.6461	36:1 PE	746.5695
34:1 DGDG	936.6618	38:6 PE	764.5225
34:0 DGDG (IS)	938.6775	38:5 PE	766.5382
36:6 DGDG	954.6148	38:4 PE	768.5538
36:5 DGDG	956.6305	38:3 PE	770.5695
36:4 DGDG	958.6461	38:2 PE	772.5851
36:3 DGDG	960.6618	40:3 PE	798.6008
36:2 DGDG	962.6774	40:2 PE	800.6164
36:1 DGDG	964.6931	40:0 PE (IS)	804.6477
36:0 DGDG (IS)	966.7087	42:4 PE	824.6169
38:6 DGDG	982.6461	42:3 PE	826.6321
38:5 DGDG	984.6618	42:2 PE	828.6477
38:4 DGDG	986.6774	28:0 PG (IS)	684.4816
38:3 DGDG	988.6931	32:1 PG	738.5279
34:6 SQDG	828.4926	32:0 PG	740.5436
34:5 SQDG	830.5082	34:4 PG	760.5123
34:4 SQDG	832.5239	34:3 PG	762.5279
34:3 SQDG	834.5395	34:2 PG	764.5436
34:2 SQDG	836.5552	34:1 PG	766.5592
34:1 SQDG	838.5708	34:0 PG	768.5749
34:0 SQDG (IS)	840.5865	40:0 PG (IS)	852.6694
36:6 SQDG	856.5239	28:0 PC (IS)	678.5074
36:5 SQDG	858.5395	32:0 PC	734.5695
36:4 SQDG	860.5552	34:4 PC	754.5382
36:3 SQDG	862.5708	34:3 PC	756.5538
36:2 SQDG	864.5865	34:2 PC	758.5695

36:1 SQDG	866.6022	34:1 PC	760.5851
36:0 SQDG (IS)	868.6178	36:6 PC	778.5382
28:0 PA (IS)	610.4448	36:5 PC	780.5538
34:6 PA	682.4442	36:4 PC	782.5695
34:5 PA	684.4462	36:3 PC	784.5851
34:4 PA	686.4755	36:2 PC	786.6008
34:3 PA	688.4912	36:1 PC	788.6164
34:2 PA	690.5068	38:6 PC	806.5695
34:1 PA	692.5225	38:5 PC	808.5851
36:6 PA	710.4755	38:4 PC	810.6008
36:5 PA	712.4912	38:3 PC	812.6164
36:4 PA	714.5068	38:2 PC	814.6321
36:3 PA	716.5225	40:5 PC	836.6164
36:2 PA	718.5381	40:4 PC	838.6321
40:0 PA (IS)	778.6326	40:3 PC	840.6477
28:0 PS (IS)	680.4503	40:2 PC	842.6634
34:4 PS	756.4810	40:0 PC (IS)	846.6952
34:3 PS	758.4967		
34:2 PS	760.5123		
34:1 PS	762.5280		
36:6 PS	780.4810		
36:5 PS	782.4967		
36:4 PS	784.5123		
36:3 PS	786.5280		
36:2 PS	788.5436		
36:1 PS	790.5593		
38:6 PS	808.5123		
38:5 PS	810.5280		
38:4 PS	812.5436		
38:3 PS	814.5593		
38:2 PS	816.5749		
38:1 PS	818.5906		
40:4 PS	840.5749		
40:3 PS	842.5906		
40:2 PS	844.6062		
40:1 PS	846.6219		
40:0 PS (IS)	848.6375		
42:4 PS	868.6062		
42:3 PS	870.6219		
42:2 PS	872.6375		
42:1 PS	874.6532		
44:3 PS	898.6532		
44:2 PS	900.6688		

Table. 11: Parameters for the quantification of glycerolipids by Q-TOF MS/MS in the positive ion mode

Lipid	**Parental Ion**	**Collision Energy [V]**	**Neutral Loss**
MGDG	$[M + NH_4]^+$	12	179.0556
DGDG	$[M + NH_4]^+$	17	341.1084
SQDG	$[M + NH_4]^+$	19	261.0518
PA	$[M + NH_4]^+$	20	115.0034
PS	$[M + H]^+$	22	185.0089
PI	$[M + NH_4]^+$	20	277.0563
PE	$[M + H]^+$	20	141.0191
PG	$[M + NH_4]^+$	20	189.0402
PC	$[M + H]^+$	35	-

7.3. Plasmids and Expression Vector Maps

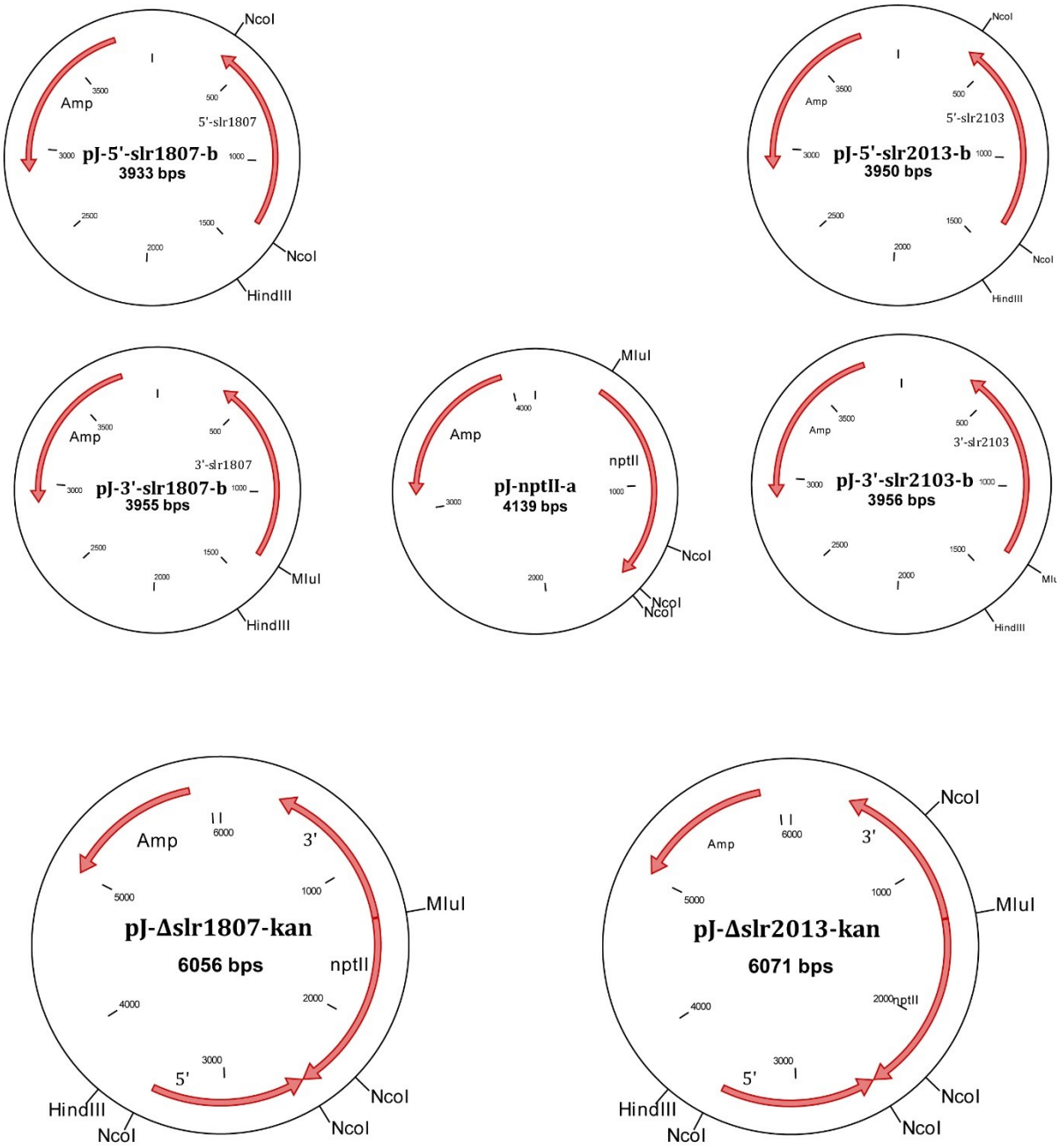

Figure 7. 3: Vectors that were used to generate the insertion mutants in *Synechocystis*. a and b represent the different directions that the PCR product can be ligated into the blunt-ended pJET1.2 vector.

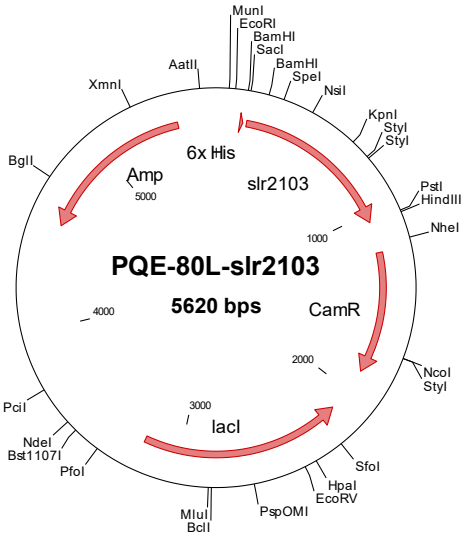

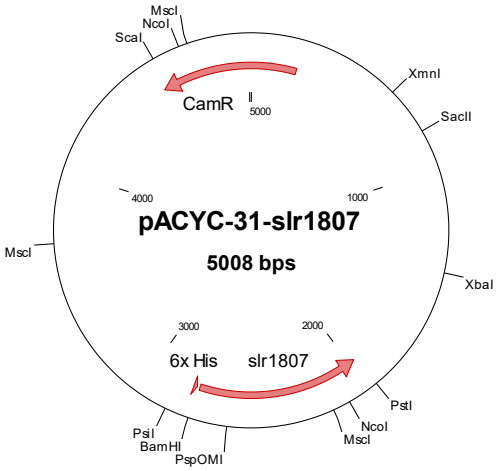

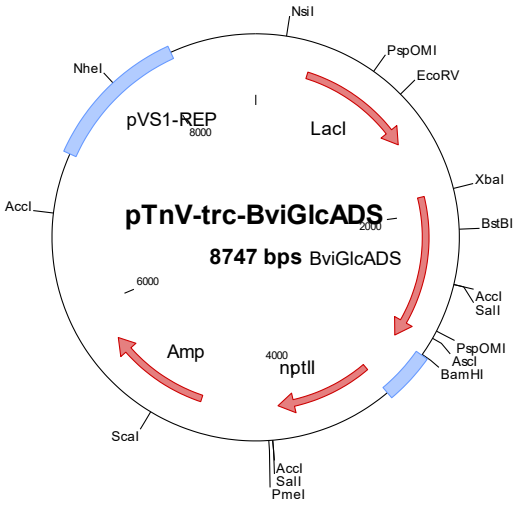

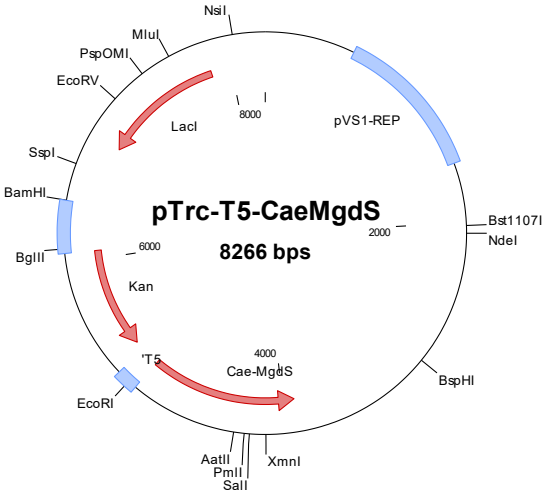

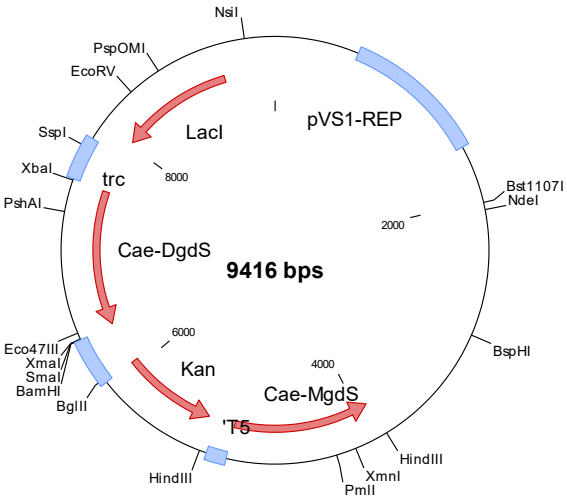

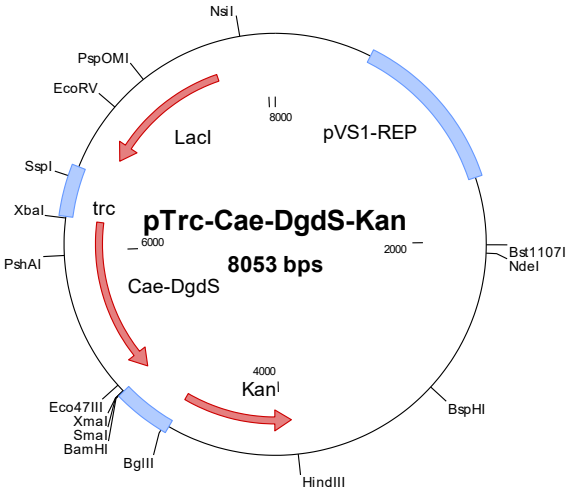

pTrc CaeDgdS-T5 CaeMgdS

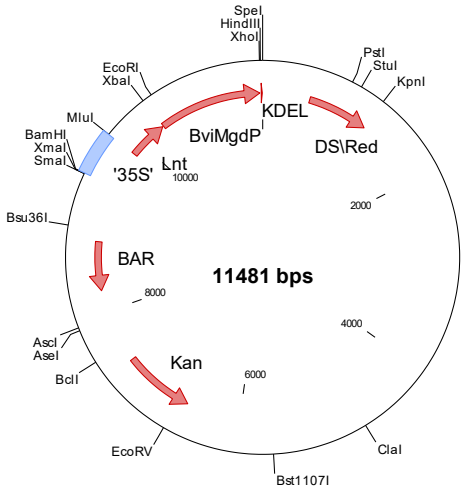

Figure 7. 4: Vectors which were used in this study

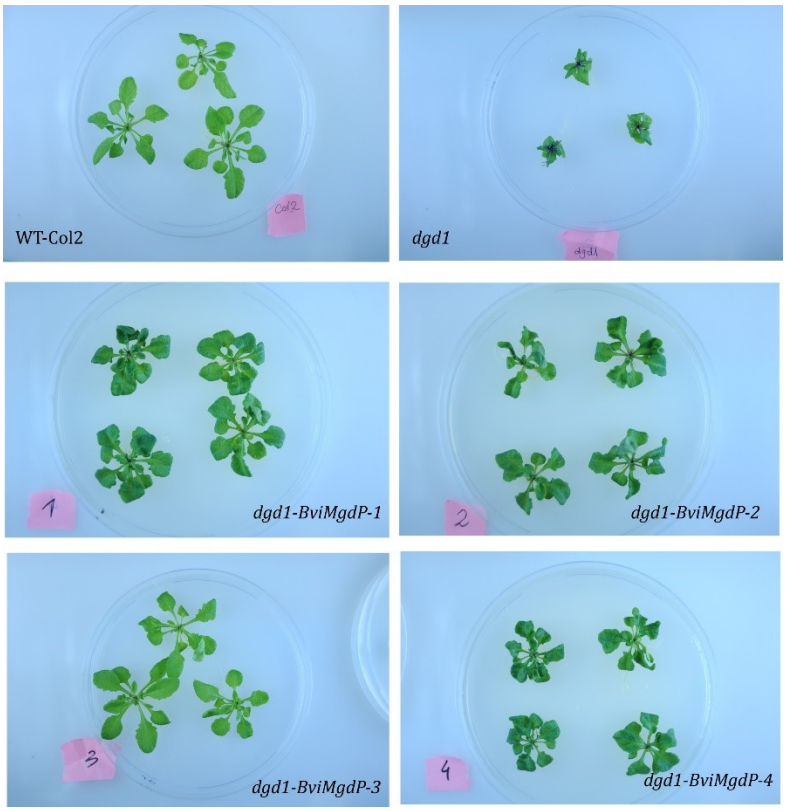

Figure 7. 5: Arabidopsis plants WT, *dgd1,* and the four transformed *dgd1* lines expressing BviMgdP

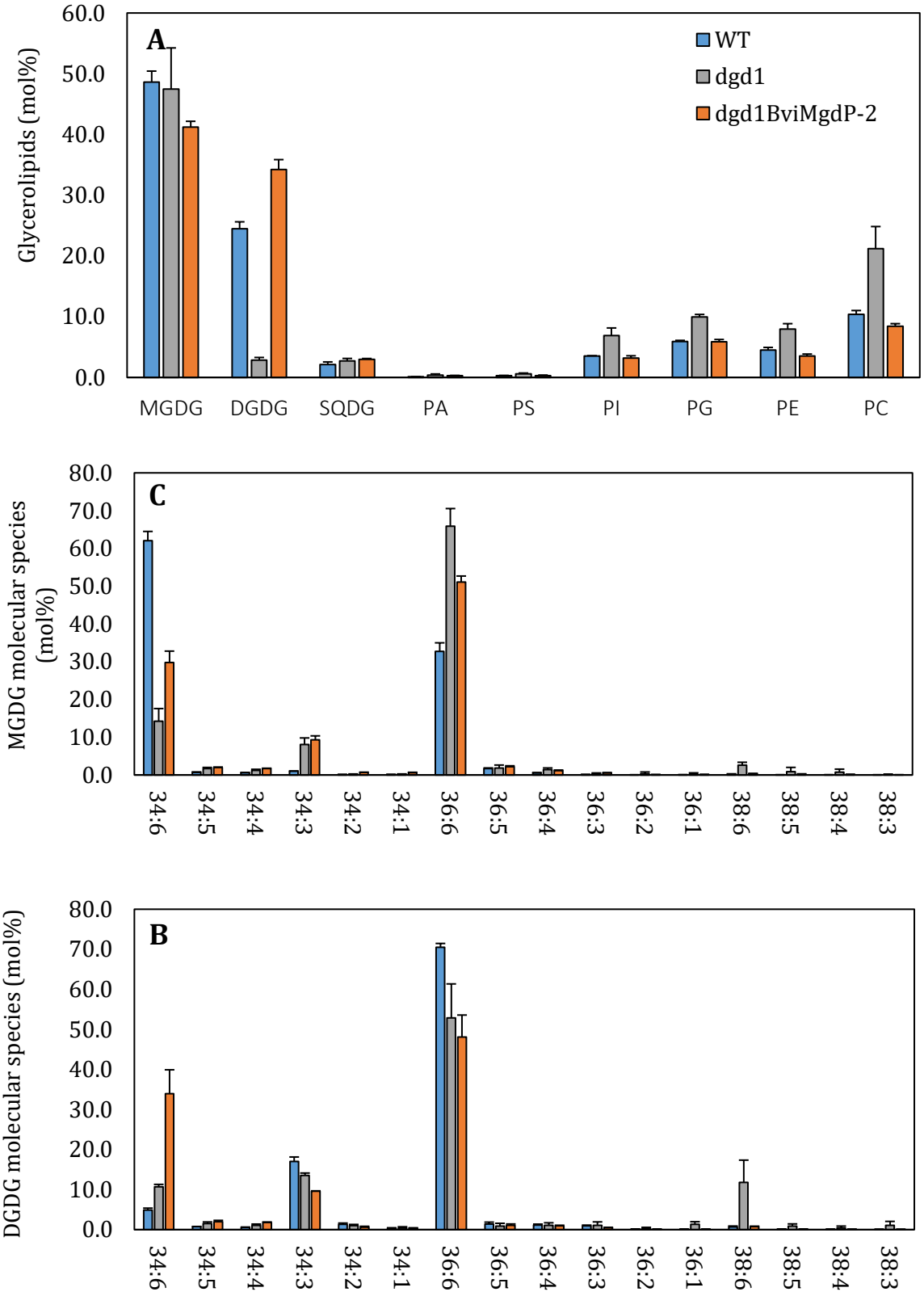

Figure 7. 6: Glycerolipid content and the molecular species oh MGDG and DGDG showed in mol% **(A)** Membrane glycerolipids were quantified in leaves of wild type, *dgd1*, and one line of *dgd1*-BviMgdP-2 using direct infusion Q-TOF MS/MS. Data are shown in mol%. **(**B**)** The fatty acid composition of DGDG in mol% **(C)** The fatty acids composition of MGDG in mol%. Mean and SD values were calculated from 3 independent replicates. DGDG in the WT is αβDGDG and in the expression lines is ββDGDG.

Parts of this thesis is published in the Proceedings of the National Academy of Sciences of the United States of America (PNAS):

Triacylglycerol and phytyl ester synthesis in *Synechocystis* sp. PCC6803

https://doi.org/10.1073/pnas.1915930117

8. Acknowledgements

كلنا يا بني نسافر وحدنا في النهاية

الطيب الصالح

''Son! Eventually, we all travel alone''

Al-Taieb Al-Saleh

I would love to warmly thank all who made my journey easier. Firstly, I am thankful to Prof. Dr. Peter Dörmann for giving me the opportunity to complete my thesis in his lab. I am thankful for his continuous support and valuable advices. Many thanks to the members of the examining committee represented by Priv. Doz. Dr. Christiane Dahl, Prof. Dr. Dorothea Bartels and Prof. Dr. Frank Hochholdinger for their time and appreciated comments. I would like to thank Dr. Michael Melzer from IPK Gatersleben for his efforts in TEM. I am thankful to the Institute of Crop Sciences and Resource Conservation (INRES) for giving the chance to use their ChemiDoc imaging system.

Dear IMBIOs ''Guten TAG''!
Katharina Gutbrod, I truly appreciate your great help and being patient while introducing me to the world of mass spectra. Thank you for your positive words, they were always helpful. Many thanks to Georg Hölzl for helping in cloning and always being there to answer all questions. I would like to acknowledge the great help of Mrs. Helga Peisker in the Q-TOF measurements. Mathias, thank you for your help with my first GC measurements, acyl-ACP and for all the tips. Payal, thank you for your help with the enzyme assay, for sharing your delicious Indian food and to be close. Jill my Cologne-Bonn way companion, thank you for your friendly attitude and all the discussions. Thank you, Philipp, and Wentao for the good time.
Previous colleagues, Regina thank you for your special kindness and being always ready to help. I would like also to thank Barbara, my sweet neighbour in the old office. Victoria thank you for helping with the tocopherol measurements. Thank you Duan and all the best for you. Thank you, Vera Wewer, for the indirect help in the untargeted LC-MS.
New colleagues, Nina, thank you for your contagious smile and for being friendly all the time. Thank you, Julia and good luck with MGDG project. Vadim and Yannic, thank you for the good time. ''Mamma mia… I swear I did nothing'' dear Andreas thank you for all these unforgettable moments and for your special way to be you. Biggi and Marlies, thanks for your help in many ways and for all the sympathy you showed. Thank you, Ellen and Christine, for your efforts. I would also like to thank the students who were involved in the lab work Hanna, Nils and Mohammed. Thank you, Dora, for helping in genotyping.

Finally, my family, Daniel thank you for the unlimited support, thank you for being there all the time a good listener and a good advisor. Anmaro thank for bearing me when I got crazy. Mom, Dad, Hiba and Karam you are the hope that makes everything achievable. Cheers!